The Role of Cell Signalling Events in Modulating the Functions of Nucleoporin Tpr
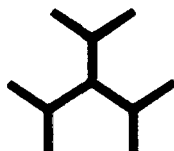
Thesis submitted to

Jawaharlal Nehru University

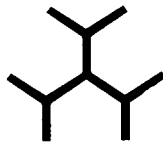in partial fulfillment of the requirements for the degree of

Doctor of Philosophy

Kalpana Rajanala

Signal Transduction Laboratory - I

National Institute of Immunology

New Delhi-110067, India

March 2012

राष्ट्रीय प्रतिरक्षाविज्ञान संस्थान
NATIONAL INSTITUTE OF IMMUNOLOGY

CERTIFICATE

This is to certify that the thesis entitled "**The Role of Cell Signalling Events in Modulating the Functions of Nucleoporin Tpr**" submitted by **Ms. Kalpana Rajanala** in partial fulfillment of degree of **Doctor of Philosophy** of Jawaharlal Nehru University, embodies the work done under the guidance of Dr. Vinay Kumar Nandicoori at the **National Institute of Immunology**, New Delhi. This work is original and has not been submitted in part or full for any other degree or diploma of any university.

Kalpana Rajanala

Dr. Vinay Kumar Nandicoori,

Ph.D Supervisor,

National Institute of Immunology,

New Delhi.

Deputy Director,

National Institute of Immunology,

New Delhi.

डॉ सतीश कुमार गुप्ता / Dr. Satish K. Gupta
स्टाफ वैज्ञानिक-VIII / उप निदेशक
Staff Scientist-VIII / Dy. Director
राष्ट्रीय प्रतिरक्षाविज्ञान संस्थान
NATIONAL INSTITUTE OF IMMUNOLOGY
अरुणा आसफ अली मार्ग / Aruna Asaf Ali Marg,
नई दिल्ली-110067 / New Delhi-110067

Acknowledgements

Nanamma, Tatagaru, Usha Atta, Sandhya Atta, Kittu Chinanna and Bujji Chinanna for all the affection and constant encouragement.

I am grateful to Ajaz for his love and consideration, his constant support and enthusiasm towards my career has played an important part in helping me accomplish this goal. I am especially thankful to him for boosting up my confidence and making me believe in myself whenever I was distressed.

When I set out to achieve my ambition of pursuing a Ph.d degree, God has been kind enough to provide me the opportunity and also bestow me with the resilience and strength to carry on, for which I am very grateful. I hope as my jouney through life continues, the blessings always remain with me.

Kalpana Rajanala
12 March 2012

Table of Contents

2. Chapter-II: Materials and Methods

3. Chapter-III: Functional role of Tpr in the nucleocytoplasmic transport of macromolecules

Appendix-I

Appendix-II

Bibliography

Synopsis

INTRODUCTION

In eukaryotes, nucleopore complex (NPC) forms a major channel of communication between the nucleus and the cytoplasm which helps in the import and export of proteins and messenger RNA. The NPC is a large protein assembly comprising of over 30 different proteins called nucleoporins (Nup's) which are arranged as sub complexes. Nucleoporin Tpr (translocated promoter region) , present at the nuclear phase of the NPC, was originally identified as the oncogenic activator of the met, raf, and trk protooncogenes [1-3]. Tpr is a large 270 kDa protein with a bipartite structure consisting of ~1600-residue α-helical coiled-coil N-terminal domain and a highly acidic noncoiled ~800 amino acid carboxy terminus [4]. Cellular transformations and human tumors have been shown to occur due to the fusion of N-terminal residues of Tpr (residues 140-230) with the protein kinase domains of the protooncogenes met, raf, and trk [1-3]. Tpr has been shown to be localized exclusively to intranuclear filaments associated with the nucleoplasmic side of the NPC, by directly binding to Nup153 [5-7]. Different metazoan species have been shown to contain only one Tpr ortholog, whereas two homologs, Mlp1 and Mlp2, are present in *Saccharomyces cerevisiae* and *Schizosaccharomyces pombe* [8-10].

The functions of Tpr include roles in intranuclear and nucleocytoplasmic transport and as a scaffolding element in the nuclear phase of the NPC [11-14]. Tpr has been shown to play a role in nuclear export of proteins containing leucine rich nuclear export signal (NES) and it also aids in the export of proteins with no apparent NES, as in the case of Huntington protein [12, 15]. The ectopic expression of mammalian Tpr has also been reported to result in the accumulation of poly $(A)^+$ RNA in the nucleus [16]. Studies performed with the yeast homolog of Tpr, Mlp1 reveals a role for the protein in the nuclear retention of unspliced RNA [17]. The association of Mad1 and Mad2 proteins with Tpr has been shown to affect mitotic spindle checkpoint signalling [18]. Depletion of Tpr causes a chromosome lagging phenotype and this phenomenon is due to the loss of interaction between Tpr and dynein complex [19]. The Tpr homolog of *Arabidopsis* has been implicated in the regulation of mRNA export and SUMO homeostasis, and has been shown to influence various aspects of plant development like flowering time [20, 21]. The interaction between transcription factor HSF-1 and Tpr has been shown to facilitate the export of stress induced Hsp-70 mRNA [22]. These observations implicate a critical

role for the human Tpr protein in modulating diverse functions. However, the role played by nucleoporin Tpr in the nucleocytoplasmic transport of macromolecules has not been reported in detail. One of the focuses of the present study is to clearly delineate the role for nucleoporin Tpr in the macromolecular transport through the NPC.

FUNCTIONAL ROLE OF TPR IN THE NUCLEOCYTOPLASMIC TRANSPORT OF MACROMOLECULES

Tpr does not play a significant role in cellular protein transport or in mRNA export.

We sought to comprehensively investigate the role of Tpr in nucleocytoplasmic transport of macromolecules. In order to examine the function of Tpr in cellular transport of proteins and nuclear export of mRNA, we depleted Tpr protein in HEK293T cells using three independent siRNA oligonucleotides. When the levels of Tpr were analyzed 48 hours post transfection, diminution in Tpr levels could be seen with all three siRNA oligos. Love et al., [23] have established an exceedingly useful system to investigate import and export of proteins in HeLa cells. In these cells, chimeric Rev- Glucocorticoid-GFP Receptor protein (chimeric GFP) is localized to the cytosol in the absence of any treatment, and upon the addition of dexamethasone it translocates into the nucleus. Subsequent to the removal of dexamethasone, the chimeric GFP is exported back to the cytoplasm. When import of the chimeric GFP protein was investigated by incubating the cells with dexamethasone, import rates were observed to be similar for both NS-siRNA and Tpr-siRNA treated cells, indicating absence of any role for Tpr in protein import. Subsequently, the export of the chimeric GFP-protein was visualized at different time intervals after the removal of dexamethasone. We did not observe any significant change in the rate of chimeric GFP protein export in the cells treated with Tpr-siRNA in comparison with those treated with NS-siRNA. These results indicate that Tpr may have a limited role in modulating the rate of protein export. To investigate the role of Tpr in export of processed poly $(A)^+$ mRNA, we knocked down Tpr expression and performed Fluorescence in situ hybridization using FITC tagged oligo(dT) probe. The distribution of poly $(A)^+$ mRNA was found to be comparable in both control and in Tpr depleted cells. Based on these

results, we conclude that Tpr does not play a role in translocation of proteins or poly $(A)^+$ mRNA across the nuclear membrane.

Tpr depletion enhances CTE mediated export of unspliced RNA from the nucleus

Conventionally in eukaryotes, unspliced RNA is retained in the nucleus, and only processed mRNA is exported through the NPC. However, retroviruses have developed mechanisms to overcome this regulation, thus enabling unspliced genomic RNA to be exported and finally packaged. Tpr homologs in *S.cerevisiae*, Mlp1 and Mlp2, were reported to play a role in export of unspliced RNA [17]. Towards analyzing the role of Tpr in the nucleocytoplasmic export of intron-containing RNA, we utilized well characterized Gag/Pol reporter constructs containing either a Rev response element (RRE) [3] or a constitutive transport element (CTE) [24-28]. These reporter constructs contain coding sequences of Gag/Pol proteins of HIV within an intron, followed by either RRE or CTE. When we examined the possibility of a role for Tpr in RRE-dependent export, we observed that when Tpr was indeed knocked down there was negligible variation in the levels of Gag protein cleavage product p24 in the cytoplasm which was quantified by ELISA, indicating that Tpr does not play any role in RRE-Rev dependent export of unspliced RNA. On the contrary, when we investigated the possible role of Tpr in regulating CTE-dependent export of unspliced RNA, we observed that knockdown of Tpr resulted in a ~8-10 fold enhancement in the levels of Gag proteins (p24) in the cytoplasm. Quantitative real time PCR analysis of the nuclear and cytoplasmic extracts of control cells and Tpr depleted cells demonstrated elevated CTE-mRNA pools in the cytoplasm of Tpr depleted cells, which were proportional to the levels of p24 protein levels. In addition, we found that ectopic and stable expression of siRNA resistant Tpr rescued CTE mediated p24 expression. Taken together, these results provided evidence of a regulatory role for Tpr in modulating CTE-dependent export of unspliced RNA.

Tpr mediated regulation of unspliced RNA export is independent of Sam68 and Tap functions

Sam68, Nxt1/p15 and Tap/Nxf1 proteins have been previously reported to play a role in enhancement of CTE function [26-29]. In an effort to understand the mechanism behind

Tpr mediated regulation, we studied the effect of Sam68 and Tap depletion as well as over-expression on CTE mediated export in Tpr deficient cells. Depletion of Tap, or Tap and Tpr together, did not significantly enhance p24 levels whereas, depletion of Tpr and Sam68 together resulted in decreased p24 in the cytosol. This may be due to the fact that Sam68 is known to be required for stabilization of unspliced RNA [30], which may have been compromised to an extent in its absence. In contrast, we observed that the simultaneous depletion of Tpr and over-expression of Sam68 resulted in a synergistic increase in the export of unspliced RNA. These results indicated that the mode of regulating unspliced RNA export by Sam68 and Tpr were likely to be different.

Localization of Tpr at the Nucleopore complex is necessary for the regulation of CTE mediated export

Subsequently, we wanted to ascertain whether other nucleoporins known to play a role in nucleocytoplasmic transport may also be involved in the modulation of CTE mediated unspliced RNA export. Towards this, specific siRNAs were used to individually deplete various FG repeat-containing nucleoporins such as Nup214, Nup358/RanBP2 which are localized to the cytoplasmic fibrils of the NPC, and Nup153, Nup98 and Nup50, shown to be present in the nucleoplasmic side of the NPC. We observed elevated levels of normalized p24 expression in samples when either Tpr or Nup153 were depleted, depletion of the other FG containing nucleoporins had no effect on CTE mediated export. Interaction between Tpr and Nup153 has been reported to be required for localization of Tpr to the nuclear pore [7]. If the increased export of Gag/Pol-CTE RNA observed upon Nup153 depletion is an independent function of Nup153, we would expect a cumulative increase when both Tpr and Nup153 are depleted. While, we observed enhanced p24 levels when either Tpr or Nup153 are depleted, with Tpr depletion enhancing p24 levels more effectively than Nup153 depletion, we did not observe a cumulative elevation of p24 levels when both of them were depleted.

Nup153 has been demonstrated to interact with Tpr and the interaction is mediated through residues L458 and M489 in the N-terminal coiled-coil region of Tpr. The interaction has been shown to be required for the localization of Tpr [7]. The fact

that we did not observe a cumulative effect upon Tpr and Nup153 double knockdown, suggested that Nup153 mediated Tpr anchoring may be essential for modulating Gag/Pol-CTE RNA export. To test this, we generated siRNA resistant localization deficient mutant of Tpr (Tpr-L458P/M489P). As expected, when cells were transfected with siRNA resistant FLAG-Tpr-Si construct, we observed decreased p24 levels. Importantly, presence of siRNA resistant FLAG-Tpr-L458P/M489P-Si did not bring down the levels of normalized p24. Taken together, these results provide compelling evidence that the localization of Tpr to the NPC is critical for regulating the export of intron containing RNA.

ROLE OF POST TRANSLATIONAL MODIFICATIONS ON THE FUNCTIONS OF TPR

In Eukaryotic cells, one of the crucial steps for mitotic entry is the breakdown of nuclear envelope. Previous reports showed that nucleoporins are extensively phosphorylated during the mitosis [31-34]. In a previous study we have identified Tpr as a substrate of MAP kinase ERK2 and identified the ERK2 mediated phosphorylation sites on Tpr [35, 36]. Tpr has been demonstrated to act as an ERK2 scaffold in NPC, in turn resulting in phosphorylation of substrates that interact with Tpr. Moreover, studies have demonstrated that nucleoporin Tpr activates mitotic spindle checkpoint by interacting with Mad proteins [18] and its association with dynein complex was shown to be important for proper segregation of chromosomes during mitosis [19]. The fact that nucleoporins are extensively phosphorylated during mitosis and the evidence of pivotal role for Tpr during the anaphase led us to investigate the role for Tpr phosphorylation in modulating the known mitotic functions of the protein.

Identification of ERK independent phosphorylation sites on Tpr

In our previous work, we identified a nuclear pore complex protein Tpr to be a novel substrate for the MAP Kinase ERK2. We identified sites on Tpr for ERK2 phosphorylation and binding, and demonstrated their functional interaction. Further, we observed that in addition to ERK2, other cellular kinases also phosphorylate Tpr protein *in vivo*. In order to identify these ERK2 independent phosphorylation sites, series of deletions were generated in the C-terminal region of Tpr from both amino and carboxy

terminal ends. These constructs were transfected in COS-1 cells and metabolically labelled with ^{32}P inorganic phosphate. Phosphoaminoacid of the *in vivo* labelled Tpr carboxy terminal fragment with mutations in ERK2 target sites indicated that ERK2 independent sites are phosphoryalted only on serine residues. Two dimensional tryptic phosphopeptide maps of in vivo phosphorylated TprC deletion fragments showed similar pattern similar to the TprC fragment for five mutants, while the spots disappeared in one fragments, thus allowing us to narrow the the target site to a region between aminoacid residues 2029 and 2129. With the help of site directed mutagenesis, metabolic labelling and peptide maping we identified the target sites to be S2059 and S2094.

Characterization of phospho specific antibodies of Tpr

In an effort to decipher the functional significance of phosphorylation of ERK2 target site T2123 and independent sites S2059 and S2094, we have raised phospho specific antibodies. In order to test the specificity of the pS2059 and pS2094 antibodies, COS-1 cells were transfected with TprC, TprC-S2059A, TprC-S2094A and TprC-T2123A mutants. Cell lysates were resolved, transferred on to membrane and probed with anti-TprC and pS2059, pS2094 and pT2123 antibodies. Tpr C-terminal fragment expressed and purified from *E. coli* was used a control for these blots. We found that while all the antibodies could detect TprC succesfully, they failed to detect either the *E. coli* expressed form or the respective alanine mutants. Interestingly, pS2059 and pS2094 antibodies also detected band corresponding to endogenous full length Tpr. Next, we characterized these antibodies for their ability to detect Tpr in immunofluoresence experiments. Immunofluroresence analysis using phospho-specific antibodies demonstrated nuclear rim staining, which co-localized with the staining with Tpr antibodies.

Tpr is phosphorylated at S2094 residue by PKA

Bioinformatics analysis and scan-site predications indicated a few putative cellular kinases that would potentially phosphorylate Tpr protein *in vivo*. Based on these predictions, *in vitro* kinase assay was carried out with these candidate kinases and the TprC protein. Results indicated that Protein Kinase A phosphorylated TprC at

S2094 residue *in vitro*. To determine whether the same site is a PKA target *in vivo*, PKA was depleted in HeLa cells by specific siRNA and the cells were analyzed by phosphoblots which clearly established the specificity of PKA phosphorylation of Tpr *in vivo*.

Cell cycle dependent phosphorylation of Tpr

Analysis of Tpr protein levels during different stages of mitosis by immunoblot provided evidence that Tpr levels are higher during the mitotic stages than during the interphase. Immunofluoresence analysis of HeLa cells by phospho-S2059 antibody showed that Tpr is phosphorylated at this specific residue during the interphase and also during the mitosis. It was particularly interesting to find a significant unphosphorylated form of Tpr protein in the cytosol and the phosphorylated form associated with the chromatin during the telophase. When a similar analysis was done with phospho-S2094 antibody, significant dephosphorylation was observed during the telophase. However, the T2123 phosphorylation was uneffected during all the mitotic stages. These results provide crucial data supporting the fact that phosphorylation of Tpr protein is modulated during the period of mitotic exit.

In the present study, we report the results of a comprehensive analysis of nucleoporin Tpr's role in modulating protein import/export, mRNA export and the export of unspliced RNA. We find that Tpr does not seem to play any significant role in regulating protein import /export and mRNA export. However, it plays a definitive role in modulating CTE- mediated export of intron-containing RNA. Depletion of Tpr results in the enhancement of CTE function ensuring an increase in the export of Gag/Pol-CTE RNA, thus leading to a subsequent proportional rise in the Gag/Pol protein levels. Our data indicates that Tpr is a novel modulator of unspliced RNA export in mammalian cells, and its function is independent of those proteins which are known to promote CTE- mediated export of unspliced RNA. The results of our study clearly establish the importance of Tpr's localization at the NPC in facilitating the regulation of export of unspliced RNA in mammalian cells. In addition, we also identified novel *in vivo* ERK2 independent phosphorylation sites on Tpr protein. We demonstrated one of the residues on Tpr protein is phosphorylated by Protein Kinase A. Phosphospecific antibodies were raised against these residues and they were found to be

specific to the phosphorylated form of the protein. Results also indicate that that Tpr protein levels and its ERK2 independent phosphorylation is regulated during the cell cycle.

CHAPTER-I

Review Of Literature

In eukaryotes, the spatial sequestration of the genetic material in the nucleus from the cytoplasm is achieved by the presence of the physical barrier called the nuclear envelope (NE). The nuclear envelope comprises of concentric double lipid bilayers, the inner nuclear membrane (INM) and the outer nuclear membrane (ONM). The INM is enriched with integral membrane proteins that interact with nuclear lamina and the chromatin [37], whereas, the ONM is in continuation with the endoplasmic reticulum and is studded with ribosomes[38]. At certain junctures, the INM and the ONM fuse to form the nuclear pores which are spanned by large, complex proteinaceous structures called the nucleopore complexes (NPC). These embedded NPC's constitute the aqueous transport channels that mediate macromolecular exchange between the nucleus and the cytoplasm. In the plane of the nuclear envelope, NPC's form an eight-fold symmetrical framework surrounding a central channel. A single NPC exhibits complex molecular architecture and is comprised of ~30 different proteins called nucleoporins. These nucleoporins are modularly arranged as subcomplexes within the NPC which provide shape and structure to the NPC and also mediate several critical cellular functions. The NPC while maintaining a highly selective permeability barrier, functions in the bidirectional transport of diverse macromolecules. Once the cargo is transported, the NPC ensures that they are retained in their respective nuclear and the cytoplasmic compartments. The integrity of the NE is maintained throughout the interphase while the maintainence, turnover and the repair of the NPC's occurs in the cell. Besides playing a significant role in the nucleocytoplasmic shuttling, the NPC and its components also function in diverse cellular processes such as gene activation and cell cycle regulation.

1.1. Structure of Nucleopore Complex

The NPC is a huge macromolecular assembly with a mass of 40 and 60 MDa in yeast and vertebrates, respectively [39, 40]. Despite the difference in size, the basic architecture of the NPC is conserved between yeast and metazoa. The overall structure of the NPC can be divided into three basic components: the nuclear basket, the central core, and the cytoplasmic fibrils. Electron microscopy, and in particular cryo-electron tomography provided useful insights to decipher the entire molecular architecture of the NPCs at high resolution. The nucleopore complexes observed under the electron microscope

appear as the cylindrical formations that span the nuclear envelope which have a diameter of ~1,000 °A [41] and demonstrate an eight-fold axial symmetry. NPCs embedded in nuclear envelopes have two coaxial rings, one on the cytoplasmic periphery and the other on the nuclear periphery with eight elongated structures termed spokes connecting the two rings [42-44]. Attached to the symmetric central core are filamentous structures extending to the cytoplasm and a basket-like structure on the nucleoplasmic side, both of which provide binding sites for the cargo [42, 45-47]. The structural proteins making up the bulk of the spokes and rings give shape and strength to the pore complex (Fig. 1). These structural core proteins which support the central channel of the NPC, help in maintaining the stability of the nuclear envelope and also mediate the juxtapositioning of the the inner and outer NE membranes. The inner rings, are comprised of the Nup170 complex (yeast) or Nup155 complex (vertebrates) [48-50] (Fig. 1). The inner rings are sandwiched between the outer rings, which are comprised of the Nup84 complex (yeast) or Nup107 complex (vertebrates) [51-55]. Together, these complexes form a scaffold that supports the curved surface of the pore membrane and help in forming the central channel of the NPC through which macromolecular transport occurs [56, 57]. Nups in the core scaffold represent roughly half the mass of the whole NPC and are composed almost entirely of either β-propeller folds, α-solenoid folds, or a distinct positioning of both in an amino-terminal β-propeller followed by a carboxy-terminal α-solenoid fold. The core scaffold is well conserved and the basic fold composition is preserved in all eukaryotes [58-60]. The framework of the NPC serves two major purposes: one, to maintain the selective permeability barrier within the pore, and second, to facilitate the selective transport of macromolecules across it. Both these crucial physiological processes are dependent on the correct arrangement of the key nucleoporins in the NPC architecture [61-63]. Attached to the inner phase of the NPC scaffold, facing the central channel, are groups of nucleoporins termed "linker nucleoporins" which provide attachment sites for the last group of nucleoporins namely the "FG nups" [57] (Fig. 1). These FG Nups, named for their phenylalanine-glycine repeats, are the direct mediators of nucleocytoplasmic transport [61-63]. The outer luminal ring in the NE lumen is formed by a set of integral membrane proteins and is connected to the core of the NPC scaffold, which assists in anchoring the NPC to the nuclear envelope. [56, 57, 64] (Fig. 1).
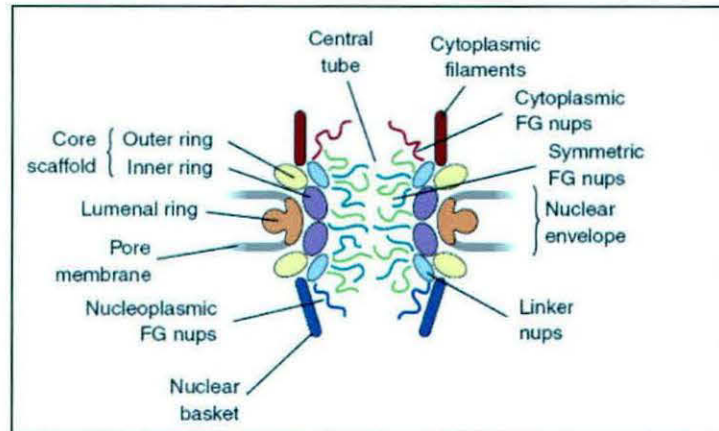
Fig 1.1: Structure of The Nucleopore complex [Source : Wente and Rout et al., 2011 [65]]

1.2. Nucleoporins

The NPC which is a very large ~60-125 MDa structure composed of a set of approximately 30 different proteins, collectively termed nucleoporins. The nucleoporins are conserved and form sub-complexes with defined composition and localization along the pore [39, 40, 60, 66, 67]. Each nucleoporin occurs in multiple copies, resulting in ~500 – 1,000 protein molecules in the fully assembled NPC. Most nucleoporins are denoted "Nup" followed by a number that in most cases refers to their molecular weight. Because of the molecular mass differences in various species, a uniform nomenclature for nucleoporins does not exist. However, based on their approximate localization within the NPC, the nucleoporins can be classified into the following six categories: (a) integral membrane proteins of the pore membrane domain of the nuclear envelope (POMs), (b) membrane apposed coat nucleoporins, (c) adaptor nucleoporins, (d) channel nucleoporins, (e) nuclear basket nucleoporins, and (f) cytoplasmic filament nucleoporins (Figure 2) [68]. Homology modeling suggests that nucleoporins are primarily constructed from one or more of the following structural units: α -helical regions, β -propellers, and unstructured phenylalanine-glycine (FG) repeats. Nucleoporins with conserved FXFG (phenylalanine and glycine) repeats in their sequence play a significant role in mediating nucleocytoplasmic transport by providing an interaction interface that aids in the translocation of receptor–cargo complexes through the NPC [69, 70]. Members of the karyopherin/importin superfamily, the mRNA

export receptor Mex67/Mtr2, and the Ran transporter Ntf2, have been shown to specifically interact with FG Nups [71, 72].

Symmetric nucleoporins			Asymmetric nucleoporins		
	Yeast	Human		Yeast	Human
Coat nucleoporins	Seh1	Seh1	**mRNA export**	Dbp5	Ddx19
	Nup85	Nup75		Gle1	Gle1
	Nup120	Nup160			
	Sec13	Sec13	**Cytoplasmic filaments**	---	Nup358
	Nup145C	Nup96		Nup82	Nup88
	Nup84	Nup107		Nup159	Nup214
	Nup133	Nup133		Nup42	CG1
	---	Nup37		Gle2	Rae1
	---	Nup43		Nup116	
Adaptor nucleoporins	Nic96	Nup93		Nup100 }	Nup98
	Nup192	Nup205		Nup145N	
	Nup188	Nup188		---	ALADIN
	Nup157 }	Nup155	**Nuclear basket**	Nup1	Nup153
	Nup170			Nup2	Nup50
	Nup53 }	Nup35		Mlp1 }	TPR
	Nup59			Mlp2	
Channel nucleoporins	Nsp1	Nup62		Nup60	---
	Nup57	Nup54			
	Nup49 {	Nup58			
		Nup45			
POMs	NDC1	NDC1			
	POM34	---			
	POM152	---			
	---	Gp210			
	---	POM121			

Fig. 1.2: The composition of the Human and Yeast Nucleopore complexes
[Source: Hoelz et al., 2011 [73]]

Fluorescence based experiments to determine the NPC residence times revealed that some Nups are dynamic in nature while the others are very stable at the NPC. In a pioneering study, 19 nucleoporins tagged with green fluorescent protein (GFP) were analyzed by inverse fluorescence recovery after photobleaching (iFRAP) and the rate of dissociation of at the NPC were calculated [74]. Based on the dynamics of nucleoporins at the NPC, they were classified into three classes: (a) Scaffold nucleoporins - which are very stable NPC proteins and had very low dissociation rates, (b) Dynamic

nucleoporins – which were highly mobile and had high dissociation rates, and (c) Adaptor nucleoporins – these were mobile and had dissociation rates intermediate between the scaffold and the dynamic nucleoporins (Table 1).

	Vertebrate Nups and Nup Subcomplexes[a]	Yeast Nups and Nup Subcomplexes[a]	Order of Assembly[b]	Dynamics[c]	Structural Folds[d]	Predicted Function(s)
Cytoplasmic Face	Nup358	–	Early	ND	FG	Structural and transport
	Nup214	Nup159	Middle	Stable	Bp, CC, FG	Structural
	CG1	Nup42	ND	Intermediate	FG	Structural and transport
	Nup88	Nup82	Middle	Stable	Bp, CC	Structural
Symmetrically Distributed	Nup62 complex	Nsp1 complex	Middle	Intermediate	FG, CC	Structural and transport
	Nup107-160 complex	Nup84 complex	Early	Stable	Bp, As	Scaffold
	Nup93 complex	Nic96 complex	Early	Intermediate	Bp, As, FG	Structural and transport
	Rae1/Gle2	Gle2	ND	Dynamic	Bp	Transport
	Nup98	Nup100, Nup116 and Nup145N	ND	Dynamic	FG, Nup98 fold	Transport
Transmembrane	Pom121	–	Early	Stable	TMH, FG	Structural
	gp210	Pom152	Late	Dynamic	TMH	Transport
	Ndc1	Ndc1	ND	ND	TMH	Structural
	–	Pom34	ND	ND	TMH	Structural
Nuclear Face	Nup50/Npap60	Nup2	ND	Dynamic	FG	Transport
	Nup153	Nup1	Early	Dynamic	FG	Structural and transport
	–	Nup60	ND	Dynamic	FG	Transport
	TPR	Mlp1 and 2	Late	ND	CC	Structural and transport

Bp, β propeller; As, α solenoid; FG, FG repeat domains; CC, coiled coil; ND, not determined.
[a]The Nup components of the vertebrate (v) and yeast (y) NPC complexes are as described (Hetzer et al., 2005; Loiodice et al., 2004; Mansfeld et al., 2006; Schwartz, 2005), and subcomplex members are as follows:
vNup62 complex: Nup62, Nup58, Nup54, Nup45; yNsp1 complex: Nsp1, Nup57, Nup49; vNup107-160 complex: Nup160, Nup133, Nup107, Nup96, Nup75/85, Nup43, Nup37, Sec13, Seh1, ALADIN; yNup84 complex: Nup145C, Nup133, Nup120, Nup85, Nup84, Sec13, Seh1; vNup93 complex: Nup205, Nup188, Nup155, Nup93, Nup35/53; yNic96 complex: Nic96, Nup192, Nup188, Nup170, Nup157, Nup59, Nup53.
[b]Reviewed in Hetzer et al. (2005).
[c]Compiled from Griffis et al. (2002); Lindsay et al. (2002); Pritchard et al. (1999); Rabut et al. (2004).
[d]Devos et al. (2006) and references therein.

Table 1.1: A summary of Vertebrate and Yeast nucleoporin subcomplexes

[Source: Tran and Wente et al., 2006 [75]]

1.3. Life Cycle of the Nucleopore Complexes

1.3.1. Assembly

The formation or assembly of nucleoporecomplexes is very critical for the proliferation and the proper functioning of the cellular machinery. The biogenesis of the nucleopores occurs at two distinct phases during the cell cycle, first, during the post mitotic stage, when the nuclear envelope forms around the segregated daughter nuclei and second, during the interphase where the nuclear membrane expands and the pore number is doubled in order to prepare for the subsequent cell division [76]. Though the objective during both stages is the formation of pore complex, the mechanisms differ specifically with respect to the time taken and the order of events during the assembly [77,78].

1.3.1.1. Mitotic assembly

NPC assembly during mitosis occurs when the nuclear envelope forms around the chromatin of the two segregated daughter nuclei [76,79]. During this, the NPCs are rebuilt from the nucleopore subcomplexes that were disassembled into the cytoplasm during the start of mitosis. Studies in from mammalian cells and Xenopus egg extracts have shown that mitotic-NPC assembly is a highly organized step-wise process which begins with the recruitment of the scaffold Nup107–160 complex on chromatin [80]. This recruitment is mediated by the proteins like Elys/Mel-28 [81-84]. The interactions between the nucleoporins and their association with the chromatin is regulated by the ratio between importin-β and Ran-GTPase [80,85]. The sequestering of Nup107-160 complex, Elys/Mel-28 and other nucleoporins from the chromatin during the mitosis is mediated by importin-β [80,83]. The early step of the NPC assembly is the release of nucleoporins from importin-β which occurs due to the presence of Ran-GTP which is found highly concentrated around the chromatin. Subsequently, the chromatin bound Nup107-160 sub complex recruits other nucleoporins sequentially, the transmembrane nucleoporins followed by the peripheral nucleoporins [78,80].

1.3.1.2. Interphase assembly

During Interphase, the chromatin content is doubled and the nuclear membrane expands, which requires incorporation of new pores. The exact mechanism behind this assembly is still unclear. Recent studies revealed that Pom121 is initially recruited to

the sites where the INM and ONM are juxtaposed [86, 87] and then the Nup107–160 complex is incorporated. [77, 88, 89]. This is then followed by the assembly of newly synthesized nucleoporins present around the nuclear envelope.

1.3.2. Disassembly

The disassembly of the NPC's occurs concomitant to the breakdown of nuclear envelope at the initiation of mitosis. Several studies provided evidence that mitotic dependent phosphorylation of nucleoporins would trigger the disassembly, although the exact mechanism still remains unclear though few studies hypothesize that Ran-GTPase system may play a role [32, 33, 90-93]. The phosphorylation of the nucleoporins mediates the dissociation of subcomplexes from the pore and prevents their re–association. After the completion of mitosis, the nucleoporins are dephosphorylated and the complexes are assembled [80]. The synchronous disassembly process starts with the disassociation of basket nucleoporins followed by the release of complexes present in the cytoplasmic ring [94, 95]. The release of FG repeat nucleoporins to the cytosol results in the loss of selective permeability barrier which would aid the mitotic regulators present in the cytoplasm to access the nucleus.

1.4. Functions of the Nucleopore Complex

1.4.1. Maintainence of the permeability barrier

The Nucleopore complexes serve as the gatekeepers of the nucleus which regulate the traffic between the nuclear and cytosolic compartments. Ions and small molecules are allowed to pass through passive diffusion. The passage of cargo with a mass greater than 40 kDa requires active transport, which is mediated by transport receptors [96-98]. The natively unfolded FG-repeat containing nucleoporins are extended towards the central channel to form the diffusion barrier [63, 99]. Several models have been proposed to understand the mechanism underlying the NPC selectivity. The "virtual gate model" proposes that highly dense FG-Nups in the central channel of the NPC create an energetic barrier that prevents the passage of inert molecules [100]. The "Selective phase model" suggests that the FG-nucleoporins form a Gel like meshwork in the central channel which acts like a sieve and permits the free passage of molecules lesser than its pore size [101]. The "reduction of dimensionality model" predicts that the FG repeats

which extend from the nuclear basket region to the cytoplasmic fibrill region acts as a selective filter due to which the small molecules can diffuse through, and the larger cargo complexes with transport receptors bind to the FG repeats and are transported [102]. Due to the presence of unstructured FG repeats, the detailed characterization of the selective permeability barrier still remains unresolved.

1.4.2. Protein transport across the NPC

Although carrier-independent transport has been described for several proteins, most of the protein transport in or out of the nucleus is carried out by a family of conserved soluble factors known as karyopherins. In facilitated transport, importins and exportins recognize short peptide signals – either a nuclear localization signal (NLS) or a nuclear export signal (NES) on their cargoes and mediate either nuclear import or export. The karyopherin-cargo complex then binds to nucleoporins with phenylanine-glycine (FG) repeats, which provide a favourable environment for the passage of the complex [67, 103]. Directionality of transport is modulated by Ran, a small GTPase. GTP bound form of Ran, RanGTP is highly enriched in the nucleus due to the presence of exchange factor RanGEF (Ran-GDP-exchange factor) resulting in its dissociation from the importin-cargo complexes, which subsequently promotes the formation of cargo complexes with exportins [32]. The exportin CRM1, recognizes and transports proteins bearing a leucine-rich nuclear export signal [104-106]. CRM1 binds along with RanGTP to the cargo to form a trimeric complex NES-RanGTP-CRM1, which then translocates through the NPC. Release of the export substrates in the cytoplasmic face of the NPC is accomplished by the RanGTPase-activating protein (RanGAP) and RanBP1, which hydrolyzes RanGTP and dissociates the complex [39, 107].

1.4.3. Export of RNA through the NPC

The process of mRNA export in eukaryotes is a complex trafficking pathway as it is critical to ensure that a number of steps like transcription, splicing, and processing have been accomplished before mRNA is actually exported [108, 109]. The mRNAs are synthesised as pre-mRNAs in the nucleus by RNA polymerase (Pol II), which are further processed by capping at the 5' end, splicing of introns and the polyadenylation at the 3' end. During these steps, several RNA binding proteins, splicing and processing

factors bind to the mRNA and form a structure known as the mRNP (ribonucleoparicle) complex, due to which the identification of the export signal on the mRNA by the export machinery becomes excessively difficult. Importantly the export factors must have the capability to distinguish between a pre-mRNA and a mature processed mRNA. Therefore, the mRNA export occurs through an independent mechanism that does not involve karyopherins and Ran proteins. Of the many proteins that bind to the mature mRNA, the binding of proteins TAP:p15 or NXF1:NXT1 (Mex67:Mtr2 in yeast) marks the first step of transport which is the generation of a cargo:carrier complex. The tanslocation through the NPC is facilitated by the weak interactions of these proteins with FG-nucleoporins [71, 72]. Recent studies in budding yeast have demonstrated that the DEAD-box helicase Dbp5 facilitates removal of Mex67 after transport through the pores [110] and that the activation of Dbp5 ATPase is brought about by Gle1 and inositol hexaphosphate (IP6), which probably occurs when Dbp5 and Gle1 are bound to nucleoporins located at the cytoplasmic end of the NPC. In addition, preventing return of the mRNP to the nucleus and maintenance of transport directionality is also thought to be a function of Dbp5 which could act as a Brownian ratchet at the cytoplasmic phase of the NPC [111, 112]. The export of small nuclear RNA (snRNA), tRNA and ribosomal RNA is mediated by the exportins of the Karyopherin family and utilizes the RanGTP – Ran-GDP gradient [108].

1.4.4. Export of unspliced RNA from the nucleus

Conventionally in eukaryotes, unspliced mRNA is retained in the nucleus, and only the processed mRNA is allowed to be exported through the NPC. However, retroviruses developed mechanisms to overcome this regulation, thus enabling unspliced genomic RNA to be exported and finally packaged. These mechanisms can be classified into two types, Rev dependent and Rev independent. The Rev dependent pathway, employed by the Human Immuno deficiency Virus (HIV) utilizes retroviral Rev protein bound to Rev response element (RRE) present in the unspliced transcripts [113, 114]. Once bound to RRE, Rev recruits host cellular factors such as Exportin-1[115] and Sam68 to effect the export through NPC. Sam68 (Src associated in Mitosis 68) a member of STAR (Signal Transduction and Activation of RNA) family of proteins is functionally regulated by nuclear kinases Sik/BRK [116]. Sam68 is absolutely required for

Rev function, a single point mutation in the nuclear localization domain of Sam68 blocks RRE/Rev mediated export [30, 117, 118] and the experiments with knockdown of Sam68 by RNAi dramatically reduced the expression of two Rev-dependent reporter constructs [118].

In contrast, Mason Pfizer Monkey Virus (MMPV) utilizes Rev independent mechanism to export its unspliced RNA. This is mediated by a *cis* – acting element present in the unspliced transcript known as the Constitutive Transport Element (CTE) [119] which directly recruits host cellular factors such as Nxt1/p15 and Tap/Nxf1 [26-29]. These proteins are RNA export factors implicated in the transport of processed cellular mRNA [29]. The formation of Tap and Nxt heterodimers augments the binding of nucleoporins to Tap and results in its increased nucleocytoplasmic shuttling [120]. Association of Nxt1 to Tap-CTE mRNA increased the interaction of this mRNP complex to the NPC resulting in its efficient export [121]. Tap/Nxf1 and the Nxt1 proteins were also shown to promote polyribosome association of intron containing mRNA resulting in their efficient translation [27]. Sam68 was also shown to be important for CTE mediated export of retroviral RNA [122]. This protein was shown to enhance the cytoplasmic utilization of unspliced Gag/pol-CTE mRNA resulting in escalated Gag-Pol protein expression in the cytosol [28].

1.4.5. Transport independent functions of the NPC

In addition to mediating the nucleocytoplasmic transport, the NPC and its components are involved in diverse cellular functions, such as chromatin organization, replication coupled DNA repair, and regulation of gene expression [123-131]. Nucleopore complexes were shown to regulate the activity of the enzymes associated with sumoylation and desumoylation processes [132]. Studies have shown that Nup358 present in the cytoplasmic fibrils of the NPC is an active E3 ligase that is involved in the sumoylation reactions [133, 134]. A recent study demonstrated that Nup358 associates with the microtubules during the interphase and modulates their dynamics and thereby plays a role in the organization of the cytoskeleton [135]. Several nucleoporins like Nup153, Nup358 and gp210 were reported to function in the breakdown of nuclear membrane [136-138]. Nup155, Nup35 and Elys/Mel-28, and the transmembrane nucleoporins Pom121 and NDC1 were shown to play a role in the NE assembly [34, 137, 139-141]. The defects in

the NPC or its components are linked to a diverse set of diseases, including hematological neoplasms, heart arrhythmia, and primary biliary cirrhosis [142-144] which clearly implicates the significant role played by the NPC in cellular physiology.

1.4.6. Role of Nucleoporins in Mitosis

In the recent years, several studies shed light on the crucial role played by the components of the nucleopore complex during mitosis. Nup170p, a homolog of vertebrate Nup155 was the first nucleoporin that was demonstrated to play a role in chromosome segregation and kinetochore function [145]. Nup358 was shown to associate with the kinetochores through Crm1 and is essential for the assembly of kinetochores [138, 146]. Crm1 was also reported to target Nup358/RanGAP complex and the chromosomal passenger complex to the centromere region of the spindle [147, 148]. Nup107–160 complex that is targeted to kinetochores during mitosis, where it functions in spindle assembly and its interaction with γ-tubulin ring complex was shown to promote the association of microtubules and kinetochores [149]. Elys and Nup153 were reported to play independent functions during cytokinesis [82, 150]. Rae1 was reported to play multiple roles in mitosis like the modulation of anaphase promoting complex, spindle assembly and was also shown to be required for the mitotic spindle checkpoint [151-154]. Recent studies have demonstrated that nucleoporin Tpr activates mitotic spindle checkpoint by interacting with Mad proteins [18] and its association with dynein complex was shown to be important for proper segregation of chromosomes during mitosis [19]. Nup153 was also reported to target the Mad proteins to the kinetochore and promote mitotic spindle checkpoint [155]. Nup98, functions in mitotic spindle assembly by interacting with the microtubules. This interaction was shown to inhibit a major regulatory molecule of microtubule dynamics, mitotic centromere-associated kinesin (MCAK) [156]. These reports clearly demonstrate active roles for the nucleoporins during mitosis but detailed understanding of the molecular mechanism underlying these assigned functions still remains to be elucidated.

1.5. Phosphorylation of Nucleoporins

In eukaryotic cells, one of the crucial steps for mitotic entry is the breakdown of nuclear envelope. Nucleoporins, the vital components of the nuclear envelope, are

phosphorylated in a cell cycle or DNA damage dependent manner. Many studies reported that nucleoporins are extensively phosphorylated during the mitosis and this mitotic-specific hyperphosphorylation was demonstrated both *in vitro* and *in vivo* [31-34, 90-92]. Mitotic phosphorylation of FG-Nups was shown to be critical for the organization of spindle microtubules and the chromosomes [157-160]. A recent report demonstrated that the phosphorylation of Nup98 by various cellular kinases was necessary for NPC disassembly during mitosis [161]. Cell cycle-dependent phosphorylation of Nup153 modified by O-linked *N*- acetyl glucosamine was reported, which was shown to be phosphorylated throughout the cell cycle and hyperphosphorylated during M phase [90]. Several reports demonstrate that Cdk1 phosphorylates multiple nucleoporins, which regulate diverse nucleoporin functions. A study using temperature-sensitive Cdk1 *Drosophila* embryos showed that Cdk1 activity is required for keeping NPCs dissociated during mitosis, while the reassembly may be phosphatase-dependent providing evidence that mitotic phosphorylation regulates the assembly of the NPC [162]. Cell-cycle-dependent phosphorylation of the main components of the Nup107–160 sub complex by Cdk1 regulates the association of the subcomplex with the NPC and other proteins [32]. It is thought that phosphorylation mediated by Ser/Thr kinase Cdk1 regulates the breakdown of the nuclear envelope at mitosis and the disassembly of the NPC into different subcomplexes [33, 162, 163]. Phosphorylation of Ran-GAP1 by Cdk1 regulates its interaction with Ran, a GTPase actively involved in nucleocytoplasmic shuttling [164]. Mitotic phosphorylation of Nup50 and other FG Nups by Cdk1 were implicated to function in the importin-β mediated spindle assembly [165].

In addition to Cdk1, MAP kinase ERK2 was extensively reported to be involved in phosphorylating several nucleoporins. Nucleoporins Nup153 and Tpr interact directly with MAP kinase ERK2 [35, 98]. The phosphorylation of FG repeat containing nucleoporins Nup153 and Nup214 by ERK2 disrupts the interaction of these nucleoporins with importin- β and thus resulting in an inhibition of nuclear protein import [165]. In a previous study, we have identified Tpr as a substrate of MAP kinase ERK2 and identified the ERK2 mediated phosphorylation sites on Tpr [35, 36]. Tpr was suggested to act as an ERK2 scaffold at NPC, which in turn results in phosphorylation of proteins that interact with Tpr. Phosphorylation of Nup50 at Ser221 and S315 by ERK has been shown to be essential for ERK mediated inhibition of nuclear

translocation of impotin- β and transportin [165]. Though these studies provide evidence that ERK2 may be modulating several physiological functions at the NPC, the mechanism and the exact timing of these phosphorylation events or in regulation of nucleocytoplasmic transport has not yet been elucidated.

In addition to Cdk1 and ERK2, several other kinases such as mammalian protein kinase A (PKA), protein kinase C (PKC), the *S. cerevisiae* casein kinase and the *Aspergillus nidulands* Ser/Thr kinase NIMA have also been shown to phosphorylate NPC components [166, 167]. Phosphorylation of structural proteins of the nuclear pore complex also appears to be necessary for nuclear import [69, 168], and the kinases responsible for the phosphorylation may be cAMP-dependent protein kinase [169-171], protein kinase C [172], or both[169]. Nup214 has been shown to be phosphorylated by JNK after NGF deprivation of neurons [67]. However, the biological significance of JNK mediated phosphorylation has not been described.

Phosphorylation of NLS-binding proteins, which are part of the mobile import machinery was reported to be necessary for the nuclear import [72]. In *Saccharomyces cerevisiae*, a nuclear pore complex associated protein kinase has been shown to phosphorylate Srp1p, an NLS-binding protein essential for nuclear import [173]. The phosphorylation of RanBP3 by Ras-ERK-RSK and PI3K-Akt pathways demonstrated to modulate the Ran gradient and thereby regulating the nuclear transport [174]. Thus, reports published in the last decade suggest that the phosphorylation of FG-Nup's and non-FG Nups serves as a molecular hub for cellular signalling pathways and is important to mediate the functions like transcriptional regulation and cell cycle progression [175-177].

1.6. Nucleoporin Tpr

Nucleoporin Tpr, present at the nuclear phase of the NPC, was originally identified as the oncogenic activator of the met, raf, and trk protooncogenes [1-3]. Tpr is a large 270 kDa protein with a bipartite structure consisting of ~1600-residue α-helical coiled-coil N-terminal domain and ~800 amino acid highly acidic, unstructured carboxy terminus [4]. Cellular transformations and human tumors have been shown to occur due to the fusion of N-terminal residues of Tpr (residues 140-230) with the protein kinase domains of the protooncogenes met, raf, and trk [1-3]. Accumulation of the non-coiled

21
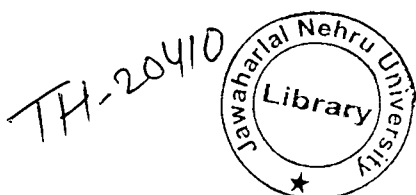
COOH terminus of Tpr in the nucleus suggested the presence of a nuclear localization signal (NLS) [16]. Tpr was reported to be imported to the nucleus by the importin α/β heterodimer [178]. Tpr localizes exclusively to intranuclear filaments associated with the nucleoplasmic side of the NPC, by directly binding to Nup153 [5-7].

Tpr and its yeast homologs Mlp proteins form homodimers via the large N-terminal α -helical coiled-coil domains [15, 179]. This domain also consists of a short sequence, essential for binding of recombinant Tpr to the NPC [179-181]. Amphibian NPCs reassembled from *Xenopus* egg extracts that had been immuno-depleted of Nup153, have been reported to be devoid not only of Nup153 but also other proteins, namely Nup93, Nup98, and Tpr [182]. Yeast two -hybrid analyses confirmed a specific interaction between Tpr and Nup153 that depends on the sequence integrity of Tpr's NPC Binding domain [183]. Site directed mutagensis of L458 and M489 residues of Tpr protein abolishes Tpr's ability to bind to the NPC but do not inhibit Tpr homodimerization [179]. These mutations abolished the binding of Tpr to Nup153 suggesting the importance of their interaction for the localization of Tpr at the NPC [7]. In a previous study we have identified Tpr as a substrate of MAP kinase ERK2 and identified the ERK2 mediated phosphorylation sites on Tpr [35, 36]. Tpr has been demonstrated to act as an ERK2 scaffold in NPC, in turn resulting in phosphorylation of proteins that interact with Tpr [36]. Tpr and its homologues in various species have been attributed several crucial functions in the cell.

1.6.1. Functions of Tpr and its homologs

1.6.1.1. Yeast homologs Mlp1 and Mlp2

While different metazoan species have been shown to contain only one Tpr ortholog, two homologs Mlp1 and Mlp2 are present in both *Saccharomyces cerevisiae* and *Schizosaccharomyces pombe*. Studies performed with the yeast homolog of Tpr, Mlp1 revealed a role for the protein in the nuclear retention of unspliced RNA [17]. Disruption of both *Mlp* genes is not lethal and does not affect any type of nucleocytoplasmic transport [15, 22]. The RNA binding proteins Yra1p and Nab2p have been shown to be essential for the docking of mRNP complexes near the Mlp export gate located at the nuclear membrane [184]. Null mutants showed increased sensitivity toward UV-induced DNA damage [15], an impairment in DNA double-strand break repair

and alterations in the spatial organization of telomeric heterochromatin [8]. Mlp2 was shown to promote spindle assembly by binding to the yeast spindle body [185]. These proteins have also been reported to function in the SUMOylation process by aiding the functional interaction of SUMO- protease Ulp1p with the nucleopore complex [132, 186].

1.6.1.2. Drosophila Ortholog of Tpr - Megator

Megator (Mtor/ Bx34 antigen), an ortholog of Tpr in *Drosophila* is an essential protein that localize to the nuclear interior [14]. Mtor has an extended coiled-coiled domain and during the mitosis, it localizes with the spindle matrix proteins Mad2 and Mps1[187]. Mtor plays a role in the recruitment of Mad2 and Mps1 proteins to the unattached kinetochores, which are critical for the progression of spindle check point and maintainence of normal mitotic duration [188]. Nup153 and Mtor have been shown to be essential for the transcriptional regulation of dosage-compensated genes [181]. Mtor and Nup153 bind to 25% of the regions in the *Drosophila* genome and play a pivotal role in coordinating dosage compensation and are also involved in the doubling of expression of the male X-chromosome [189].

1.6.1.3. Arabidopsis Homolog of Tpr – AtTpr

Arabidopsis homolog of TPR (AtTPR) is involved in various processes like maintaining the RNA homeostasis by functioning in the mRNA export pathway. AtTPR is a component in the nucleopore associated function of the Sumoylation process, and aids in regulating SUMO homeostasis in the cell [21]. Auxin signalling, flowering time and diverse aspects of plant development have been shown to be significantly affected in the AtTPR mutant plants [20, 21].

1.6.1.4. The Human Tpr protein

The functions of human Tpr include roles in intranuclear and nucleocytoplasmic transport and as a scaffolding element in the nuclear phase of the NPC [11-14]. Overexpression of Tpr has been shown to result in defective nuclear export and the nuclear import remained unaffected (Bangs et al., 1998). Further, it was demonstrated that ectopic expression of mammalian Tpr resulted in the accumulation of poly (A)$^+$ RNA in the nucleus [16]. Depletion of Tpr protein with the help of anti-Tpr antibodies

injection into the nuclei of the interphase cells resulted in inhibition of the nuclear export pathway [12, 15]. Especially, the export of proteins containing leucine rich nuclear export signal (NES) was shown to be affected by the depletion [12, 15]. In another study, the export Huntington protein, a protein with no apparent NES, has also been shown to be affected by the depletion of Tpr protein [12, 15]. In response to stress, Tpr interacts with HSF-1, a transcriptional factor for stress response genes, facilitating the export of stress induced Hsp-70 mRNA [22]. The published reports investigating the functional role of Tpr in the nucleocytoplasmic shuttling either address the question with the help of Tpr depletion using antibody or investigate its role in specific mRNA export or protein. However, global role played by nucleoporin Tpr in the nucleocytoplasmic transport of macromolecules has not been comprehensively investigated.

In the past decade, several studies demonstrated critical role played by components of NPC in orchestrating various stages of cell division. Some recent reports provide evidence of the pivotal role played by Tpr during mitosis. Spindle matrix proteins Mad1 and Mad2 interact with Tpr through its N- and C-terminal regions, respectively [18] and this interaction was demonstrated to be essential for localization of Mad proteins to NPC. Knockdown of Tpr resulted in inactive mitotic spindle checkpoint thus resulting in the formation of micronuclei and multinucleated cells after cell division [18]. Apart from Mad proteins, Tpr was also shown to associate with the Dynein light chain, which is a part of Dynein motor complex. The depletion of Dynein light chain caused the mislocalization of Tpr from the kinetochores resulting in abnormal chromosome segregation [19]. Prolonged Tpr depletion resulted in chromosome lagging and abnormal spindle polarity and had detrimental effects on the anaphase progression [19].

Apart from the suggested role of Tpr in the nucleocytoplasmic transport and mitosis, two recent reports established novel functions of Tpr at the NPC. Krull *et al* demonstrated a role for Tpr in the perinuclear hetero-chromation organization. Their results indicated that depletion of Tpr resulted in chromatin condensation all along the surface of the nuclear envelope and the disappearance of heterochromatin exclusion zones [190]. Tpr depletion was reported to result in a p53 dependent senesence-like phenotype due to its impact on the Crm1-dependent nuclear export pathway [191]. The partial co-depletion of Nup153 protein resulting upon Tpr knockdown was shown to

affect the SENP2 function at the NPC, thereby influencing the overall cellular SUMOylation [191].

These observations implicate critical roles for the human Tpr protein in modulating diverse functions. One of the objectives of the study is to delineate the precise role for nucleoporin Tpr in the macromolecular transport through the NPC. Previous data from the lab indicated that Tpr protein is phosphorylated in ERK2 dependent [36] and independent manner. The fact that nucleoporins are extensively phosphorylated during mitosis and the evidence of pivotal role for Tpr during the mitosis, led us to believe that phosphoryaltion of Tpr may have implications on the functional roles of Tpr. Second objective of the study is to identify ERK2 independent phosphorylation sites on Tpr and to determine the functional significance of these phosphorylations.

CHAPTER-II

Materials And Methods

2.1 Plasmid Constructs and siRNA Oligonucleotides

siRNA oligonucleotides (including Tpr-siRNA targeting 5'gcacaacaggataaggtta3' of the *tpr* gene) were purchased from either Dharmacon or Invitrogen. The construction of pcDNA3-FLAG plasmids expressing full-length Tpr (TprFL) and C-terminal region of Tpr (TprC), TprCM4, TprCM417 and Tpr-M4-Si have been reported previously (Vomastek et al., 2008). The Tpr-Si clone which is resistant to RNA interference by the Tpr-siRNA oligo was created by overlapping PCR. Various deletion constructs of Tpr, such as C-terminal deletion fragments of Tpr, Tpr-N, Tpr-M, Tpr-NM and Tpr-MC, were made using pcDNA3-Tpr-Si construct as template and specific forward and reverse primers, with Phu DNA polymerase (New England Biolabs). The amplicons were digested with NotI and ApaI and cloned into the corresponding sites on pcDNA3-FLAG. Tpr-L458P/M489P mutations were made by overlapping PCR using specific primers and the Tpr-Si clone as template. The amplicon was cloned into pENTR-Topo vector (Invitrogen). The BstEII- PmlI fragment from the pcDNA3-Tpr-Si plasmid clone was then subcloned into the BstEII-EcoRV sites of the pENTR-L458P/M489P plasmid construct. The full-length FLAG-Tpr-L458P/M489P was made by subcloning the NotI-PpuMI fragment from pENTR-TprN-L458P/M489P into the corresponding sites in FLAG-TprC. The TprC-M4-(S2046,2047,2049A), TprC-M4-(S2059A) and TprC-M4-(S2094A) constructs were generated by introducing the respective mutations by site directed mutagenesis by overlapping PCR using specific primers and subsequently cloning the amplicons into pcDNA3-FLAG vector at NotI-ApaI sites.

pCMV-GagPol-CTE, pCMV-GagPol-RRE and pCMV-β-Gal constructs were kindly provided by Dr. Marie-Louise Hammarskjold (University of Virginia), Dr. Hans-Georg Krausslich (University of Hamburg) and Dr. Sagar Sengupta (National Institute of Immunology) respectively. For the generation of Luc-CTE construct, the 5' Splice site (5'SS) region, and 3' Splice site with a part of Pol region (3'SS+Pol), were amplified by using specific adaptor primers, and pNL4.3-HIV DNA as template, (a gift from Dr. A.C.Banerjea, National Institute of Immunology). The luciferase gene was amplified from pCDNA3-luciferase plasmid kindly provided by Dr. Sudanshu Vrati (National Institute of Immunology), and the CTE region was amplified from pCMV-GagPol-CTE plasmid. The PCR products were then individually cloned into pENTR

entry vector. The full cassette was created by ligating the HindIII–KpnI fragment from pENTR-Luciferase, KpnI-EcoRV fragment from pENTR- 3'SS+ Pol and the EcoRV-XhoI fragment of pENTR-CTE, and subcloning into HindIII-XhoI sites of pENTR-5'SS vector to create the plasmid pENTR-Luc-CTE. The pcDNA3-Luc-CTE construct was then generated by cloning the NotI-XbaI fragment from pENTR-Luc-CTE into the corresponding sites in pcDNA3.1 vector. pcDNA3-FLAG-Rev was made by amplifying the coding region of Rev from pNL4.3-HIV and cloning it into pcDNA3-FLAG vector. HA tagged Tap and Nxt-1 clones were generated by amplifying the respective ORF's from the cDNA clones of Tap and Nxt-1 (Origene) and then cloning them into NotI and XbaI sites of pcDNA3-HA vector. The HA-Sam68 clone was purchased from Addgene. The CMV-PKA and the HA-Cdk1 plasmids were kindly provided by Dr. Pushkar Sharma (National Institute of Immunology).

2.2 Cell Culture and Transfection

HEK293T, COS-1 and HeLa cells were grown in DMEM supplemented with 10% fetal bovine serum (FBS). All transfections in HEK293T cells were performed in 6 well plates using calcium phosphate method. The transfections in HeLa, and COS-1 cells were performed by using Lipofectamine 2000 (Invitrogen) as per the manufacturer's recommendations. To analyze CTE- mediated export, cells were transfected with 250 ng pCMV-Gag/Pol-CTE, 100 ng pCMV- β-Gal and 1 μg of appropriate siRNA. In all the transfections, the final amount of plasmid DNA present in the transfection mix has been equalized by addition of appropriate amount of pCDNA3-FLAG vector. Cells were harvested 48 hours after transfection for further analysis unless mentioned otherwise.

2.3 Generation of Stable cell lines

FLAG-Tpr and FLAG-Tpr-Si stable cell lines were generated by transfecting the constructs into HEK293T cells using Lipofectamine 2000 (Invitrogen). Twenty four hours after transfection, 10^4 cells were plated in a 100 mm dish in medium containing 600 μg/ml Geneticin (Invitrogen), and incubated for 10 days. The colonies obtained were individually expanded and checked for expression of the introduced genes by

Western Blot and indirect immunofluorescence analysis using anti-FLAG antibodies (Sigma).

2.4 p24 ELISA and β-Galactosidase assay

Harvested cells were lysed with M2 Lysis buffer (50mM Tris-HCl, 150mM NaCl, 10% Glycerol, 1% Triton X-100, 0.5mM EGTA and 0.5mM EDTA) containing protease inhibitor cocktail (Roche). Lysates were clarified by high speed centrifugation. p24 expression levels were determined by sandwich ELISA using anti-mouse and anti-rabbit p24 monoclonal antibodies (obtained from AIDS Research and Reference Reagent program). β -Galactosidase (β-Gal) activity was assayed by incubating the lysate with 400 μg of o-nitrophenyl-β-D-galactopyranoside (ONPG) in Z buffer (40mM $Na_2HPO_4.7H_2O$, 60mM $NaH_2PO_4.H_2O$, 10mM KCl, 1mM $MgSO_4.7H_2O$) for 15 to 30 minutes and measuring absorbance at 420 nm. The p24 readings obtained from ELISA were then normalized with respect to β-Galactosidase readings. The data presented in the figures are average values obtained from three independent transfections; the error bars represent the standard deviation.

2.5 Antibodies and Immunoblotting

The mouse monoclonal antibody against Tpr (ab58344), anti-Nup153, anti-Nup98, anti-Nup214, anti-Sam68 and anti-Tap antibodies were from Abcam, anti-Nxt-1 and anti-cyclinA antibodies were from Santa Cruz Biotechnology. All the above mentioned primary antibodies were used at a dilution of 1: 5000. The anti-53BP1 antibody was kindly provided by Dr. Sagar Sengupta, anti-Erk2, anti-LaminA/C, anti-CREB, anti-PKA and anti-Tubulin antibodies were purchased from Cell Signalling Technology and used at a dilution of 1: 1000. Anti-Nup358 antibody was kindly provided by Dr. Jomon Joseph. All secondary antibodies (1:10,000 dilution) were obtained from Jackson Immuno Research Laboratories. The phospho specific antibodies (1: 1000 dilution) used in this study were custom generated from Phopho Solutions. Typically, 50 μg of the lysate were analyzed in Western Blot analysis after resolution on 10% SDS-PAGE. For the immunoblotting with the phospho specific antibodies, the membrane was blocked with 5% BSA in PBST for 2 hours followed by incubation with primary antibodies diluted in 1% BSA in PBST overnight at 4^0C and subsequently

followed by the incubation with the appropriate secondary antibody diluted in plain PBST for one hour.

2.6 Immunofluorescence

Immunofluorescence analysis was carried out with cells fixed with 4% paraformaldehyde, followed by permeabilization with 0.1% Triton X-100 for 10 minutes. Blocking was carried out with 10% normal chicken serum (NCS) at 4^0C (12 hours), followed by incubation with appropriate antibodies. For immunofluoresence, all the primary antibodies were used at a dilution of 1:100 and the secondary antibodies at a dilution of 1:250. Coverslips were mounted using mounting medium containing DAPI (Vectashield) and visualized with the help of Carl Zeiss Axiovision LSM 510 Meta confocal microscope.

2.7 Protein Transport Assay

The HeLa cell line stably expressing a chimeric Rev-GFP-Glucocorticoid Receptor protein (RGG) [23] was kindly provided by Dr. Jomon Joseph. Two 60 mm dishes of the above cells (8×10^5 cells /dish) were transfected with 4 µg of NS-siRNA or Tpr-siRNA. 24 hours post-transfection, cells were trypsinized and plated on to coverslips (10^5 cells/ coverslip) and allowed to recover for 24 hours. We monitored the import of chimeric GFP by fixing the cells with 4% paraformaldehyde at different times post dexamethasone treatment. To study nuclear export, the cells treated with 1 µM dexamethasone for 60 minutes were washed to remove the hormone, and were replenished with fresh medium for different time intervals, as indicated.

2.8 Analysis of mRNA export

An FITC-conjugated oligod(T) 23mer probe was procured from Integrated DNA Technologies (USA). Fluorescence in situ hybridization was performed with this probe to analyze poly (A)$^+$ mRNA export in HEK293T cells. 48 hours after siRNA transfection to induce Tpr knockdown, the cells (grown on coverslips) were fixed with 4 % paraformaldehyde and permeabilized with 0.2% Triton X-100. The cells were incubated in a moist chamber for 3 hours at 37°C with the hybridization mix containing 20X SSC, 50% dextran sulphate, 1µg/µl yeast tRNA and 1pmol/µl of the labelled

probe. Stringent post hybridization washes were done with 4X SSC and 0.1% Tween 20. Blocking was carried out with 10% normal chicken serum (NCS), followed by incubation with appropriate antibodies.

2.9 RNA Isolation and qRT-PCR

HEK293T cells were harvested 48 hours after transfection with either NS-siRNA or Tpr-siRNA. Cells were lysed in Hypotonic Lysis Buffer (20 mM HEPES-NaOH, 2mM EGTA and 2mM MgCl$_2$) for 10 min and subsequently centrifuged at 1200 r.p.m to sediment the nuclei and to obtain the cytoplasmic fraction as the supernatant. The nuclear pellet was washed once in the Cell fractionation buffer (PARIS Kit, Ambion). The Nuclear lysis and preparation of RNA from both cytosolic and nuclear extracts was performed using the PARIS kit according to manufacturer's recommendations. Synthesis of cDNA using an oligo (dT) primer was carried out by RETROscript Kit (Ambion). This cDNA was used for real time quantitative PCR analysis of Gag-Pol-CTE and *ERK2* (reference) genes using gene specific primers. The results obtained from real-time PCR data are represented as CT values, where CT is defined as the threshold cycle number at which there is a detection of amplified product. The average CT was calculated for both the target gene (Gag-Pol-CTE or Luc-CTE) and *ERK2* (Control) and the ΔCT was determined as (the mean of the triplicate CT values for the CTE gene) minus (the mean of the triplicate CT values for *ERK2*). The ΔΔCT represents the difference between the Tpr knockdown cells and Control cells, as calculated by the formula ΔΔCT = (ΔCT of Tpr Knockdown cells - ΔCT of control cells). The N-fold differential expression of the target gene (Gag-Pol-CTE or Luc-CTE) in Tpr depleted cells versus the control cells transfected with NS-siRNA, was expressed as $2^{-\Delta\Delta CT}$ [192].

2.10 Immunoprecipitation

100 mm dishes of COS-1 cells cells were transfected using Lipofectamine 2000 (Invitrogen) according to the manufacturer's recommendations. Cells were allowed to recover overnight, and transfected cells were then serum starved for 4 h and stimulated with epidermal growth factor (EGF) (20 ng/ml) for 10 min. The cells were washed once with cold PBS and then lysed with hypotonic lysis buffer at 4°C (20 mM HEPES pH

7.4, 2 mM EGTA, 2 mM MgCl$_2$, 200 mM sodium orthovandate, 2 mg/ml aprotinin, 0.4 mM microcystin and 2 mM phenylmethylsulphonyl flouride (PMSF). The lysate was clarified by centrifugation at 13,000 rpm in a microfuge for 20 min. and the immunoprecipitation of the lysates was carried out with anti-Flag Beads (Sigma) or anti-HA beads (sigma) for 2 h at 4^{0}C. After binding, the beads were washed thrice in Hypotonic Lysis Buffer and resuspended in 2× SDS-sample buffer. The samples were then boiled for 5 min and then were resolved on a 10% SDS-PAGE gel.

2.11 Metabolic Labelling

Dishes (100 mm) of COS-1 cells were transfected with 10 μg of FLAG-Tpr constructs and were allowed to recover overnight. Cells were washed twice with phosphate-free DMEM medium (GIBCO) and starved for 1 h in phosphate-free DMEM medium (GIBCO). Cultures were metabolically labeled in phosphate-free RPMI medium containing 3 mCi/ml carrier-free 32Pi (Perkin Elmer) for 3 h. For EGF-stimulated samples, EGF (20 ng/ml for 10 min) was added to the above medium.

2.12 Phosphopeptide Mapping

Metabolically labelled cells were lysed in M2 lysis buffer (50mM Tris-HCl, 150mM NaCl, 10% Glycerol, 1% TritonX-100, 0.5 mM EDTA, 0.5 mM EGTA, 40mM β-Glycerophosphate and 5mM Sodium pyrophosphate) followed by immunoprecipitation with anti FLAG M2 agarose beads. Immunoprecipitates were washed five times with M2 lysis buffer, resolved on 10% SDS-PAGE gels and transferred to nitrocellulose membranes followed by autoradiography. Bands corresponding to the labeled Tpr were excised, processed, and were digested with 1 μg of mass spectrometry grade Trypsin Gold (Promega). The peptides thus generated were then resolved on two dimensional thin layer cellulose plates. In the first dimension, the peptides were resolved based on their charge in pH 1.9 buffer (50 ml Formic acid, 156 ml Glacial acetic acid and 1794 ml deionized water) by electrophoresis. The plates were allowed to dry and the samples were resolved in the second dimension based on their R$_f$ in phospho-chromatography buffer (500ml of pyridine , 750 ml of n-butanol , 150 ml of glacial acetic acid and 600 ml of deionized water). The resolved radiolabelled phospho-peptides were then visualized as spots in the autoradiogram.

2.13 Phosphoaminoacid analysis

Metabolically labelled cells were lysed in M2 lysis busffer and immunoprecipitated as described above. Immunoprecipitated samples were resolved on 10% SDS-PAGE gels and transferred to PVDF membranes followed by autoradiography. Bands corresponding to the labeled Tpr were excised, and were subjected to complete hydrolysis using 6N HCl as described [36]. Hydrolysed aminoacid pellet was resuspended in 9 µl of pH 1.9 buffer and 2 µl phosphoaminnoacid standards (1 mg/ml each of pTyr, pThr and pSer). The samples were resolved by two dimensional thin layer chromatography using pH 1.9 buffer for the first dimension and pH 3.5 buffer (glacial acetic acid 100ml, pyridine 10 ml and deionized water 1890 ml) for the second dimension. Spots in the positions corresponding to phosphoaminoacid standards were visualized by ninhydrin staining (2% ninhydrin solution in acetone) and the radiolabelled spots were visualized by autoradiography. The phosphorylated aminoacids were determined by superimposing the autoradiogram to the ninhydrin stained TLC plate.

2.14 In vitro Kinase Assay

After transfection and immunoprecipitation as described above, the immunoprecipitated FLAG-TprFL, FLAG-TprC, and mutants of FLAG-TprC or the vector control were mixed with immunoprecipitated ERK2 or PKA proteins, and kinase reactions were performed in 25 mM HEPES (pH 7.4), 20 mM magnesium acetate, and 1mM dithiothreitol containing 10 µCi [γ-^{32}P]ATP (Perkin Elmer, Boston, MA), for 10 min at 30°C. The reactions were stopped by adding 4X SDS sample buffer followed by heating at 95°C for 5 min. Reactions were resolved on SDS-PAGE gels and were transferred on to nitrocellulose membrane. The membranes were then exposed to X-ray films for autoradiography.

2.15 Purification of C-terminal fragment of Tpr from E.Coli

Plasmid pQE2-TprC overexpressing carboxy terminal fragment of Tpr was transformed into *E. coli* BL21 (DE3) Codon Plus cells (Stratagene). Cultures were induced with 0.1 mM isopropyl 1-thio-β-D-galactopyranoside (IPTG) and further grown for 3 h at 37°C. Cells were harvested and lysed by sonication in lysis buffer (20

mM Tris-HCl (pH 7.5), 200 mM NaCl, and 10 mM β-mercaptoethanol). The cell lysates containing His fusion proteins were nutated with equilibrated Ni-NTA agarose (GE Healthcare) affinity resin. His tagged proteins were eluted with lysis buffer containing 50-200 mM imidazole. Peak fractions were dialysed against dialysis buffer (10 mM Tris-HCl pH 7.4, 50 mM NaCl and 20% glycerol).

2.16 Cell cycle synchronization experiments

HeLa cells were grown in 100 mm dishes and the cells were treated with 40 ng/ml of nocadazole. After 16 hours of nocadazole treatment, the cells were subjected to mitotic shake off and the mitotic cells were replated and released. Cells were harvested at various time points post replating to analyze the various stages of the cell cycle by Flow cytometry. The cells were also analyzed by western blot in order to assess the level of Tpr and the phosphorylation status during cell cycle.

2.17 Propidium Iodide staining and Analysis of Cells by Flow cytometry

The cells harvested after different time points of Nocadazole treatment and were fixed in 70% ethanol at 4°C with constant twirling for 16-18 hours. After fixation, the cells were washed thrice with PBS and the cell pellet was resuspended in approppriate amounts of propidium iodide (PI)/RNAse staining solution (BD Biosciences). After 15min of PI staining, the cells were analysed by Flow cytometry (BD FACS Calibur). The FACS analysis for the cells at different stages of cell cycle was done with the help of Cell Quest Software.

2.18 Micro Array Analysis

Total RNA was isolated from HEK293T cells transfected either with NS-Si or TSi using the Paris Kit (Ambion). Microarray was performed by Ocimum biosolutions as described below. RNA extracted from each sample was used as a starting template to synthesize double-stranded cDNA with random hexamers tagged with T7 promoter sequence. The fragmented DNA was labeled and used for overnight hybridization with Affymetrix Gene ST 1.0 arrays, followed by washing, staining and scanning. Microarray data was generated on two samples – TSi and NS-Si, each with two replicates, using Affymetrix Human Gene 1.0 ST Array chip. Data QC was performed

on arrays as recommended by Affymetrix, and RMA summarized data was subsequently analyzed for differential expression. The differentially expressed genes were subsequently evaluated for their biological relevance through Gene Ontology (GO) and Pathways analysis. The QC analysis was carried out using Affymetrix Expression Console (EC), and the statistical analysis was performed using R-programming language. The biological analysis was carried out using GenowizTM software.

CHAPTER-III

Functional Role of Tpr In The Nucleocytoplasmic Transport Of Macromolecules

3.1 Introduction

In the past few years, several groups have focused their research on the cellular functions of nucleoporins, including those, which localize to the nuclear basket region such as Tpr and Nup153. Tpr has been shown to activate mitotic spindle checkpoint [18] and its association with dynein complex was shown to be important for proper segregation of chromosomes during mitosis [19]. A recent study has shown that nucleoporin Tpr is important for establishing perinuclear heterochromatin exclusion zones [190]. These observations implicate a critical role for the human Tpr protein in modulating diverse functions. However, the role played by nucleoporin Tpr in the nucleocytoplasmic transport of macromolecules has not been comprehensively investigated. Studies performed with the yeast homolog of Tpr, Mlp1 reveals a role for the protein in the nuclear retention of unspliced RNA [17].

3.2 Results

3.2.1. Tpr does not play a significant role in cellular protein transport or in mRNA export

Nucleoporin Tpr has been reported to play a role in nuclear export of proteins containing leucine rich nuclear export signal, [12] and the ectopic expression of mammalian Tpr has also been reported to result in the accumulation of poly $(A)^+$ RNA in the nucleus [16]. We sought to comprehensively investigate the role of Tpr in nucleocytoplasmic transport of macromolecules. In order to examine the function of Tpr in cellular transport of proteins and nuclear export of mRNA, we depleted Tpr protein in HEK293T cells using three independent siRNA oligonucleotides (Fig. 3.1.A). When the levels of Tpr were analyzed 48 hours post transfection, diminution in Tpr levels could be seen with all three siRNA oligos (Fig. 3.1.B). Indirect immunofluorescence microscopy using mouse monoclonal anti-Tpr antibodies corroborated these findings (Fig. 3.1.C).

Love et al., [23] have established an exceedingly useful system to investigate import and export of proteins in HeLa cells. In these cells, chimeric Rev-Glucocorticoid-GFP Receptor protein (chimeric GFP) is localized to the cytosol in the absence of any treatment, and upon the addition of dexamethasone it translocates into the nucleus. Subsequent to the removal of dexamethasone, the chimeric GFP is exported
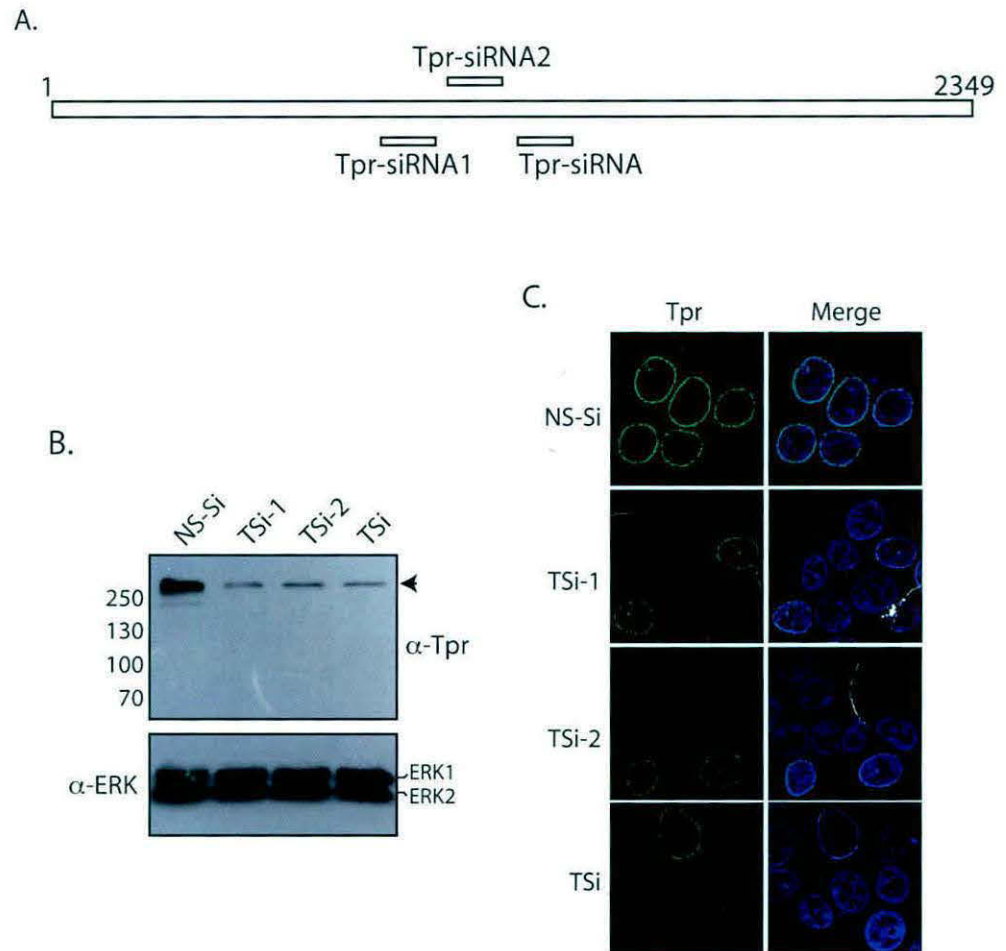
Figure 3.1. Tpr knockdown in HEK293T cells mediated by RNA interference. (A) Schematic representation of the regions of Tpr targeted by three independent siRNA oligonucleotides – Tpr-siRNA (TSi), Tpr-siRNA1 (TSi-1) and Tpr-siRNA2 (TSi-2). (B) Western blot analysis of whole cell extracts made from cells after 48 hours after treatment either with Non-specific siRNA (NS-Si) or three different Tpr siRNA's (TSi, TSi-1, TSi-2), probed with anti-Tpr and anti-ERK antibodies. (C) Immunofluorescence analysis of cells 48 hours after transfection with various Tpr siRNA oligonucleotides. Clear staining of nuclear membrane is seen in cells treated with NS-Si whereas only traces of staining is detected in cells where Tpr is knocked down.

back to the cytoplasm. Cells expressing this chimeric GFP protein were transfected with either the Non-Specific siRNA (NS-Si) or Tpr-siRNA (TSi) oligonucleotides and incubated for 48 hours to achieve the knockdown of Tpr protein (Fig. 3.2.A). When import of the chimeric GFP protein was investigated by incubating the cells with dexamethasone, import rates were observed to be similar for both NS-Si and TSi treated cells (Fig. 3.2.B), indicating absence of any role for Tpr in protein import. Subsequently, the export of the chimeric GFP-protein was visualized at different time intervals after the removal of dexamethasone. Interestingly, we observed slight, but reproducible, decrease in the rate of chimeric GFP protein export in the cells treated with TSi in comparison with those treated with NS-Si, at 30 and 60 min after washing off the drug/hormone. However, 2 h after the drug was removed, complete translocation of chimeric GFP to the cytosol was noticed in both cases (Fig. 3.2.C). These results indicate that Tpr may have a limited role in modulating the rate of protein export. To investigate the role of Tpr in export of processed poly $(A)^+$ mRNA, we knocked down Tpr expression (Fig. 3.3.A) and performed Fluorescence in situ hybridization using FITC tagged oligo (dT) probe (Fig. 3.3.B). The distribution of poly $(A)^+$ mRNA was found to be comparable in both control and in Tpr depleted cells (Fig. 3.3.B). Similar results were observed when in situ hybridization was performed 96 hours post siRNA transfection (Fig. 3.3.C & D). Based on these results, we conclude that Tpr does not play a role in translocation of proteins or poly $(A)^+$ mRNA across the nuclear membrane.

3.2.2. Tpr modulates CTE dependent export of unspliced RNA

Tpr homologs in *S.cerevisiae*, Mlp1 and Mlp2, were reported to play a role in export of unspliced RNA [17]. Towards analyzing the role of Tpr in the nucleocytoplasmic export of intron-containing RNA, we utilized well characterized Gag/Pol reporter constructs containing either a Rev response element (RRE) [3] or a constitutive transport element (CTE) [24-28]. These reporter constructs contain coding sequences of Gag/Pol proteins of HIV within an intron, followed by either RRE or CTE. We first examined the possibility of a role for Tpr in RRE-dependent export. Western blot analysis showed that when Tpr was indeed knocked down there was negligible variation in the Gag protein cleavage products p55, p41 and p24 (Fig. 3.4.A). The levels of Gag protein in the cytoplasm were quantified with the help of p24 ELISA, which
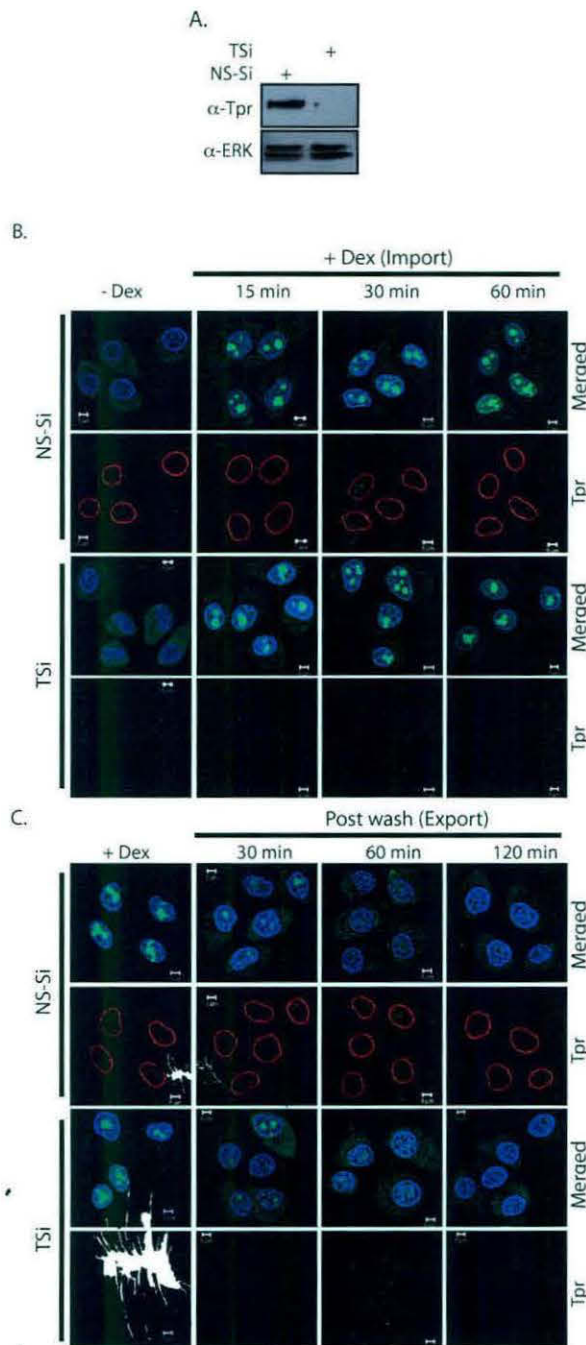
Figure 3.2. Depletion of Tpr has no significant effect on cellular protein transport.
(A) Western blot analysis of extracts of HeLa cells made 48 hours after treatment with TSi. (B) HeLa cells which stably express hormone responsive GFP reporter construct (RGG) were transfected with NS-Si or TSi. Import of chimeric GFP was monitored by fixing the cells with 4% paraformaldehyde at different times post dexamethasone treatment. (C) Export of RGG construct was tracked at indicated time points after removal of the hormone.
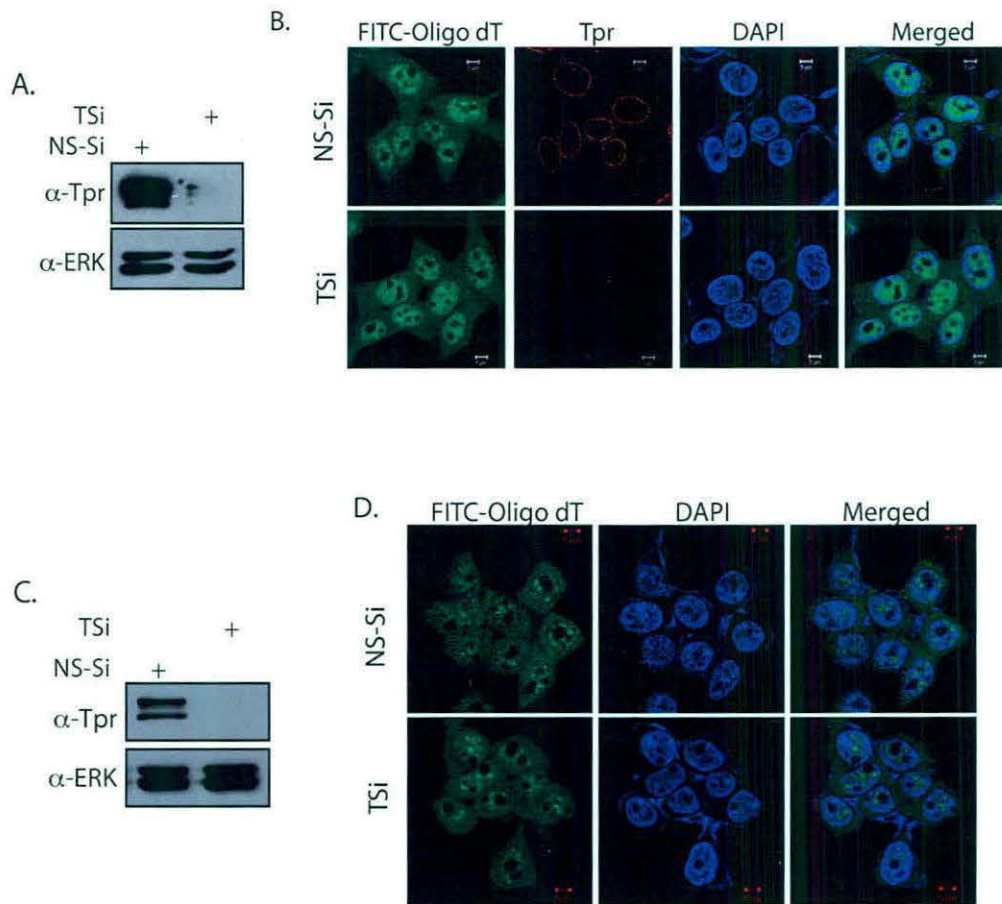
Figure 3.3. The distribution of poly(A)+ mRNA remains unaffected upon Tpr knockdown. (A) Western blot depicting Tpr knockdown in HEK293T cells after 48 hours after siRNA transfection. (B) Fluorescence in situ hybridization with FITC-oligo (dT) probe to assess distribution of poly(A)+ mRNA in HEK293T cells transfected with TSi. (C) Western blot depicting Tpr knockdown in HEK293T cells 96 hours after siRNA treatment was carried out. (D) Fluorescence in situ hybridization with FITC-oligo-d(T) probe to assess distribution of poly(A)+ mRNA in HEK293T cells 96 hours after siRNA transfection.
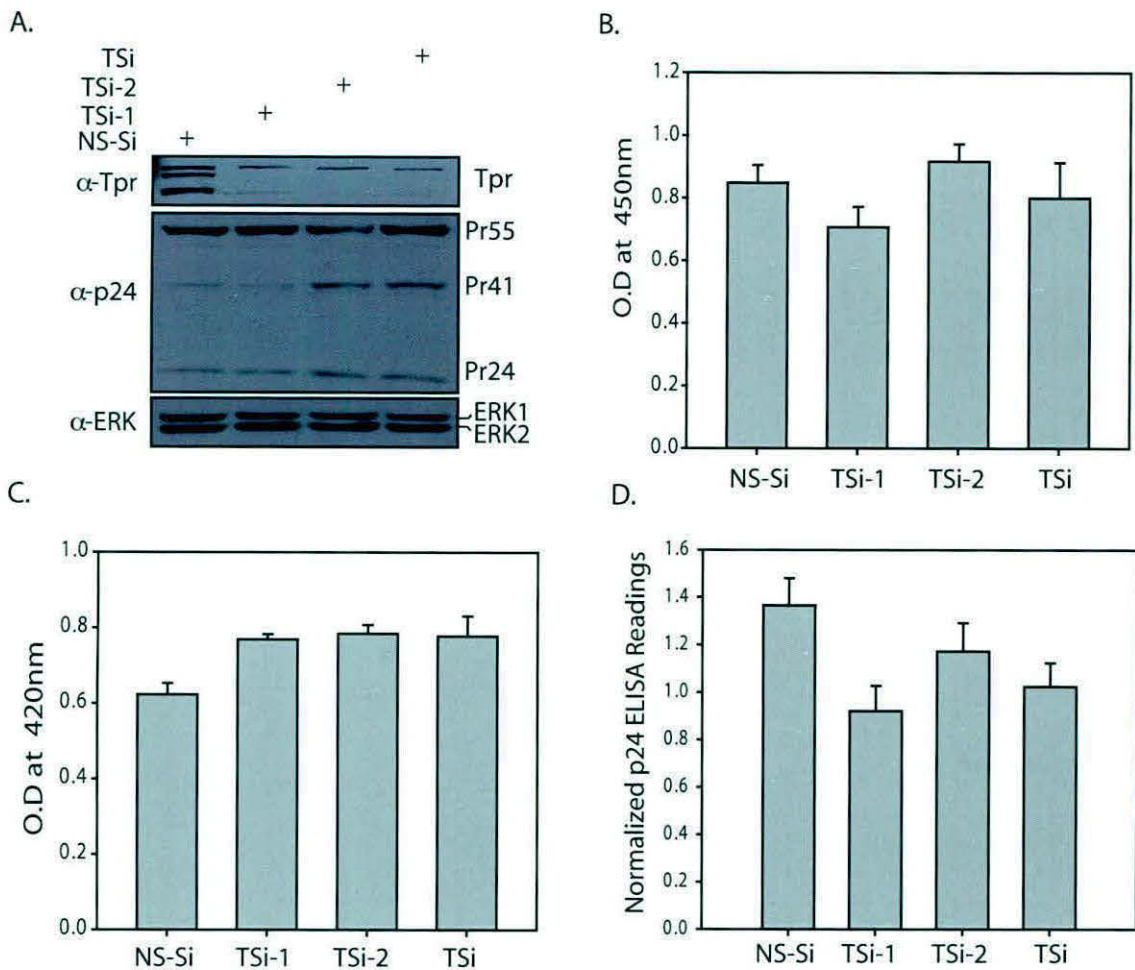
Figure 3.4. Role of Tpr in Rev dependent export of unspliced RNA. (A) HEK293T cells were transfected with either NS-Si or with different siRNA oligos against Tpr along with 100 ng of Gag/PR-RRE, 75 ng of pcDNA3-Flag-Rev and 100 ng of CMV- β-Gal constructs. 48 hours post transfection the lysates were resolved on SDS-PAGE, transferred on to nitrocellulose membrane and probed with anti-Tpr, anti-ERK and anti-p24 antibodies. (B) 48 hours later, the lysates were assayed for p24 expression. (C) β-Galactosidase levels in each of the samples were assayed. Bars represent the mean of values obtained and the error bars represent the standard deviation (s.d) of values obtained from three independent trans-fections. (D) The p24 values were then adjusted against variations in β-Gal readings and the normalized values are presented here. Average values of three independent transfections are presented; the error bars represent the standard deviation.
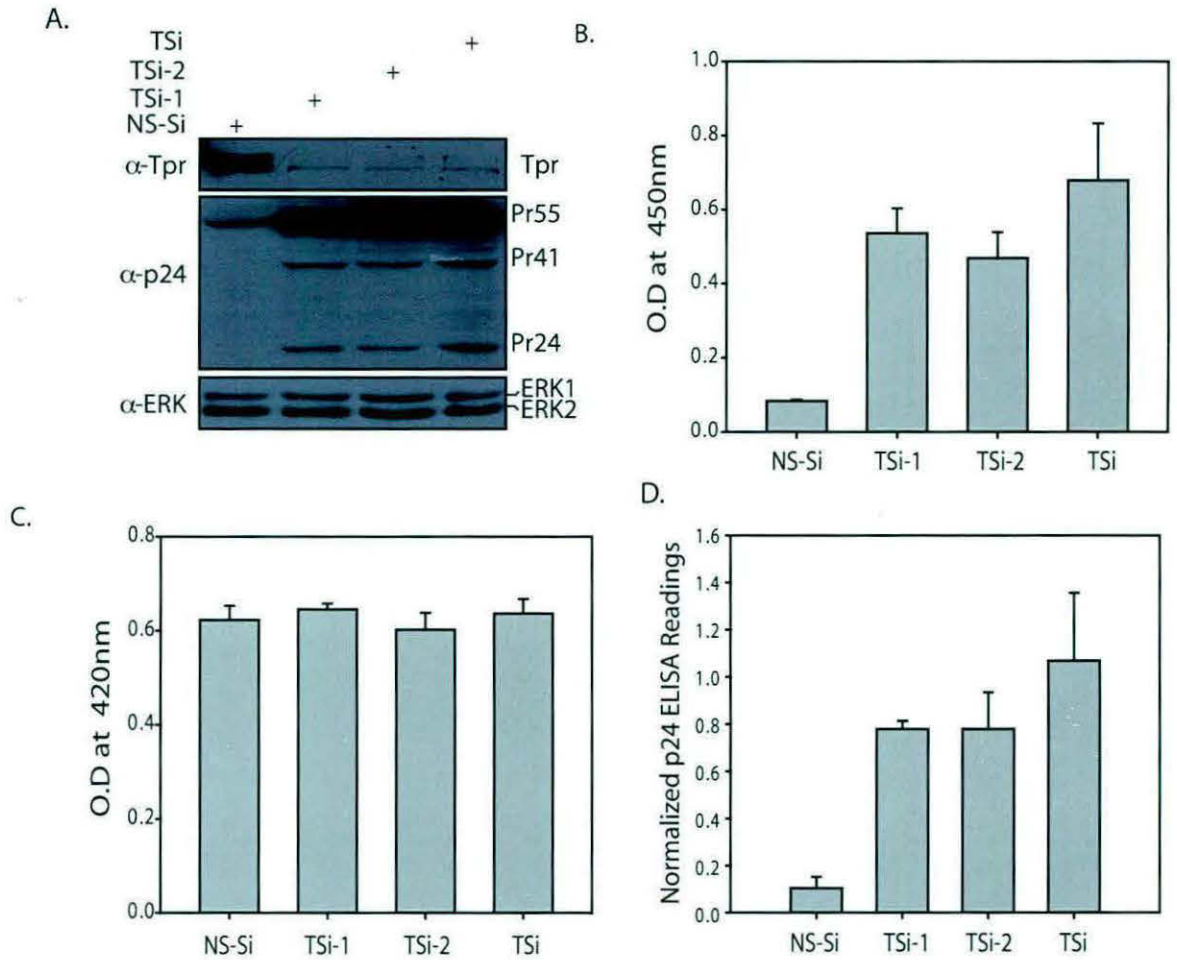
Figure 3.5. Elevated p24 levels resulting from enhanced CTE function are observed in Tpr knockdown cells. (A) Western blot of HEK293T cell extracts depicting elevated levels of Gag/pol protein cleavage products in cells transfected with Gag/Pol-CTE reporter construct, CMV- β-Gal and different Tpr siRNA's. (B) p24 ELISA readings of HEK293T cell extracts depicting elevated levels of Gag/Pol protein cleavage products in cells harvested 48 hours after transfection. (D) The β-Galactosidase activity is estimated in each of the samples. (D) Effect of Tpr knockdown on p24 expression from Gag/pol-CTE reporter as demonstrated by p24 ELISA readings after normalization against β-Galactosidase levels.
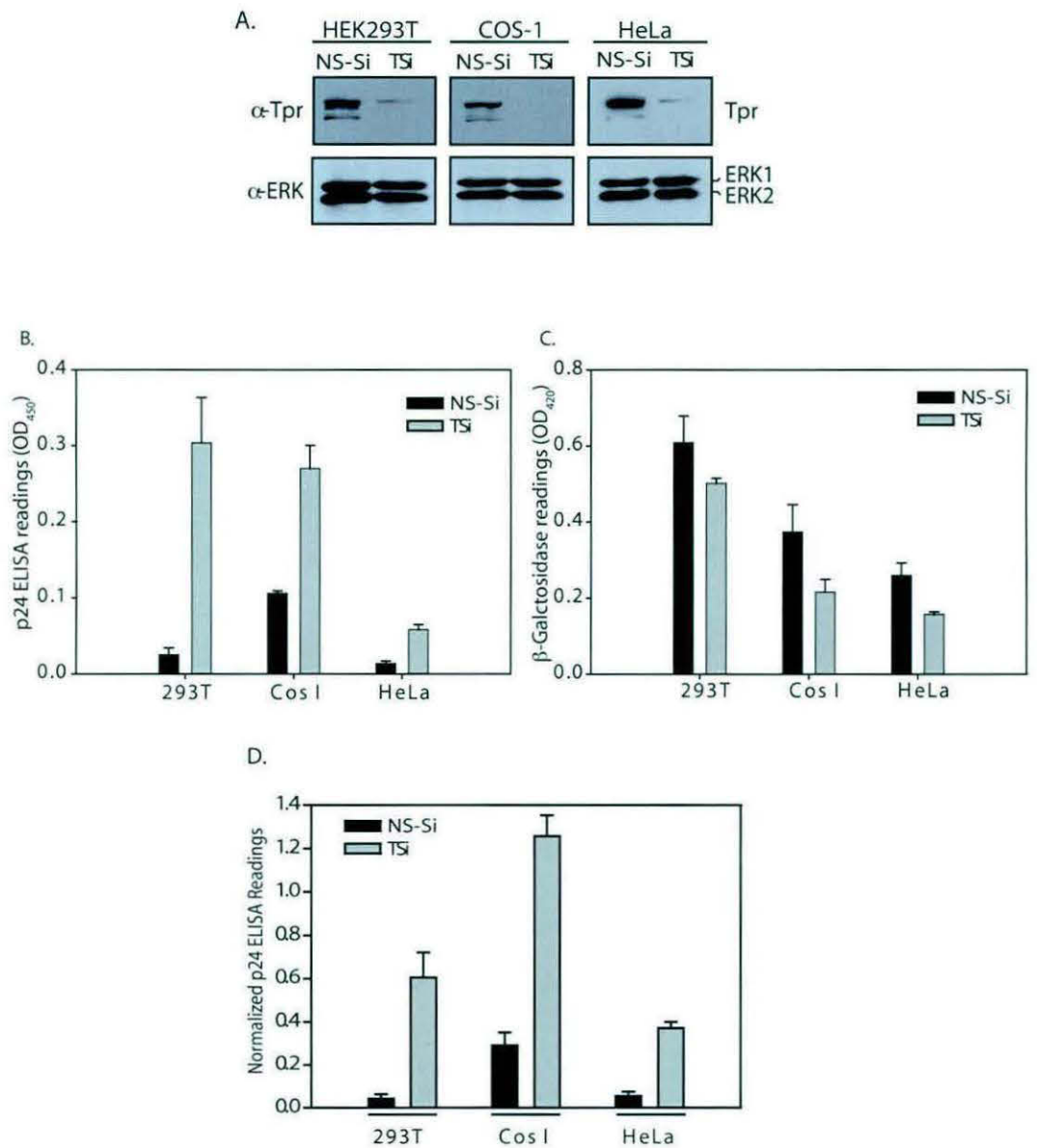
Figure 3.6. Depletion of mammalian Tpr significantly enhances CTE function. (A) HEK293T, COS-1 and HeLa cells were transfected with either NS-Si or TSi along with Gag/Pol-CTE reporter construct, and the lysates were probed with anti-Tpr, anti-ERK antibodies. (B&C) 48 hours after the transfection, the lysates were assayed for p24 (Panel B) and β-Gal expression (Panel C). (D) The p24 levels were normalized against the variations in the β-Gal readings. Bars represent the mean of values and the error bars represent the s.d. of values obtained from three independent transfections.
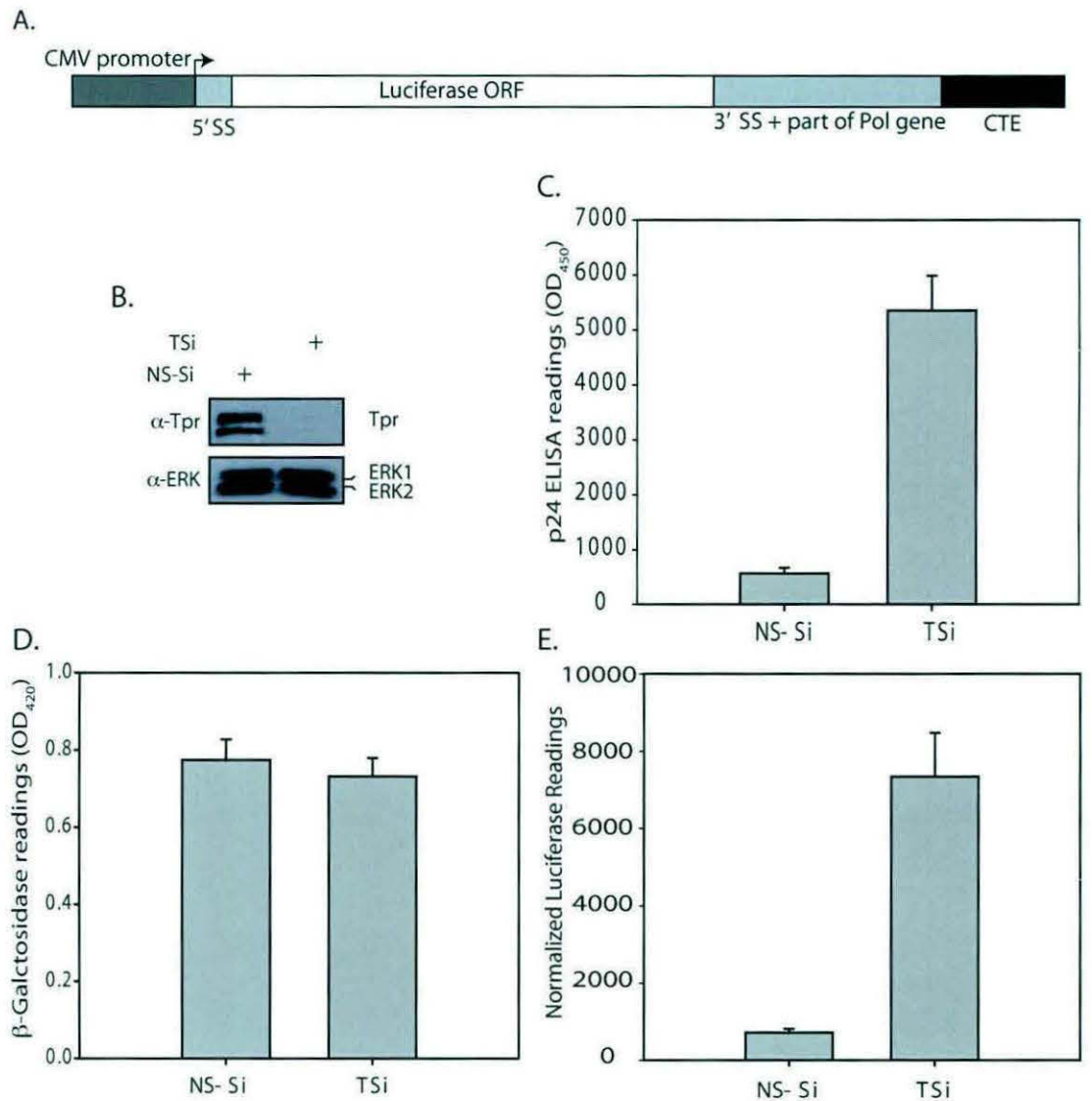
Figure 3.7. CTE dependent export in the presence of Luciferase based reporter construct. (A) Schematic representation of the Luciferase-CTE (Luc-CTE) reporter construct. (B) Western blot analysis of extracts of HEK293T cells co-transfected with NS-Si or TSi, CTE-Luc and CMV-β-Gal, to examine Tpr knockdown 48 hours after transfection. (C) The luciferase activity in the lysates was determined 48 hours post transfection. (D) β-Galactosidase levels in the samples was assayed. (E) The recorded luciferase activity in the samples was adjusted against variations in β-Gal readings. Bars represent the mean of values and the error bars represent the s.d. of values obtained from three independent transfections.

measures the amount of processed Gag protein (p24). It is apparent from the data presented (Fig. 3.4.B-D), that the levels of p24 in the extracts remained the same, irrespective of Tpr protein levels, indicating that Tpr does not play any role in RRE-Rev dependent export of unspliced RNA.

We then investigated the possible role of Tpr in regulating CTE-dependent export of unspliced RNA. Western blot analysis of extracts made from cells treated with Tpr siRNA showed that decrease in Tpr expression significantly increases levels of Gag protein cleavage products p55, p41 and p24 (Fig. 3.5.A). We observed an ~8-10 fold increase in the normalized p24 levels in the extracts prepared from TSi transfected cells compared with the NS-Si transfected cells (Fig. 3.5.B-D). Next, we sought to investigate if the phenomenon of Tpr mediated regulation of unspliced RNA export can be observed in cells other than HEK293T. Results demonstrated enhanced CTE function upon Tpr depletion in COS-1 and HeLa cell lines (Fig. 3.6.A-D). Though the fold increase in the export of unspliced RNA is different for different cell lines, the key finding that Tpr plays a role in retention of unspliced RNA in the nucleus could be consistently observed in all three cell lines. In order to rule out the possibility that the detected increase in nuclear export of reporter gene is limited to *gag/pol* gene, we created a Luciferase (Luc) reporter construct, in which the coding sequence of the *luc* gene was sandwiched between 5' and 3' splice site sequences originating from the HIV *gag/pol* gene followed by CTE (Fig. 3.7.A). As evident from Figure 4, diminution of Tpr levels (Fig. 3.7.B) resulted in ~6-8 fold increase in the normalized luciferase activity (Fig. 3.7.C-E). Taken together, these results suggest a regulatory role for Tpr in modulating CTE-dependent export of unspliced RNA.

3.2.3. Ectopic and stable expression of siRNA resistant Tpr rescues CTE mediated unspliced RNA export

To reinforce our findings we attempted to rescue the phenotype of increased export of unspliced RNA by co-transfecting cells with a plasmid containing siRNA-resistant *tpr* gene and TSi oligonucleotide. In order to generate an siRNA resistant Tpr clone, we have introduced silent point mutations into the wobble positions in the TSi's target sequence by overlapping PCR (Fig. 3.8.A). As expected, in the cells co-transfected with TSi and FLAG-Tpr construct the levels of the Tpr detected are similar to those observed in TSi transfected cells (Fig. 3.8.B; compare lane 4 with 2). However,
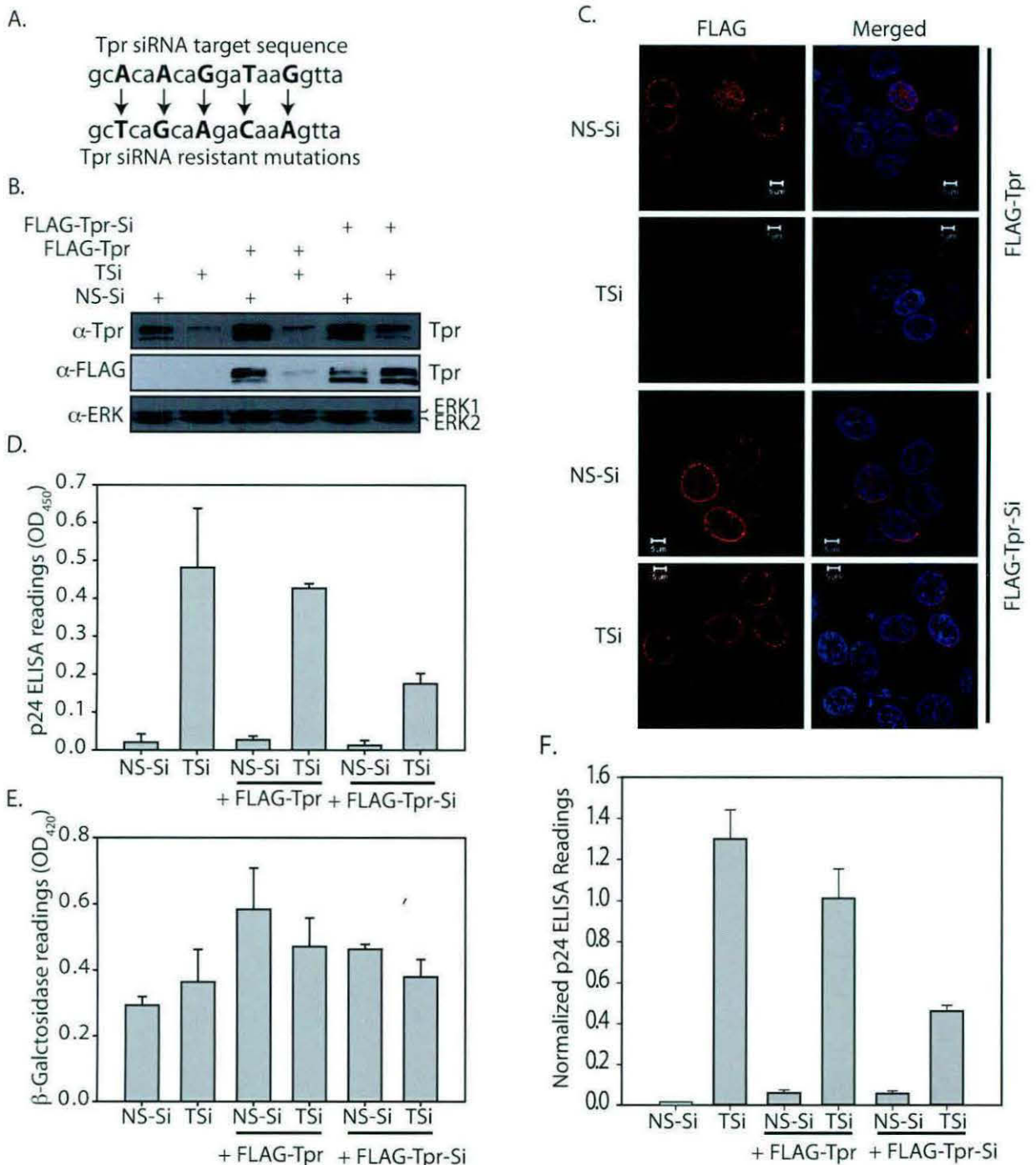
Figure 3.8. Reduction in p24 levels is observed upon rescue with siRNA resistant clone of Tpr. (A)
Schematic representation of the silent point mutations that were introduced into the nucleotide sequence
of Tpr, to protect it from being targeted by siRNA duplexes. (B) Immunoblot demonstrating the restora-
tion of Tpr levels upon co- transfection of FLAG-Tpr-Si construct with TSi. 2 μg of Flag-Tpr or Flag-
Tpr-Si were used for transfection. (C) Indirect immunofluorescence microscopy of HEK293T cells
transfected with Wild-type Flag-Tpr clone or siRNA resistant clone of Tpr along with NS-Si or TSi using
mouse monoclonal anti-Flag antibodies (D & E) The p24 expression (Panel D) and β-Galactosidase
levels (Panel E) in each of the samples were analyzed 48 hours post transfection. (F) The p24 values
were then adjusted against variations in β-Gal readings. Bars represent the mean of values and the error
bars represent the s.d. of values obtained from three independent transfections.

when the cells are co-transfected with TSi and FLAG-Tpr-Si construct, the Tpr levels detected were almost equivalent to control (Fig. 3.8.B; compare lane 6 with 1), indicating that the rescue plasmid is indeed resistant to siRNA. Indirect immunofluorescence microscopy using mouse monoclonal anti-Flag antibodies indicated that the efficiency of transfection is ~40-60% (Fig. 3.8.C). Similar to the results in Fig. 3.5, we observed significant increase in the levels of normalized p24 when the intracellular Tpr was knocked down using TSi, which predictably did not alter when the cells were co-transfected with FLAG-Tpr (Fig. 3.8.D-F). We observed an almost threefold reduction in the p24 levels when Tpr levels were restored by co-transfecting the cells with the siRNA resistant construct. However, even with repeated experimentation, the levels of the normalized p24 did not lower to control levels. This is most likely due to the fact that all Tpr knockdown cells do not express FLAG-Tpr-Si and the expression levels varied from cell to cell (Fig. 3.8.C). In order to address this problem, we generated HEK293T stable cell lines expressing either the wild-type FLAG-Tpr or FLAG-Tpr-Si. Indirect immunofluorescence data suggests similar and uniform expression of FLAG-Tpr and FLAG-Tpr-Si constructs (Fig. 3.9.B). Importantly, when the lysates were probed with FLAG antibodies we observed the expression levels of FLAG tagged Tpr in stably transfected cells to be almost equivalent (Fig. 3.9.A). The normalized p24 levels resulting from Tpr depletion in Flag-Tpr stable cell line were similar to those obtained with parental 293T cells (Fig. 3.9.C-E). When Flag-Tpr-Si stable cells were transfected with either NS-Si or TSi and Gag/Pol-CTE, we observed almost fourfold reduction in the p24 levels compared to FLAG-Tpr stable cell line (Fig. 3.9.C-E). These findings show that the regulation of CTE mediated p24 gene expression can be specifically attributed to the alterations of Tpr levels in HEK293T cells.

3.2.4. Tpr depletion enhances CTE mediated export of unspliced RNA from the nucleus

Increase in the normalized p24 levels can also be attributed to increased translation of *gag/pol* RNA in the cytosol. In order to ascertain if the Tpr dependent increase in the p24 protein levels is indeed due to the export of unspliced RNA, we performed quantitative real time PCR analysis. Nuclear and cytoplasmic fractionation was performed as described and RNA and protein fractions were prepared from the
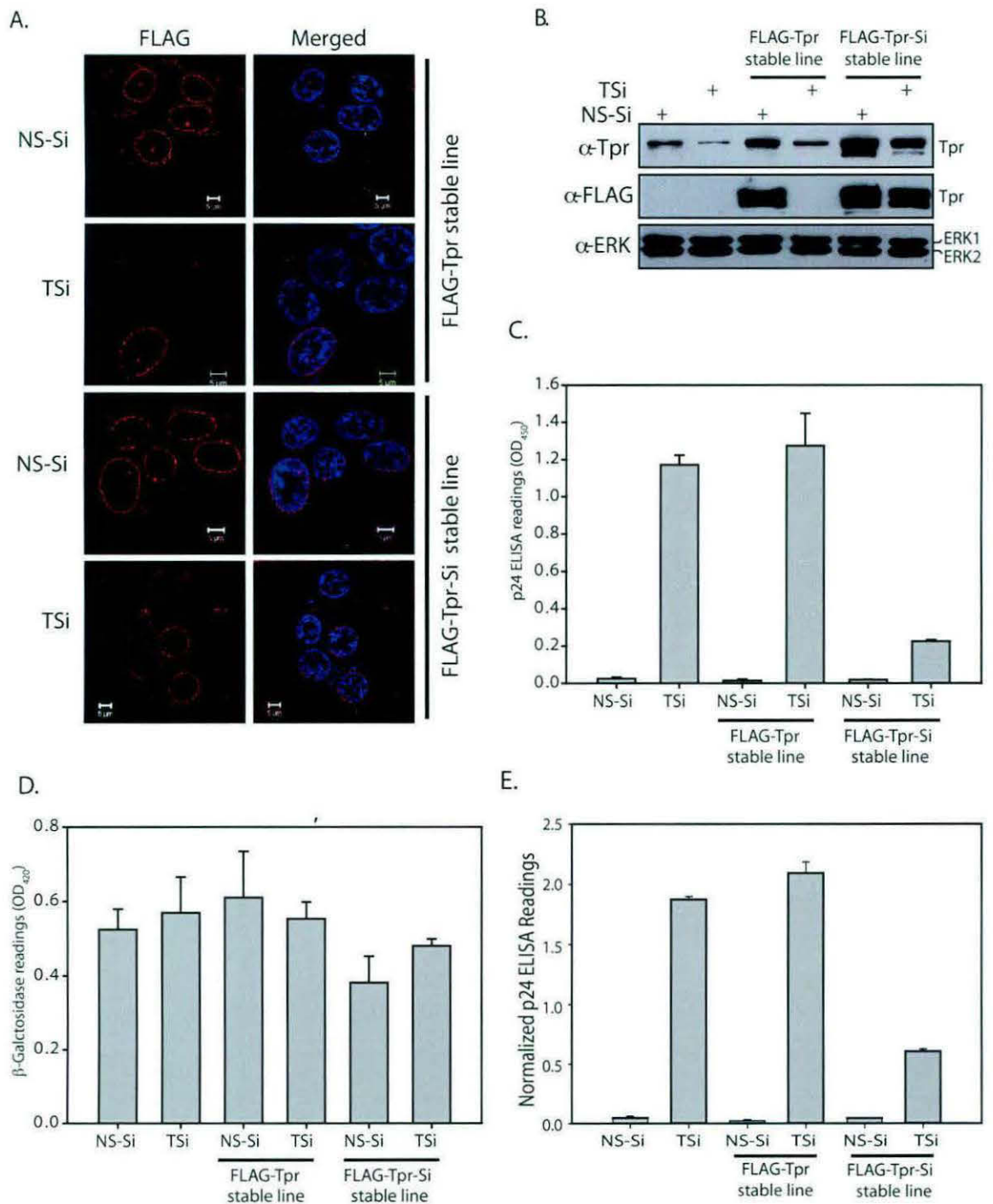
Figure 3.9. Stable expression of siRNA resistant Tpr rescues CTE mediated unspliced RNA export. (A) HEK293T cells stably expressing Flag-Tpr or Flag-Tpr-Si were transfected with either NS-Si or TSi together with Gag/Pol-CTE and CMV- β-Gal plasmids. Western blot of whole cell extracts probed with anti-Tpr, anti-FLAG and anti-ERK antibodies depicting stable expression. (B) Immunofluorescence analysis of Flag-Tpr or Flag-Tpr-Si stable cells after 2 days of transfection with either NS-Si or TSi oligonucleotides. (C&D) The cell lysates were assayed for p24 (Panel C) and β-Gal expression (Panel D). (E) The p24 levels were normalized against the variations in the β-Gal readings. Bars represent the mean of values and the error bars represent the s.d. of values obtained from three independent transfections.

extracts. Western blotting analysis (Fig. 3.10.A) clearly showed presence of Tpr in nuclear fraction and tubulin in the cytoplasmic fraction. Further, soluble nuclear proteins 53BP1, CyclinA and the nuclear marker Lamin could be detected only in the nuclear fraction indicating the fractions obtained were free of any contamination. Real time PCR analysis established that the cytoplasmic unspliced Gag/Pol-CTE RNA was significantly higher in the Tpr depleted cells compared with NS-Si treated cells, suggesting increased export of unspliced RNA transcripts (Fig. 3.10.B). Similar fold change in the nuclear and cytoplasmic mRNA levels was also observed in case of unspliced Luc-CTE RNA (Fig. 3.10.C). The increase in the cytoplasmic unspliced RNA levels is reflected in the proportionate increase in the p24 levels shown in Figures 3, 4, and 5, reinforcing the fact that Tpr regulates CTE-mediated export of intron containing mRNA. To our surprise, we found that nuclear CTE mRNA levels were also ~2-3 fold higher in the absence of Tpr (Fig. 3.10.B and 3.10.C). Yeast homologs of Tpr, the Mlp proteins have been shown to downregulate the expression of genes in response to the presence of aberrant RNA transcripts [184]. We speculate that the increase in the CTE-mRNA pools in the nucleus could be due to increased expression of the CTE-mRNA transcripts in Tpr depleted cells and/or increased stability of these transcripts in the nucleus when Tpr is knocked down. It is possible that in addition to regulating the export of unspliced RNA by causing them to be retained in the nucleus, Tpr may play a role in modulating the processing of mRNA molecules before the transcripts are actually exported

3.2.5. Tpr mediated regulation of unspliced RNA export is independent of Sam68 and Tap functions

Previous reports have demonstrated a critical role for Sam68 and Tap proteins in the enhancement of CTE function by increasing the stability and utilization of unspliced RNA [27, 28]. In an effort to understand the mechanism behind Tpr mediated regulation, we studied the effect of Sam68 and Tap depletion as well as overexpression on CTE mediated export in Tpr deficient cells. HEK293T cells were co-transfected with Gag/Pol-CTE and CMV- β-Gal reporter constructs along with NS-Si or TSi in combination with either Tap-siRNA or Sam68-siRNA and analyzed 96 hours after siRNA treatment in order to obtain efficient knockdowns. Western blot analysis of the lysates showed decrease in the protein levels of Tpr and Sam68 in the response to
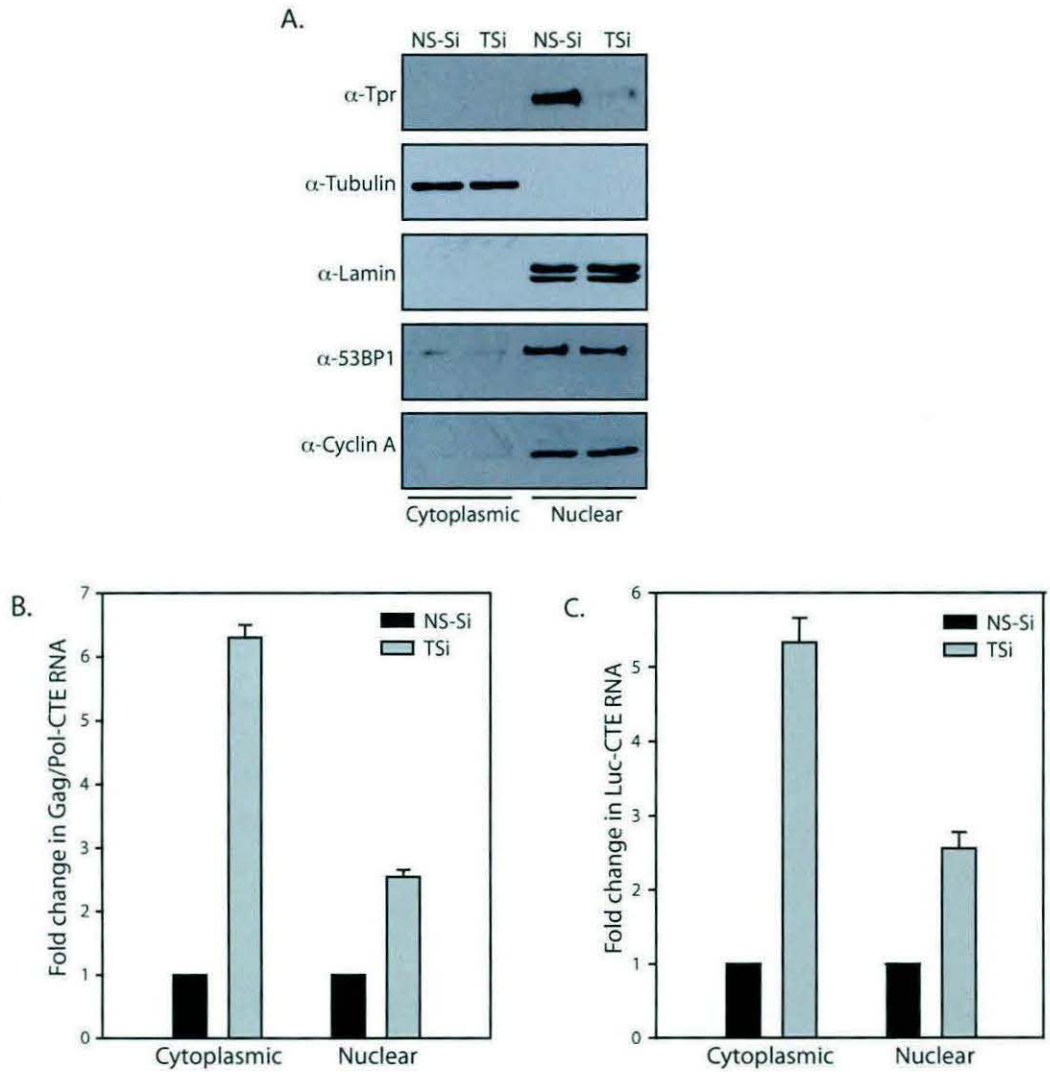
Figure 3.10. Tpr Depletion enhances CTE mediated unspliced RNA export from the nucleus. (A) Western blot analysis of cytosolic and nuclear fractions using anti-Tubulin, anti-Lamin, anti-Tpr, anti-53BP1 and anti-CyclinA antibodies. (B) Real-Time PCR analysis of mRNA isolated from nuclear and cytoplasmic fractions of HEK293T cells co-transfected with Gag/Pol-CTE construct and NS-Si or TSi. (C) Luc-CTE RNA levels in the nucleus and cytoplasm of cells transfected with pcDNA3-Luc-CTE construct and NS-Si or TSi measured by real time PCR.

treatment with their respective siRNA (Fig. 3.11.A). However, the depletion of Tap upon siRNA treatment was not very efficient (Fig. 3.11.A). Analysis of normalized p24 in the cells lysates showed that depletion of Tap or Sam68 by themselves do not greatly influence the export of unspliced RNA (Fig. 3.11.B-D). Interestingly, depletion of Tpr and Sam68 together resulted in decreased p24 in the cytosol. This may be due to the fact that Sam68 is known to be required for stabilization of unspliced RNA [30], which may have been compromised to an extent in its absence. Tap/Nxf1 has been shown to have an effect on the export of mRNA from the nucleus in various model systems [193-196]. Yet we did not observe noticeable decrease upon partial depletion of Tap either in p24 or β-GAL levels (Fig. 3.11.B & C). Differences between the earlier Tap siRNA studies and our results could be due to the differences in the efficiency of siRNA in knocking down the Tap expression, as the knockdown detected in our experiment is not as efficient as those presented in the earlier reports. In order to address this concern, we repeated the experiment including two additional siRNAs, one an alternate siRNA (Tap-siRNA-2) and the second, a pool of four different siRNAs (Tap-siRNA-SP), to deplete Tap/Nxf1 protein. While the knockdown obtained with Tap-siRNA was similar to our earlier observation, both Tap-siRNA-2 and Tap-siRNA-SP were quite effective in depleting Tap protein (Fig. 3.11.E). We also observed that the recovery of cells was lower after the treatment with the newer siRNAs compared to the cells transfected with Tap-siRNA. Consistent with the previous studies, when we depleted Tap with siRNA2 and siRNA-SP, we observed significant decrease in the β-galactosidase activity in the lysates (~50%; Fig. 3.11.F). Since the β-galactosidase activity was affected by the TAP depletion, we have not normalized the p24 readings. Interestingly, we did not detect substantial reduction in the p24 levels, indicating that the export of unspliced RNA seems to be independent of TAP depletion (Fig. 3.11.G).

Overexpression of Sam68 has been shown to enhance the stability and utilization of unspliced RNA, thus resulting in increased p24 levels [28]. Tap overexpression has been shown to improve the cytoplasmic utilization of Gag/Pol-CTE mRNA [27]. If Tpr depletion and Sam68 overexpression were to enhance the export in an inter-dependent manner, a combinatorial effect of depletion and overexpression would not be more than the independent effects. However, if they were to modulate the process independently, one would expect a cumulative effect. To address these two
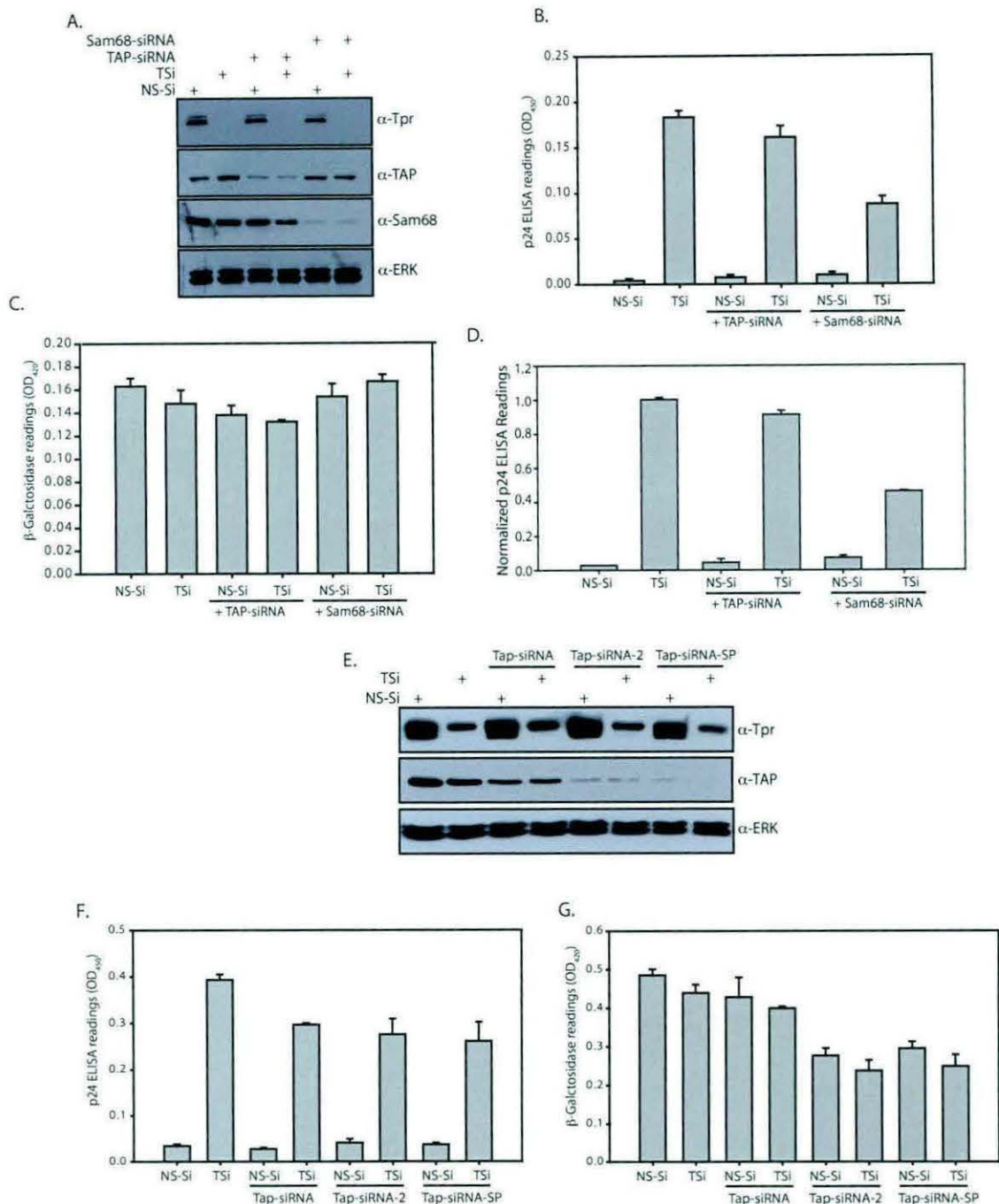
Figure 3.11. Tpr mediated regulation of unspliced RNA export is independent of Tap/Nxf1 and Sam68's functions. (A) Cells were transfected with 1 µg of siRNA against either Sam68 or Tap/Nxf1 along with NS-Si or TSi. The cells were replated the next day and 24 hours after replating, the cells were transfected once again with siRNA oligos and the reporter constructs. Western blot analysis of extracts of transfected HEK293T cells confirming the depletion of Tpr, Sam68 and Tap/Nxf1 proteins on treatment with respective siRNA's. (B & C) 48 hours after the second transfection, the amount of reporter gene expression from transfected Gag/Pol-CTE (Panel B) and CMV- β-Gal (Panel C) constructs was assayed. (D) The p24 ELISA readings obtained from the samples were adjusted against variations in the β-Galactosidase readings. (E) Cells were transfected with 1 µg of different siRNA oligos against Tap/Nxf1 along with NS-Si or TSi. The cells were replated the next day and 24 hours after replating, the cells were transfected once again with siRNA oligos and the reporter constructs. Western blot of extracts of transfected HEK293T cells to analyze the depletion of Tpr and Tap/Nxf1 proteins. (F & G) The amount of reporter gene expression from transfected CMV- β-Gal and Gag/Pol-CTE constructs were assayed.

51

possibilities, we overexpressed either HA-Sam68 or HA-Tap in the cells transfected with either NS-Si or TSi and measured the normalized p24 levels in the extracts. Western blot data depicted in Figure 3.12.A shows effective depletion of Tpr and overexpression of HA-Tap and HA-Sam68. In the samples where Tap or Sam68 were overexpressed in presence of NS-Si, we detected increase in the normalized p24 in the extracts as compared to NS-Si only (Fig. 3.12.D). Depletion of Tpr by itself had significant effect on p24 levels in the extract (Fig. 3.12.D). Interestingly, in the sample where Tap was overexpressed in the presence of TSi, we did not observe any further increase (Fig. 3.12.B-D). In contrast, when Sam68 was overexpressed in Tpr depleted cells, we observed a modest synergistic increase in the p24. Further, analysis of Gag/Pol-CTE RNA levels in these samples by quantitative real time PCR demonstrated the same trend (Fig. 3.12.E). Depletion of Tpr by itself increased the Gag/Pol RNA levels both in nucleus and cytoplasm, which did not substantially alter when Tap was overexpressed (Fig. 3.12.E). This is not very surprising as Tap is shown to improve the cytoplasmic utilization of Gag/Pol-CTE RNA, which can only happen after its export[27]. However, when Sam68 was overexpressed in Tpr depleted samples, we observed significant increase in the Gag/Pol RNA levels (Fig. 3.12.E), which was in turn reflected in increased p24 levels (Fig. 3.12.D). Based on these results we believe that both Tpr and Sam68 regulate unspliced RNA export at different stages and a combinatorial effect of depletion and overexpression results in synergistic effect.

3.2.6. Nucleoporin Nup153, a Tpr anchoring protein is also involved in regulating unspliced RNA export

Our results thus far firmly established a role for Tpr in regulating CTE mediated unspliced RNA export. However, there exists the possibility that in addition to Tpr, other nucleoporins known to play a role in nucleocytoplasmic transport may also be involved in this modulation. Nucleoporins with conserved FXFG (phenylalanine and glycine) repeats in their sequence play a significant role in mediating nucleocytoplasmic transport by providing an interaction interface that aids in the translocation of receptor-cargo complexes through the NPC [69]. Various FG repeat-containing nucleoporins such as Nup214, Nup358/RanBP2, which are localized to the cytoplasmic fibrils of the NPC, and Nup153, Nup98 and Nup50, shown to be present in the nucleoplasmic side of the
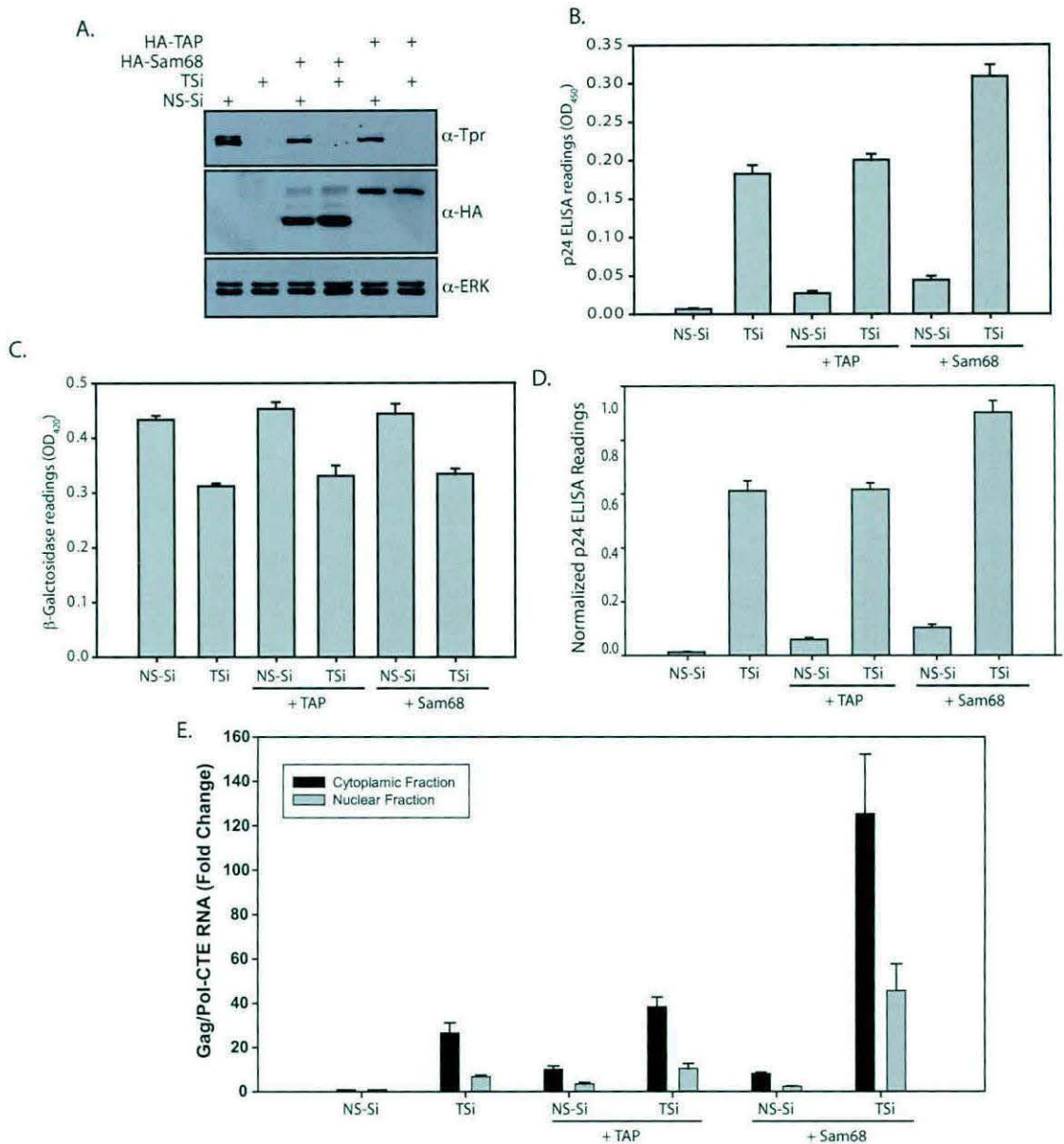
Figure 3.12. Overexpression of Sam68 in Tpr depleted cells leads to synergistic increase in the unspliced RNA export. (A) 48 hours after transfection with NS-Si and TSi, HEK293T cells were re-transfected with the same siRNA oligos along with Gag/Pol-CTE and CMV- β-Gal plasmids and 2 µg of HA-Sam68 or HA-Tap/Nxf1 constructs. The lysates thus obtained were analyzed by Immunoblot for knockdown of Tpr and overexpression of HA-Sam68 and HA-Tap (B&C) The lysates thus obtained were analyzed for the amounts of p24 (Panel B) and β-Gal expression (Panel C). (D) The p24 ELISA readings obtained from the samples were adjusted against variations in the β-Galactosidase readings. (E) Real-Time PCR analysis of mRNA isolated from nuclear and cytoplasmic fractions of HEK293T cells co-transfected with either NS-Si or TSi along with HA-Sam68 or HA-Tap/Nxf1 constructs and Gag/Pol-CTE reporter plasmid.

NPC, were considered for this study. Specific siRNAs were used to individually deplete the above mentioned nucleoporins (Fig. 3.13.A) and the export of Gag/Pol-CTE RNA was quantitated by measuring the normalized p24 levels in the protein extracts. While we observed elevated levels of normalized p24 expression in samples when either Tpr or Nup153 were depleted, depletion of the other FG containing nucleoporins had no effect (Fig. 3.13.B-D). Interaction between Tpr and Nup153 has been reported to be required for localization of Tpr to the nuclear pore [7]. If the increased export of Gag/Pol-CTE RNA observed upon Nup153 depletion is an independent function of Nup153, we would expect a cumulative increase when both Tpr and Nup153 are depleted. We observed enhanced p24 levels when either Tpr or Nup153 are depleted, with Tpr depletion enhancing p24 levels more effectively than Nup153 depletion (Fig. 3.14.A and 3.14.B-D). However, we did not observe a cumulative elevation of p24 levels when both of them were depleted, rather, we detected p24 levels similar to those observed for Tpr knockdown by itself. These results suggest that Tpr and Nup153 both regulate the export of unspliced RNA and they are most likely functioning through the same pathway.

3.2.7. Localization of Tpr at the Nucleopore complex is necessary for the regulation of CTE mediated Export

In order to determine the region of Tpr that is necessary and sufficient for regulating export of unspliced RNA, we produced a series of siRNA resistant deletion constructs of Tpr (Fig. 3.15.A). Results showed that only the N-terminal fragment and the Tpr-NM fragment containing both the N- and Middle regions was able to rescue the phenotype (Fig. 3.15.B and 3.15.C). Tpr has previously been shown to possess a nuclear localization signal in the carboxy terminal region, and the N-terminal fragment is reported to contain a NPC associating domain [16]. When we carried out immunofluorescence analysis to ascertain the subcellular localization of various Tpr fragments, we found TprN and NM to largely localize to the cytosol (Fig. 3.15.E). However, we cannot rule out the possibility of at least some amounts TprN and TprNM may be able to associate with NPC even though they do not localize to the nuclear interior. Another possibility is that the overexpression of TprN and TprNM coupled to their largely cytosolic localization may result in other hitherto unkonwn cellular factors
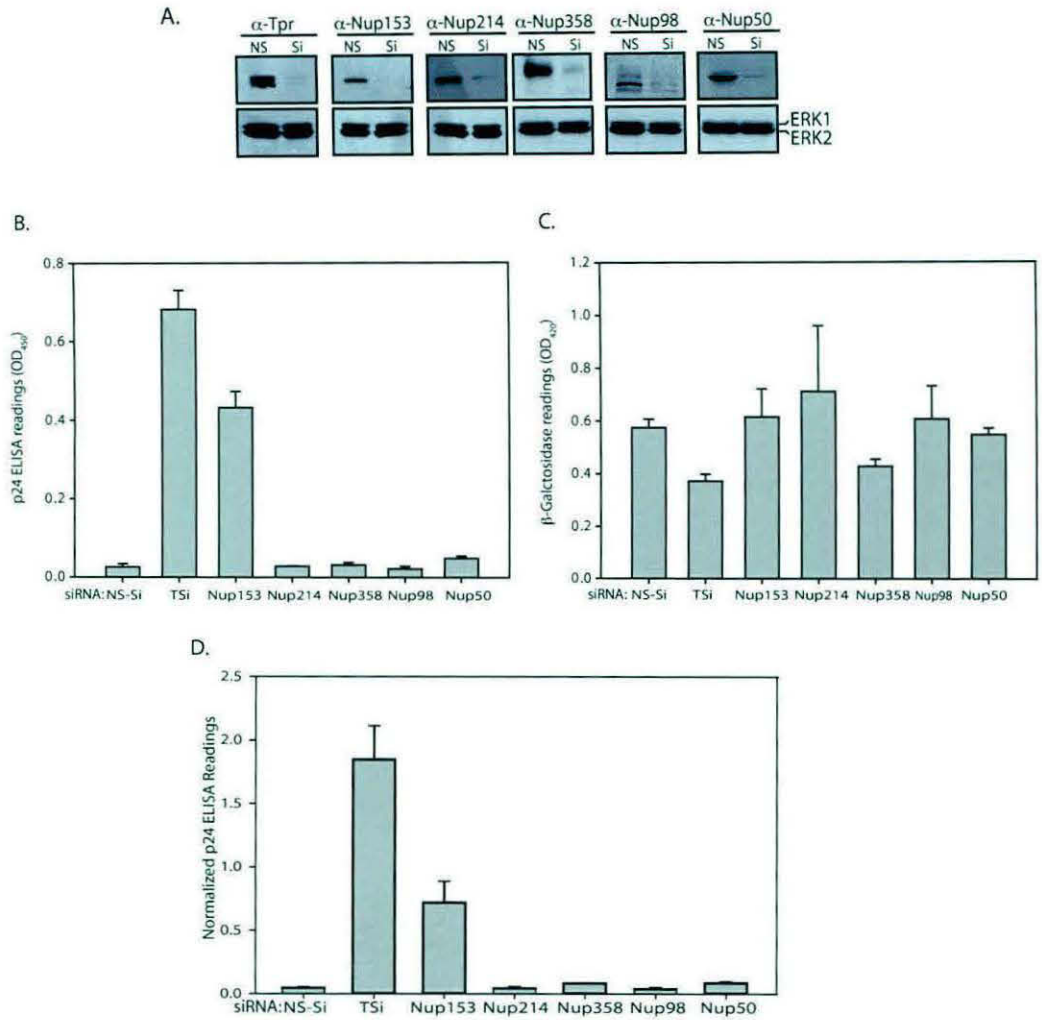
Figure 3.13. Nucleoporin Nup153, a Tpr anchoring protein is also involved in regulating unspliced RNA export. (A) HEK293T cells were transfected with siRNA's against different nucleoporins together with Gag/Pol-CTE and CMV- β-Gal constructs. Western blot of cell extracts confirming the depletion of various nucleoporins on treatment with respective siRNA's. (B & C) 48 hours post transfection, the amount of p24 and β-Gal expression was estimated in the lysates. (D) The obtained p24 levels were normalized against the variations in the β-Gal readings. Bars represent the mean of values and the error bars represent the s.d. of values obtained from three independent transfections.
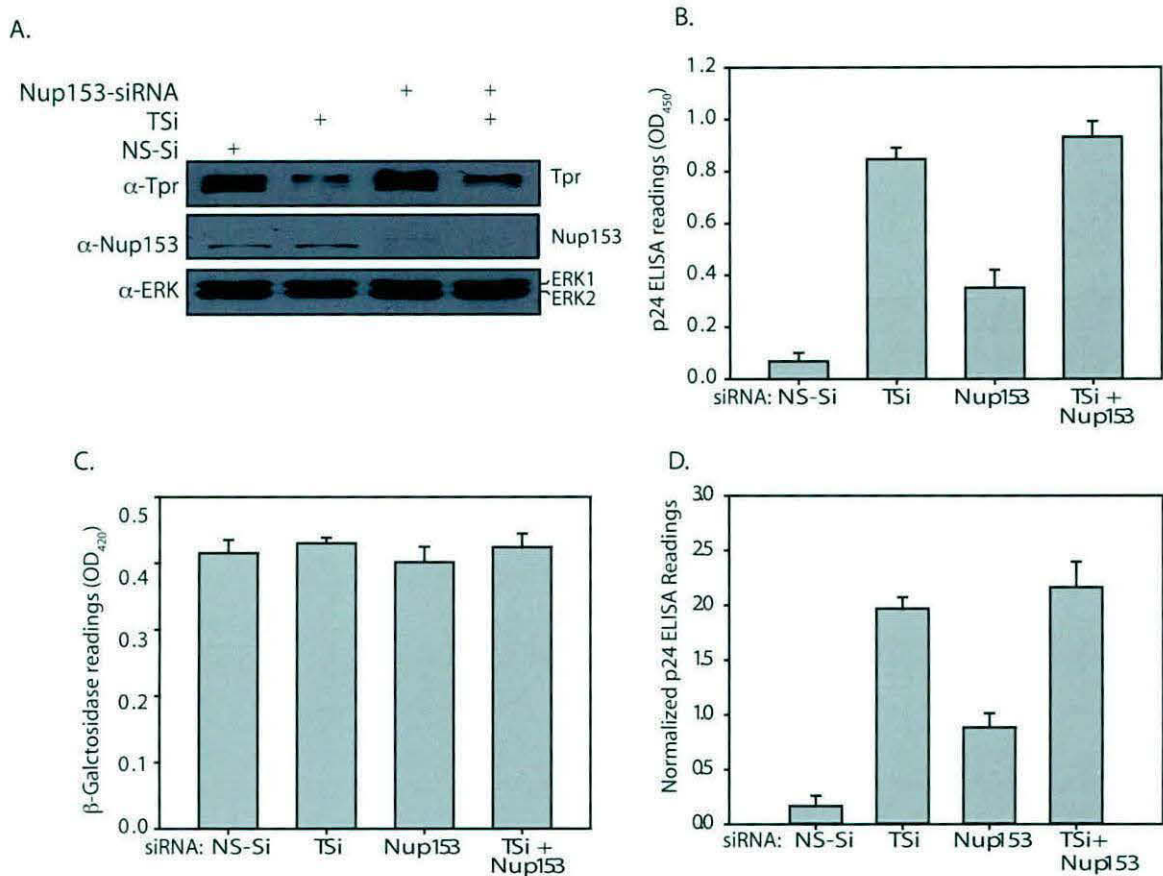
Figure 3.14. Depletion of Nup153 also has an effect on CTE dependent export. (A) Cells were transfected with siRNA's against Nup153 or Tpr or Nup153 + Tpr together with Gag/Pol-CTE and CMV- β-Gal constructs. Western blot of cell extracts confirming the depletion of Nup153 and Tpr on treatment with respective siRNA's. (B and C) The lysates thus obtained were analyzed for the amounts of p24 (Panel B) and β-Gal expression (Panel C). (D) The p24 levels were normalized against the variations in the β-Gal readings. Bars represent the mean of values and the error bars represent the s.d. of values obtained from three independent transfections.
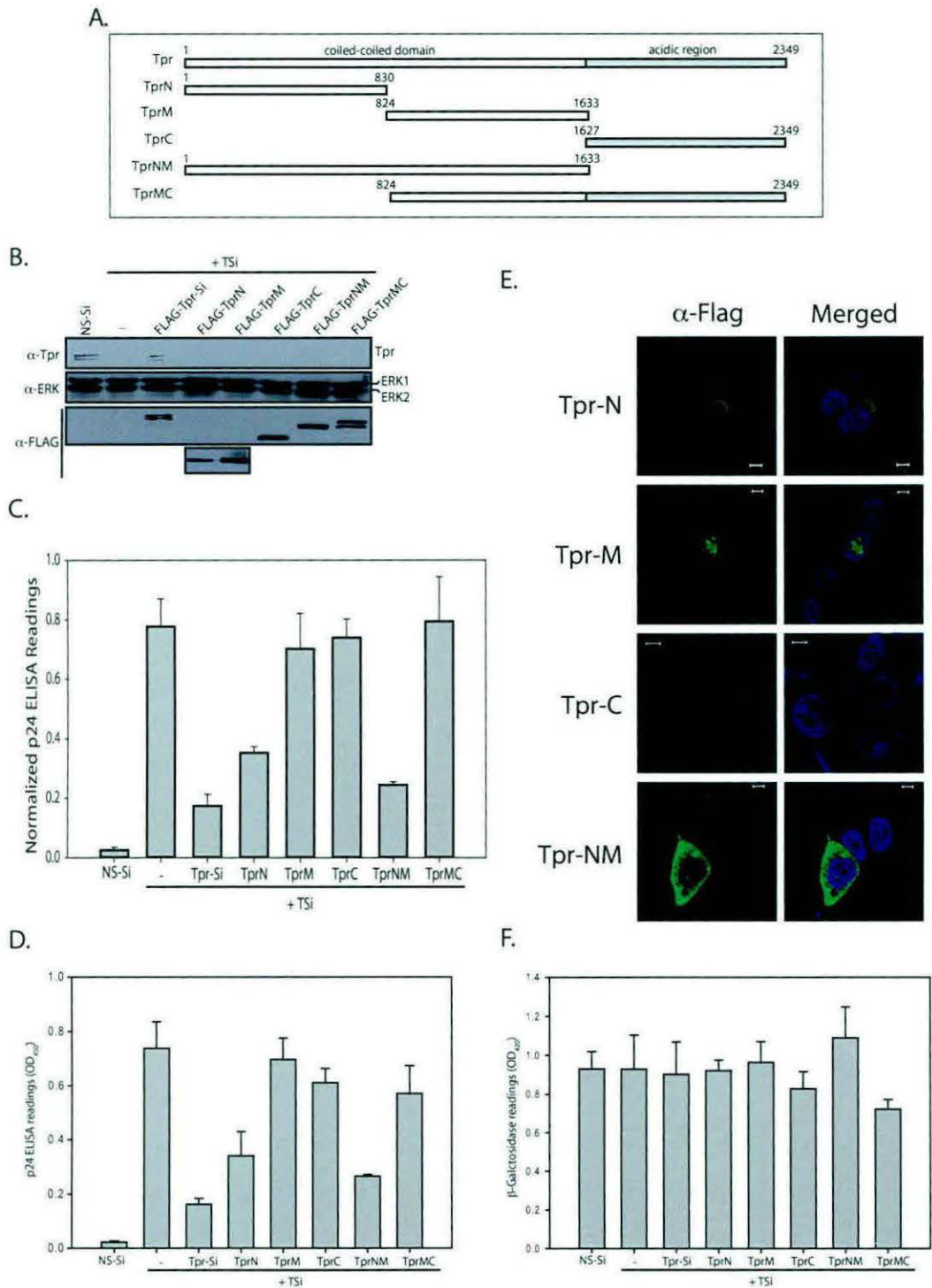
Figure 3.15. The N-terminal region of Tpr is necessary for the regulation of CTE mediated unspliced RNA export. (A) Schematic representation of various Tpr deletion fragments. (B) Immunoblot depicting the expression of various Flag-tagged Tpr deletion fragments in cells devoid of endogenous Tpr. (C and D) p24 levels (Panel C) and β-Galactosidase readings (Panel D) observed in cells transfected with Gag/Pol-CTE and CMV- β-Gal reporter constructs along with TSi and rescued with different deletion constructs of the protein. (E) Immunofluorescence microscopy of the cells transfected with different deletion constructs of Tpr. (F) Normalized p24 ELISA readings in HEK293T cells treated with TSi for 48 hours and rescued with different deletion constructs of the protein.

57

essential for CTE mediated unspliced RNA export and subsequent gene expression, being titrated out by TprN and TprNM. Further, we observed aberrant nuclear blebbing when TprN and TprNM are overexpressed, and this too may impact CTE mediated RNA export. These aspects need to be further investigated before any definitive conclusions may be drawn as some of the effects may be overexpression phenotypes.

Nup153 has been demonstrated to interact with Tpr and the interaction is mediated through residues L458 and M489 in the N-terminal coiled-coil region of Tpr. The interaction has been shown to be required for the localization of Tpr [7]. The fact that we did not observe a cumulative effect upon Tpr and Nup153 double knockdown, and that Tpr-NM fragment rescued the phenotype, suggested that Nup153 mediated Tpr anchoring may be essential for modulating Gag/Pol-CTE RNA export. To test this, we generated siRNA resistant localization deficient mutant of Tpr (Tpr-L458P/M489P). As expected, FLAG-Tpr-Si was localized to the nuclear membrane (Fig. 3.16.A). However, in agreement with the earlier reports [7], the localization of Tpr-L458P/M489P-Si mutant was observed to be intranuclear (Fig. 3.16.A and 3.16.B). As expected, when cells were transfected with siRNA resistant FLAG-Tpr-Si construct, we observed decreased p24 levels (Fig. 3.16.C-F). Importantly, presence of siRNA resistant FLAG-Tpr-L458P/M489P-Si did not bring down the levels of normalized p24, though its expression was similar to FLAG-Tpr-Si (Fig. 3.16.C-F). Taken together, these results provide compelling evidence that the localization of Tpr to the NPC is critical for regulating the export of intron containing RNA.

3.2.8. Identification of genes that are differntially regulated upon Tpr knockdown

It was apparent that Tpr localized at NPC plays a critical role in modulating unspliced mRNA export. However, it is not clear as to how Tpr functions as the gate keeper at the NPC. It is likely that Tpr interacts either directly with the unspliced mRNA or through another protein, which in turn associates with unspliced mRNA. In order to determine the effect of Tpr knockdown on the alteration in the global expression levels of cellular genes, we performed microarray analysis of HEK293T cells treated either with NS-Si or Tsi was carried out. We were specifically interested in down-regulation or up-regulation of genes that may play a role in mRNA transcription, splicing and processing. Data indicated up-regulation of genes like *hnrnpa1l2 eif4a2 ,*
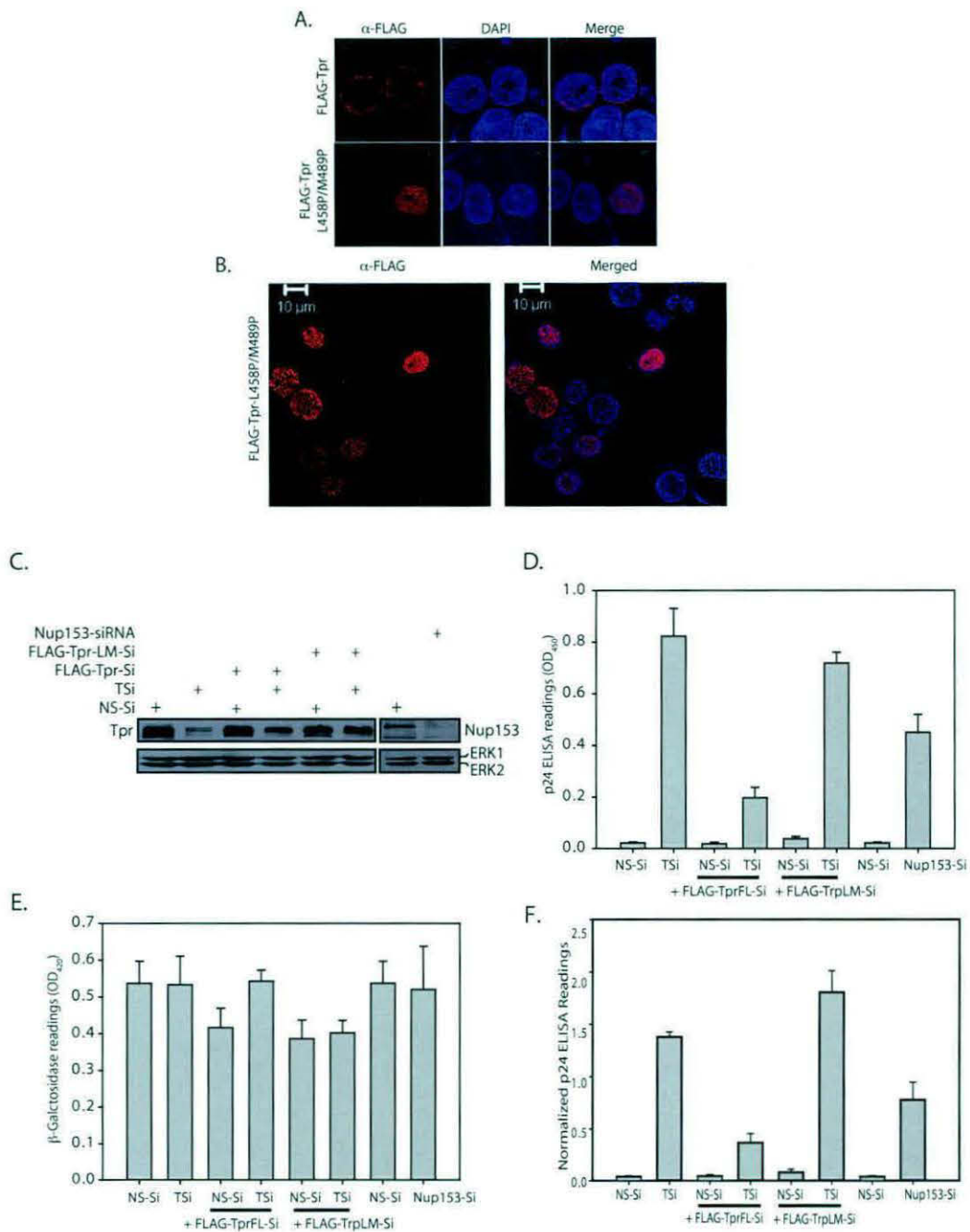
Figure 3.16. Localization of Tpr at the Nucleopore complex is important for the regulation of CTE mediated Export. (A) Immunofluorescence analysis of 293T cells transfected with Flag-Tpr or Flag-Tpr-L458P/M489P-Si constructs. (B) Overview image of HEK293T cells transiently transfected with Flag-Tpr-L458P/M489P-Si construct. (C) 293T cells were co-transfected with NS-Si or TSi or Nup153-siRNA, along with Gag/Pol-CTE and CMV-β-Gal reporter constructs, and 2 μg of Tpr-Si or Flag-Tpr-L458P/M489P-Si (Tpr-LM-Si) constructs. Western blot analysis indicating similar expression levels of Tpr-Si and Tpr-LM-Si constructs after depletion of endogenous Tpr. (D & E) p24 and β-Galactosidase levels in the whole cell extracts of each of the samples were analyzed 48 hours post transfection. (F) The obtained p24 levels were normalized against the variations in the β-Gal readings. Bars represent the mean of values and the error bars represent the s.d. of values obtained from three independent transfections.

59

eif5a, *ireb2, parn, a2bp1, rpl27a, card17*, which are known to associate with RNA, and especially *hnrnpa1l2* is known to be a part of spliceosome complex (Table 3.1). Gene expression profiles of Tpr depleted cells demonstrated down regulation of several genes that are known to function in transcription (*jun*, and *prox1*) and microtubule organization (*cdc14a*, and *cep350*). Interestingly, a significant number of genes that were upregulated were found to be a part of the nucleus and the perinuclear region of the cytoplasm. Several genes that were upregulated were found to have DNA or RNA binding properties (Table 3.2). Future work would be aimed at validating microarray data and determine if knock down of any of the interesting candidates using specific siRNA, would have any impact on export of unspliced RNA.

Table 3.1: Genes Downregulated after Tpr Knockdown

Probe Set ID	Seq.	Accession	Gene ID	Gene Symbol	Gene Description	Map ID	Csi1	Csi2	Tsi1	Tsi2	Log FC	FC	t	P Value
Splicosome complex														
7969263	chr13	+	NM_001011724	144983	HNRNPA1L2	heterogeneous nuclear ribonucleoprotein A1-like 2	13q14.3	6.77	7	6.38	6.42	-0.49	0.71	-2.64	0.044618
7939424	chr11	+	NM_001142930	8539	API5	apoptosis inhibitor 5	11p11.2	10.43	10.43	10.02	9.58	-0.63	0.65	-2.9	0.032834
Nucleolus														
7999562	chr16	-	NM_002582	5073	PARN	poly(A)-specific ribonuclease (deadenylation nuclease)	16p13	9.4	9.36	8.94	8.75	-0.54	0.69	-2.99	0.029488
8092095	chr3	-	NM_015028	23043	TNIK	TRAF2 and NCK interacting kinase	3q26.2-q26.31	8.46	8.64	8.02	7.97	-0.56	0.68	-3.12	0.025505
7975779	chr14	+	NM_005252	2353	FOS	FBJ murine osteosarcoma viral oncogene homolog	14q24.3	6.54	6.3	5.9	5.62	-0.66	0.63	-3.24	0.022236
Nucleoplasm														
7984540	chr15	+	NM_138555	9493	KIF23	kinesin family member 23	15q23	9.9	9.85	9.36	8.95	-0.72	0.61	-3.4	0.018613
U6 snRNA binding														
8004325	chr17	+	NM_001143760	1984	EIF5A	eukaryotic translation initiation factor 5A	17p13-p12	6.61	6.72	5.74	6.11	-0.74	0.6	-3.57	0.015309
Specific RNA polymerase II transcription factor					FOS									
mRNA 3'-UTR binding					PARN									
RNA polymerase II transcription factor activity, enhancer binding														
7955425	chr12	+	NM_005171	466	ATF1	activating transcription factor 1	12q13	9.11	9.1	8.69	8.62	-0.45	0.73	-2.65	0.044243
			NM_001025077	10659	CELF2	CUGBP, Elav-like family member 2	10p13	5.73	5.77	5.22	5.1	-0.59	0.66	-3.41	0.018250
RNA Binding														
7926127	chr10	+	NM_001011724	144983	HNRNPA1L2	heterogeneous nuclear ribonucleoprotein A1-like 2	13q14.3	6.77	7	6.38	6.42	-0.49			
7969263	chr13	+	AB209021	1974	EIF4A2	eukaryotic translation initiation factor 4A2	3q28	7.11	6.83	6.34	5.72	-0.94	0.52	-3.47	0.017190
8084704	chr3	+	NM_001143760	1984	EIF5A	eukaryotic translation initiation factor 5A	17p13-p12	6.61	6.72	5.74	6.11	-0.74	0.6	-3.57	0.015309
8004325	chr17	+	NM_004136	3658	IREB2	iron-responsive element binding protein 2	15q25.1	10.15	9.88	9.63	9.26	-0.57	0.67	-2.58	0.048255
7985166	chr15	+	NM_002582	5073	PARN	poly(A)-specific ribonuclease (deadenylation nuclease)	16p13	9.4	9.36	8.94	8.75	-0.54	0.69	-2.99	0.029488
7999562	chr16	-	ENST00000432184	54715	A2BP1	ataxin 2-binding protein 1	16p13.3	2.54	2.55	1.76	2.04	-0.65	0.64	-3.4	0.018509
7993110	chr16	+	NM_000990	6157	RPL27A	ribosomal protein L27a	11p15	9.91	9.98	9.11	9.2	-0.79	0.58	-4.59	0.005528
7938286	chr11	+	NM_001007232	440068	CARD17	caspase recruitment domain family, member 17	11q22.3	3.99	4.32	2.82	3.37	-1.06	0.48	-4.05	0.009324

Table 3.2: Genes Upregulated after Tpr Knockdown

			Gene ID	Gene Symbol	Gene Description	Map ID	Csi1	Csi2	Tsi1	Tsi2	Log FC	FC	t	P Value
				Accession										
RNA Binding														
Probe Set ID	Seq.													
8147065	chr8	+	NM_173848	138046	RALYL	RALY RNA binding protein-like	8q21.2	3.56	3.4	4.19	3.84	0.54	1.45	2.59	0.047876
8085676	chr3	-	NM_001351	1618	DAZL	deleted in azoospermia-like	3p24.3	3.2	3.3	3.75	3.97	0.61	1.53	3.31	0.020528
7898278	chr1	+	NM_015001	23013	SPEN	spen homolog, transcriptional regulator (Drosophila)	1p36.33-p36.11	9.82	10.2	10.47	10.64	0.55	1.46	2.56	0.049328
8013908	chr17	-	NM_020772	57532	NUFIP2	nuclear fragile X mental retardation protein interacting protein 2	17q11.2	9.6	9.1	10.47	9.92	0.85	1.8	2.95	0.031056
8022856	chr18	-	NM_003787	8715	NOL4	nucleolar protein 4	18q12	5.47	5.62	6.41	6.22	0.77	1.71	4.17	0.008254
Double stranded RNA Binding														
8098611	chr4	+	NM_003265	7098	TLR3	toll-like receptor 3	4q35	3.52	3.78	4.87	4.68	1.13	2.18	5.74	0.002075
RNA polymerase II transcription factor activity, Enhancer Binding														
7916609	chr1	-	NM_002228	3725	JUN	jun oncogene	1p32-p31	10.12	10.26	10.91	10.75	0.64	1.56	3.54	0.015930
7909681	chr1	+	NM_002763	5629	PROX1	prospero homeobox 1	1q32.2-q32.3	5.11	5.03	5.68	6.12	0.83	1.78	3.8	0.012119
Nuclear Matrix														
8056323	chr2	-	NM_018086	55137	FIGN	fidgetin	2q24.3	6.86	6.9	7.28	7.79	0.66	1.57	2.82	0.035985
Guanyl-nucleotide exchange factor complex														
8041422	chr2	+	NM_170672	25780	RASGRP3	RAS guanyl releasing protein 3 (calcium and DAG-regulated)	2p25.1-p24.1	3.99	3.96	4.68	4.61	0.67	1.59	3.94	0.010410
7990774	chr15	-	NM_002891	5923	RASGRF1	Ras protein-specific guanine nucleotide-releasing factor 1	15q24.2	5.76	5.42	6.65	6.48	0.98	1.97	4.73	0.004857
Nuclear envelope lumen														
8091867	chr3	-	NM_000055	590	BCHE	butyrylcholinesterase	3q26.1-q26.2	4.2	4.27	4.91	4.84	0.64	1.56	3.74	0.012829
Nucleoplasm														
8081953	chr3	+	NM_005513	2960	GTF2E1	general transcription factor IIE, polypeptide 1, alpha 56kDa	3q21-q24	7.52	7.34	7.94	8.04	0.56	1.47	3.11	0.025729
8130739	chr6	-	NM_021135	6196	RPS6KA2	ribosomal protein S6 kinase, 90kDa, polypeptide 2	6q27	7.41	7.16	7.92	7.72	0.54	1.45	2.73	0.040069
8067113	chr20	-	NM_006526	7764	ZNF217	zinc finger protein 217	20q13.2	7.31	7.07	7.72	7.77	0.56	1.47	3	0.029113

Nucleolus															
8141140	chr7	-	NM_005221	1749	DLX5	distal-less homeobox 5	7q22	6.71	7.01	7.52	8.12	0.96	1.95	3.57	0.015350
8061746	chr20	+	NM_006892	1789	DNMT3B	DNA (cytosine-5-)-methyltransferase 3 beta	20q11.2	6.82	6.75	7.21	7.25	0.45	1.36	2.62	0.046239
7898278	chr1	+	NM_015001	23013	SPEN	spen homolog, transcriptional regulator (Drosophila)	1p36.33-p36.11	9.82	10.2	10.47	10.64	0.55	1.46	2.56	0.049328
8040190	chr2	+	NM_198182	29841	GRHL1	grainyhead-like 1 (Drosophila)	2p25.1	5.98	5.76	6.49	6.42	0.59	1.5	3.2	0.023296
8030950	chr19	+	NM_018260	55762	ZNF701	zinc finger protein 701	19q13.41	5.01	4.74	5.77	5.73	0.88	1.83	4.64	0.005301
7954398	chr12	+	NM_030572	80763	C12orf39	chromosome 12 open reading frame 39	12p12.1	4.7	4.37	5.37	5.74	1.02	2.03	4.46	0.006260
8022856	chr18	-	NM_003787	8715	NOL4	nucleolar protein 4	18q12	5.47	5.62	6.41	6.22	0.77	1.71	4.17	0.008254
7938834	chr11	+	NM_182964	89797	NAV2	neuron navigator 2	11p15.1	5.99	6.03	6.41	6.64	0.52	1.43	2.81	0.036611
Perinuclear region of cytoplasm															
7948987	chr11	-	NM_007069	11145	PLA2G16	phospholipase A2, group XVI	11q12.3	7.72	7.87	8.25	8.64	0.65	1.57	3.05	0.027460
7916541	chr1	-	NM_021080	1600	DAB1	disabled homolog 1 (Drosophila)	1p32-p31	5.94	6.1	6.71	6.56	0.62	1.53	3.39	0.018832
8041422	chr2	+	NM_170672	25780	RASGRP3	RAS guanyl releasing protein 3 (calcium and DAG-regulated)	2p25.1-p24.1	3.99	3.96	4.68	4.61	0.67	1.59	3.94	0.010410
7956488	chr12	+	NM_004984	3798	KIF5A	kinesin family member 5A	12q13.13	6.25	6.29	7.09	6.86	0.71	1.63	3.84	0.011517
8113234	chr5	-	NM_000439	5122	PCSK1	proprotein convertase subtilisin/kexin type 1	5q15-q21	3.33	3.19	3.76	3.69	0.47	1.38	2.65	0.044128
8022986	chr18	-	NM_020783	6860	SYT4	synaptotagmin IV	18q12.3	4.62	4.25	5.18	4.96	0.64	1.55	2.95	0.031012
8135594	chr7	+	NM_001753	857	CAV1	caveolin 1, caveolae protein, 22kDa	7q31.1	6.86	6.92	7.33	7.53	0.54	1.45	2.99	0.029448
Nuclear heterochromatin					DNMT3B										
NuRD complex															
8001387	chr16	-	NM_002968	6299	SALL1	sal-like 1 (Drosophila)	16q12.1	8.38	8.89	9.2	9.65	0.79	1.73	2.91	0.032247
Nuclear chromosome and Chromatin					JUN										
Nuclear outer membrane															
8130211	chr6	-	NM_182961	23345	SYNE1	spectrin repeat containing, nuclear envelope 1	6q25	6.01	6.01	6.66	6.39	0.52	1.43	2.74	0.039925
Nuclear speck															
8102862	chr4	-	NM_018717	55534	MAML3	mastermind-like 3 (Drosophila)	4q28	5.54	5.63	6.31	6.31	0.73	1.65	4.25	0.007663
Microtubule organizing center															
7903334	chr1	+	NM_003672	8556	CDC14A	CDC14 cell division cycle 14 homolog A (S. cerevisiae)	1p21	7.27	7.37	7.78	7.83	0.49	1.4	2.82	0.036006

7907790	chr1	+	NM_014810	9857	CEP350	centrosomal protein 350kDa	1p36.13-q41	8.21	8.32	8.8	8.92	0.59	1.51	3.38	0.018837
Nucleus															
7994769	chr16	+	NM_007074	11151	CORO1A	coronin, actin binding protein, 1A	16p11.2	6.72	6.59	7.64	7.24	0.79	1.72	3.68	0.013721
8162744	chr9	-	NM_003389	7464	CORO2A	coronin, actin binding protein, 2A	9q22.3	6.6	6.42	7.3	7.17	0.73	1.65	3.98	0.009986
7975066	chr14	+	NM_004857	9495	AKAP5	A kinase (PRKA) anchor protein 5	14q21-q24	4.25	4.32	5.04	5.04	0.76	1.69	4.45	0.006325
8074606	chr22	-	NM_017414	11274	USP18	ubiquitin specific peptidase 18	22q11.21	8.61	8.69	9.18	9.06	0.47	1.39	2.7	0.041806
8141140	chr7	-	NM_005221	1749	DLX5	distal-less homeobox 5	7q22	6.71	7.01	7.52	8.12	0.96	1.95	3.57	0.015350
7981514	chr14	-	NM_138420	113146	AHNAK2	AHNAK nucleoprotein 2	14q32.33	5.75	6.06	6.72	6.76	0.84	1.78	4.29	0.007354
7956120	chr12	+	NM_001982	2065	ERBB3	v-erb-b2 erythroblastic leukemia viral oncogene homolog 3 (avian)	12q13	6.2	6.1	6.88	6.62	0.6	1.52	3.17	0.024056
7964460	chr12	-	NM_004083	1649	DDIT3	DNA-damage-inducible transcript 3	12q13.1-q13.2	9.47	9.78	10.28	10.45	0.74	1.67	3.68	0.013729
8161211	chr9	-	NM_016734	5079	PAX5	paired box 5	9p13	5.71	5.62	6.46	6.38	0.76	1.69	4.38	0.006765
8040419	chr2	+	NM_005378	4613	MYCN	v-myc myelocytomatosis viral related oncogene, neuroblastoma derived (avian)	2p24.1	5.63	5.9	6.36	6.43	0.63	1.55	3.32	0.020138
7909681	chr1	+	NM_002763	5629	PROX1	prospero homeobox 1	1q32.2-q32.3	5.11	5.03	5.68	6.12	0.83	1.78	3.8	0.012119
8013908	chr17	-	NM_020772	57532	NUFIP2	nuclear fragile X mental retardation protein interacting protein 2	17q11.2	9.6	9.1	10.47	9.92	0.85	1.8	2.95	0.031056
8121649	chr6	+	NM_173560	222546	RFX6	regulatory factor X, 6	6q22.1	3.29	3.21	4.11	3.9	0.76	1.69	4.14	0.008527
Sequence specific DNA Binding															
8016609	chr17	-	NM_005220	1747	DLX3	distal-less homeobox 3	17q21	5.25	5.23	5.66	5.86	0.52	1.43	2.9	0.033005
8128247	chr6	-	NM_021813	60468	BACH2	BTB and CNC homology 1, basic leucine zipper transcription factor 2	6q15	5.97	5.92	6.33	6.49	0.47	1.38	2.64	0.044946
8147000	chr8	+	NM_024721	79776	ZFHX4	zinc finger homeobox 4	8q21.11	7.11	7.39	7.67	8.19	0.68	1.6	2.72	0.040547
8066266	chr20	-	NM_005461	9935	MAFB	v-maf musculoaponeurotic fibrosarcoma oncogene homolog B (avian)	20q11.2-q13.1	6.88	7.03	7.53	7.46	0.54	1.45	3.07	0.026977

3.3. Discussion

In mammalian cells, mRNA transcripts with unspliced introns are restricted to the nucleus. Retroviruses overcome this retention and export their full-length genomic RNA containing introns with the help of *cis*-acting elements like RRE (and transactivator protein Rev) or CTE [114, 197, 198]. We observed a significant enhancement of CTE function in Tpr depleted 293T cells, suggesting that Tpr plays a critical role in restricting the CTE-mediated export of intron-containing RNA. The fact that the protein transport, poly(A)$^+$ mRNA distribution and the Rev-mediated unspliced RNA export remained unperturbed by Tpr knockdown, indicates that Tpr may specifically interact either directly or indirectly with the CTE-mRNP complexes in order to modulate their export through the NPC. Moreover, an increase in the nuclear CTE-RNA levels observed in the absence of Tpr also suggests that this nucleoporin may play an additional role in regulating the processing of these transcripts.

Sam68, Nxt1/p15 and Tap/Nxf1 proteins have been previously reported to play a role in enhancement of CTE function [26-29]. The formation of Tap and Nxt heterodimers augments the binding of nucleoporins to Tap, and results in its increased nucleocytoplasmic shuttling [120]. Association of Nxt1 to Tap-CTE mRNA enhances the interaction of the mRNP complex to the NPC, resulting in its efficient export [121]. These proteins have also been shown to promote polyribosome association of intron-containing RNA, resulting in their efficient translation [27]. Since depletion of Tpr and expression of Sam68, Tap and Nxt1 regulate the export of unspliced RNA, we investigated the possibility of direct interactions between Tpr and Tap, Nxt1 or Sam68. While we observed an interaction between endogenous Tpr with immunoprecipitated ERK2 [36], we could not detect any interaction of Tpr with Sam68, Tap or Nxt1 proteins (Fig. 3.17). Tap/Nxf1 has been shown to have an effect on the export of mRNA from the nucleus in various model systems [193-196]. In our study, upon partial depletion of Tap we observed a slight reduction in the p24 and β-GAL levels (Fig. 3.11A-D). However, when Tap was efficiently depleted (Fig. 3.11E-G), consistent with the previous findings, we observed a substantial reduction in β-GAL readings. On the contrary, depletion of Tap, or Tap and Tpr together, did not significantly alter the p24 levels over the levels observed upon Tpr depletion alone, suggesting that the change in Tpr levels is sufficient for the release of CTE-mRNP complexes into the cytosol. Further, we
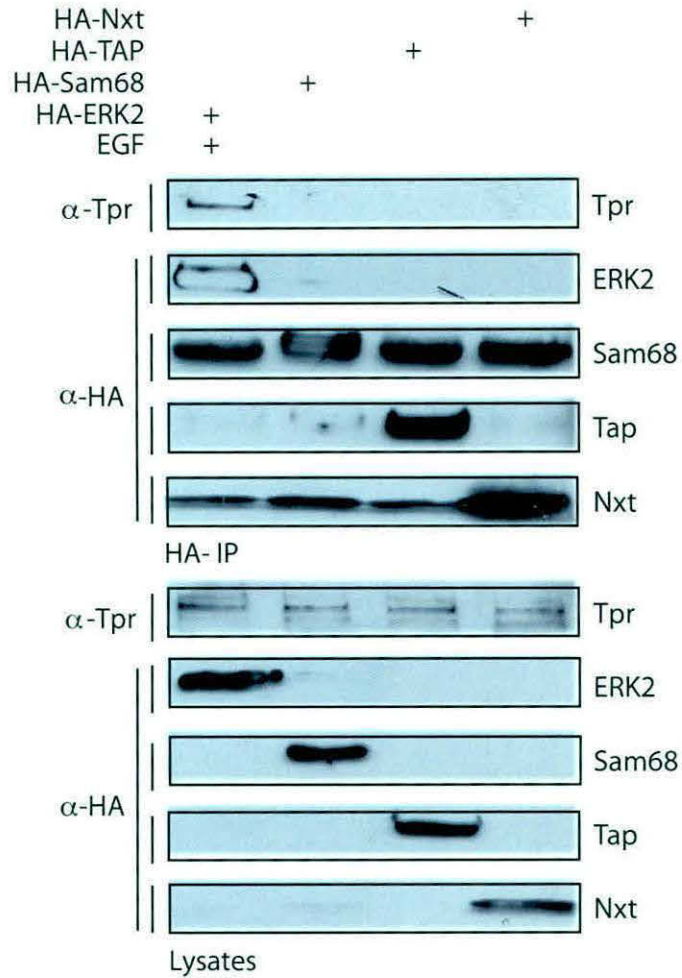
Figure 3.17. Nucleoporin Tpr does not interact with Tap/Nxf1 and Sam68 proteins.
(A) Cells were transfected with HA-ERK2, HA-Sam68, HA-Nxt/p15 or HA-Tap/Nxf1 constructs. 24 hours post transfection, cells were lysed, and the lysates were immunopre-cipitated with HA-antibodies. The immunoblots were probed with anti-HA and anti-Tpr antibodies to determine the interactions between Tpr and HA-tagged proteins. Co-immunoprecipitation of endogenous Tpr along with HA-ERK2 validates the approach.

observed that the simultaneous depletion of Tpr and overexpression of Sam68 resulted in a synergistic increase in the export of unspliced RNA. These results indicate that the mode of regulating unspliced RNA export by Sam68 and Tpr are likely to be different. As has been shown earlier, Sam68 is most likely required for stabilizing the mRNA and for improved cytosolic utilization of unspliced RNA [28], while the function of Tpr is and may be mediated by either direct interaction, or through some unidentified RNA binding protein. In yeast, the RNA binding proteins Yra1p and Nab2p have been shown to be essential for the docking of mRNP complexes near the Mlp export gate located at the nuclear membrane [184]. A recent study demonstrated that depletion of a RNA endonuclease protein Swt1 resulted in nuclear poly (A)+ mRNA accumulation and enhanced the cytoplasmic leakage of unspliced pre-mRNAs in mlp1Δ and nup60Δ Mutants [199]. The homologs of Swt1 in humans, Smg5 and Smg6 proteins which were shown to play a role in nonsense- mediated mRNA decay [200-202]. Our preliminary data with the depletion of Smg5 and Smg6 proteins in Tpr knockdown cells to study the CTE dependent unspliced RNA export revealed no significant effect of these proteins (data not shown). Future studies would be aimed at investigating the role of mammalian homologs of yeast proteins in regulating Tpr mediated unspliced RNA export.

FG repeat containing nucleoporins in the NPC are known to be required for transport of macromolecules across the nuclear pore [69, 70]. Members of the karyopherin/importin superfamily, the mRNA export receptor Mex67/Mtr2, and the Ran transporter Ntf2, have been shown to specifically interact with FG Nups [71, 72]. We did not detect increased p24 levels, when we depleted Nup98, Nup214, Nup358 and Nup50. Nup98 is a nucleoporin that has been shown to associate with the intranuclear Tpr filaments [11]. Powers, et al., have shown that the injection of monospecific polyclonal anit-Nup98 antibodies into the nucleus, inhibited export of multiple classes of RNA, including mRNA [203]. Nup98 has also been shown to interact with mRNA transport factors such as Rae1 and Tap/Mex67 [195, 204]. We observed that siRNA mediated depletion of Nup98 did not significantly affect either p24 or β-GAL readings, suggesting that Nup98 does not play a significant role in the export of unspliced RNA or mRNA. The differences detected in our observations could be due to the variance in the methods used for investigation. However, one needs to perform a systematic

investigation using multiple methods to delineate the role played by Nup98 in mRNA export.

Interestingly, depletion of Nup153, an FG repeat containing nucleoporin that plays a critical role in various cellular processes including cell cycle progression [150], resulted in increased p24 levels. The overexpression of Nup153 has been shown to cause an accumulation of poly $(A)^+$ mRNA in the nucleus [205], and the injection of antibodies against Nup153 were reported to block NES mediated export of proteins, U1 snRNA, 5sRNA and spliced mRNA [206]. The observed increase in p24 levels upon Nup153 depletion, though significant, was not as effective as that seen upon depletion of Tpr. A combined knockdown of Nup153 and Tpr did not show synergistic effect on the p24 levels, indicating that both of them most likely are functioning through the same pathway. In a previous study, Nup153 has been demonstrated to be required for anchoring Tpr to the NPC [7], and the L458 and M489 residues in the N-terminal region of Tpr have been shown to be necessary for their interaction. Taken together, the effect shown by Nup153 on CTE-mediated export may be due to the possibility that Nup153 depletion prevents or destabilizes NPC binding of Tpr, and demonstrates that the association of Tpr with the NPC is critical for its function. The results we obtained with localization-deficient Tpr mutant whereupon mislocalization of Tpr to the interior of the nucleus resulted in failure to regulate the RNA export, suggests that perinuclear localization of Tpr is an important step in regulating CTE mediated export.

While the work was under progress, Hammarskjold's group reported that Tpr regulates the export of mRNA with a *cis*- acting CTE element and that the transport of intron-containing mRNA's through the Crm1 pathway is unaffected by Tpr [116]. The authors also showed that rescue with siRNA resistant form of Tpr suppresses the effect on CTE mediated export and that the co-expression of Sam68 and Tpr-shRNA led to significant enhancement of p24 expression. These results corroborate our findings[116]. The authors suggest that the additive effect seen upon Sam68 over expression and Tpr knockdown, may be due to cross- talk between the two proteins, however, in our study we did not detect any direct interaction between Tpr and Sam68 (Fig. 3.17). Based on their experimental results Coyle et al also suggest that freshly formed Tpr molecules, which constitute minor but dynamic nuclear Tpr protein pools, which are involved in transcriptional regulation of CTE-mRNP complexes are sufficient for enhancement of

p24 expression. The fact that we observe an increase in the nuclear CTE-mRNA levels upon Tpr depletion is in support of this hypothesis. The results of our experiments with Nup153 siRNA-mediated knockdown, as well as Tpr localization mutant studies, indicate that Tpr localized to the NPC plays a critical role in regulating unspliced RNA export. Apart from the regulatory role of Tpr in nuclear export, the authors report that depletion of Tpr leads to an increased association of CTE-mRNP complexes at the polyribosomal complexes, demonstrating a role for nucleoporin Tpr in the cytoplasm. However, Tpr depletion had no bearing on the stability of Gag/Pol protein in the cytosol. While our study does not address possible roles of Tpr in the cytoplasm, an increase in the nuclear CTE-mRNA pool upon Tpr depletion (Fig. 3.10) suggests a role for Tpr in the nucleoplasm. Microarray indicated upon Tpr knockdown that (Table 3.1 and 3.2), multiple genes required for mRNA processing are either up or down-regulated. Further experiments would be directed towards validating the data and identifying the functional role, if any, of these identified proteins in conjunction with Tpr towards modulating CTE mediated unspliced RNA export.

Taking together the findings of both studies, it appears the regulation of CTE-mediated unspliced RNA export is a complex and controlled phenomenon involving a plethora of proteins acting at various levels in the nucleus, of which nucleoporin Tpr is an important modulator. Future investigations would be directed towards identifying the key RNA binding proteins interacting with Tpr, and deciphering the precise mechanism by which Tpr modulates CTE-dependent unspliced RNA export.

CHAPTER-IV

Role Of Post Translational Modifications On The Functions Of Tpr

4.1 Introduction

Nucleoporins, the vital components of the nuclear envelope, are phosphorylated in a cell cycle dependent or DNA damage dependent manner. Studies by various groups showed that nucleoporins are extensively phosphorylated during mitosis and the mitotic-specific hyperphosphorylation was demonstrated both *in vitro* and *in vivo*. Many cellular kinases namely Cdk1, MAP Kinase ERK2, Protein Kinases A and C are have been reported to phosphorylate nucleoporins. Mitotic phosphorylation of FG-Nups was shown to be critical for the organization of spindle microtubules and the chromosomes. The phosphorylation of FG repeat containing nucleoporins Nup153 and Nup214 by ERK2 were shown to be important for the nuclear transport. Reports published in the last decade suggest that the phosphorylation of FG-Nups and non-FG nups serves as a molecular hub for cellular signalling pathways and is important to mediate functions like transcriptional regulation and cell cycle. Though these studies provide evidence that phosphorylation of nucleoporins may be modulating several physiological functions at the NPC, the spatio-temporal regulation of these phosphorylation events and their influence on nucleocytoplasmic transport has not yet been deciphered. In a previous study, Nucleoporin Tpr was identified as a candidate substrate for MAP Kinase ERK2 in cell lysates using a method that originally developed by Shokat and colleagues, in which a structural "pocket" is engineered into protein kinases so that they can utilize ATP analogs that have bulky substituents (37). Nucleoporin Tpr is phosphorylated *in vivo* in ERK2 dependent and independent manner. We identified sites on Tpr for ERK2 phosphorylation and binding, and demonstrated their functional interaction. Data provided direct evidence that Tpr is a *bona fide* substrate of ERK2 *in vivo,* and that activated ERK2 stably associates with this substrate after phosphorylation where it could play a continuing role in nuclear pore function. Recent studies have demonstrated that nucleoporin Tpr activates mitotic spindle checkpoint by interacting with Mad proteins and its association with dynein complex was shown to be important for proper segregation of chromosomes during mitosis. The fact that nucleoporins are extensively phosphorylated during mitosis and given the evidence of pivotal role for Tpr during the anaphase led us to investigate the role for Tpr phosphorylation in modulating the known mitotic functions of the protein

4.2 Results

4.2.1 Identification of ERK independent Phosphorylation sites on Tpr

Previously, based on the analysis of phospho peptide maps of metabolically labelled TprFL and TprC, we demonstrated that Tpr is phosphorylated *in vivo* in ERK2 dependent and independent manner and all the phosphorylation sites are located in the carboxy terminal 800 amino acids [36]. We identified threonine 2123 and serine 2141 to be the major target sites and threonine 2102 and 2200 to be the minor target sites for ERK2 (Fig 4.1A). However, in order to decipher the role of Tpr phosphorylation on the functions of Tpr, it was necessary to identify ERK2 independent phosphorylation sites. To achieve this objective, we performed metabolic labelling of wild type Tpr C-terminal fragment, TprC and the mutant TprC-M417, in which ERK2, target sites as well as the ERK2 interaction residues have been mutated to alanine residues (Fig. 4.1B). Autoradiogram of metabolically labelled TprC and TprC-M417 showed significant *in vivo* phosphorylation (Fig. 4.1B). Analysis of tryptic phosphopeptides maps obtained clearly demonstrated the disappearance of ERK2 target peptides in TprC-M417 (Fig. 4.1C). In agreement with our previous findings, we observed presence of three additional spots in both TprC and TprC-M417 (Indicated by black arrows in Fig. 4.1C). The phosphoaminoacid analysis of the metabolically labelled TprC-M417 revealed that the phosphorylation occurs mostly on serine residues, though we observed minor phosphorylation also on threonine residues (Fig 4.1D). The presence of radiolabelled phosphopeptide spots in TprC-M417 and the results of phosphoamino acid analysis suggested that other cellular kinases phosphorylate Tpr majorly on serine residues.

To identify the target phosphorylation sites, we embarked on narrowing down the target phosphorylation regions on TprC to a smaller stretch of ~100-200 aa. To accomplish this objective, we generated series of deletion fragments from both N- and C- terminal ends of TprC-M4, a mutant of TprC in which all the ERK2 target sites are mutated to alanine residues (Fig. 4.2A). TprC-M4 and the deletion constructs were transfected into COS-1 cells and lysates were resolved, transferred and probed with anti-FLAG antibodies to confirm the expression of deletion fragments (Fig 4.2B). In order to determine which deletion would alter the two dimensional tryptic phosphopeptide maps, COS-1 cells transfected with TprC or TprC-M4 or TprC-M4

A.

1627   2349
TprC

T2102A S2141A
TprC-M417
T2123A   T2200A

B. TprC TprC-M417

← TprC

Autoradiogram

C. TprC

TprC-M417

D.

pSer
pThr
pTyr
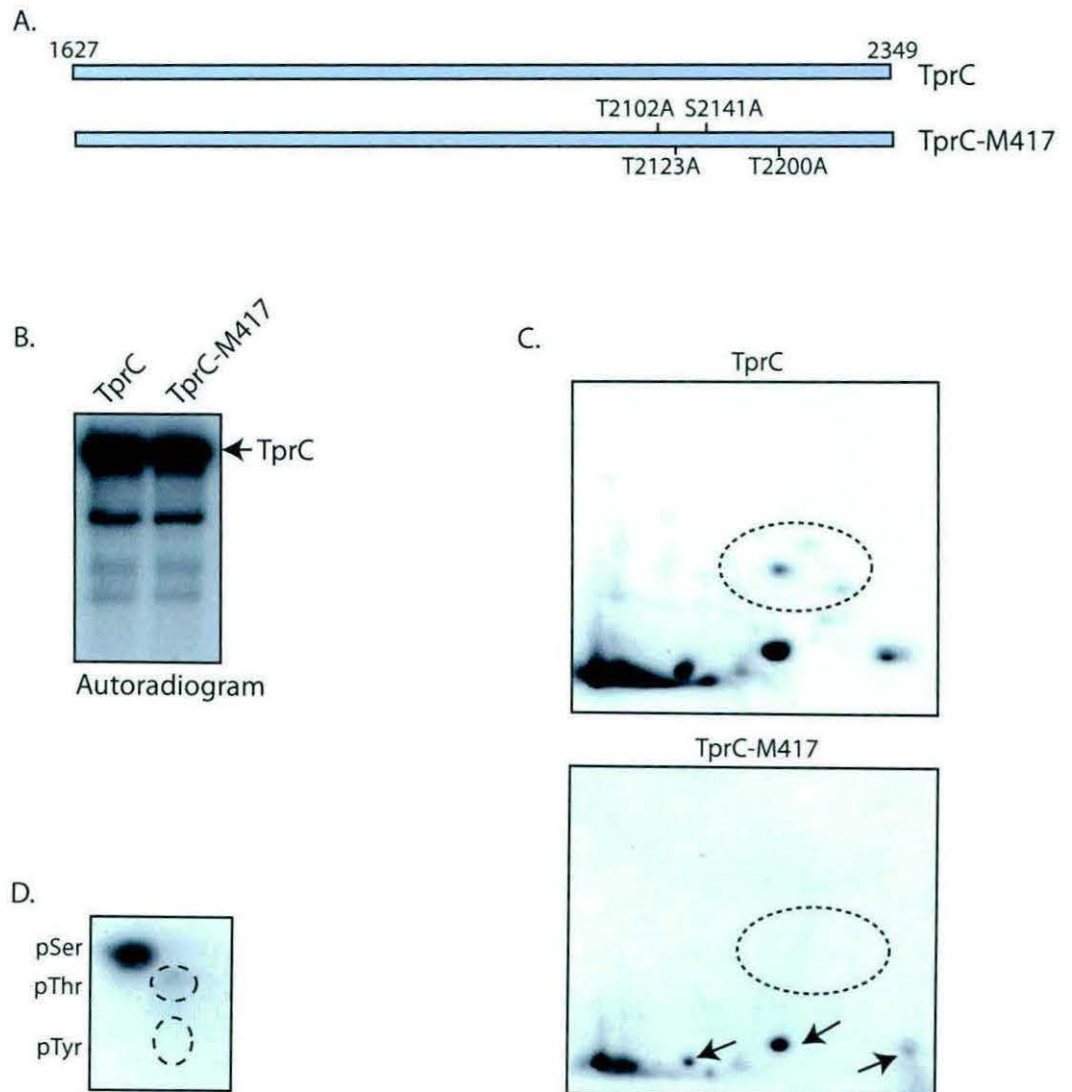
Figure 4.1. Nucleoporin Tpr is phosphorylated in vivo by kinases other than ERK2 – (A) Schematic representation of the TprC and TprCM417 constructs indicating the ERK dependent phosphorylation sites. (B) 100 mm dishes of COS-I cells were individually transfected with 8 μg each of FLAG-TprC or FLAG-TprC-M417 constructs. The cells were metabolically labelled for 3 hours and stimulated with 20 ng/ml EGF was added to the labelling cells for 10 min. FLAG-tagged TprC and TprC-M417 were immunoprecipitated, resolved, transferred, and autoradiographed. (C) In vivo-labeled TprC and TprC-M417 were digested with trypsin, and the resulting phosphopeptides were mapped by two-dimensional TLC. Arrows indicate the labelled phospho peptides that were persistent in the in vivo map of TprCM417. (D) Phosphoamino acid analysis of in vivo labelled TprCM417.

A.

1627 — Tpr (C- terminal region) — 2349		TprC-M4
1627 — 2249		TprC-M4-ΔC1
1627 — 2146		TprC-M4-ΔC2
1627 — 2029		TprC-M4-ΔC3
1728 — 2349		TprC-M4-ΔN1
1826 — 2349		TprC-M4-ΔN2
1926 — 2349		TprC-M4-ΔN3

B.

C.

TprC   TprC-M4   Tpr-M4-ΔC1   Tpr-M4-ΔC2

Tpr-M4-ΔC3   Tpr-M4-ΔN1   Tpr-M4-ΔN2   Tpr-M4-ΔN3
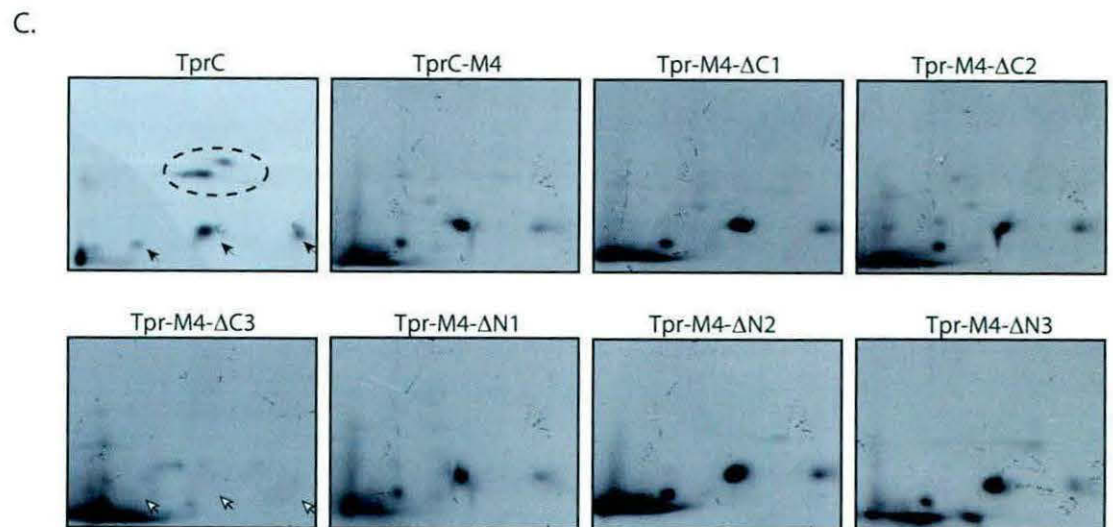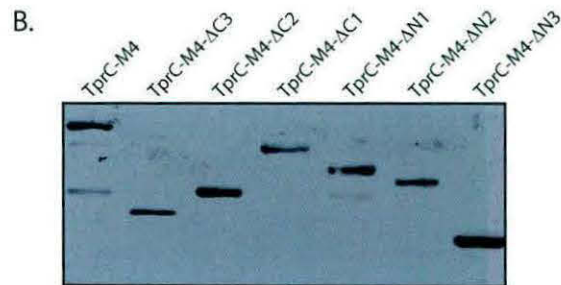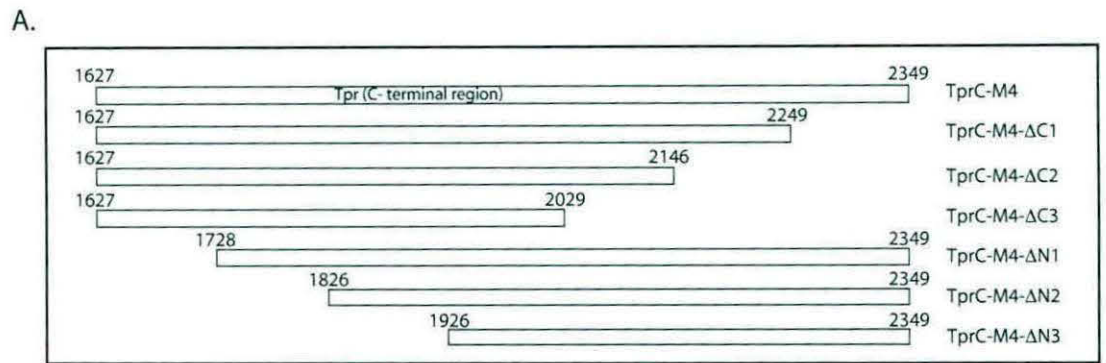
Figure 4.2. The region of ERK independent phosphorylation lies between the aminoacid residues 2029 and 2129 of Tpr - (A) Schematic representation of the various deletion constructs of TprC. (B) 100 mm dishes of COS-I cells were individually transfected with 8 μg each of TprC or TprC-M4 or the deletion constructs. The cell lysates were resolved, transferred and probed with anti-FLAG antibodies to check the expression. (C) The COS-I cells transfected with different FLAG-tagged constructs were metabolically labelled for 3 hours. The cell lysates were immunoprecipitated using anti-FLAG antibodies and the samples were resolved, transferred, and autoradiographed. Metabolically labeled FLAG-Tpr fragments were digested with trypsin, and the phosphopeptides generated were resolved by two-dimensional TLC.

deletion mutants were metabolically labelled and FLAG- tagged proteins were immunoprecipitated, digested with trypsin and followed by resolution of tryptic phopho peptides by 2D-TLC. While, five out of the six deletion fragments had the same pattern of tryptic phosphopeptides as TprC-M417, deletion fragment TprC-ΔC3 displayed altered map, where in all the spots corresponding to ERK2 independent sites disappeared (Fig 4.2C; missing spots are indicated by numbered white arrows). As the map obtained for TprC- ΔC2 (1627-2129 aa) was similar to the TprC-M4, results narrow down the target region to 100 aa stretch between aa 2029-2129.

4.2.2 Tpr is phosphorylated at residues S2059 and S2094 in vivo.

Phosphoamino acid analysis (Fig 4.1D) suggested that majority of ERK independent phosphorylation takes place on serine residues. Analysis of primary sequence within the target region showed presence of six serine containing tryptic peptides of which two peptides have overlaps with regions beyond 2029-2129 (Fig. 4.3A). Among the four remaining peptides (Table 1), peptide 4 could be eliminated as it harbours major ERK2 target site T2123, which based on our previous data (Fig 4.1C; indicated by arrow) migrates higher up in 2D-TLC. All the serine residues in the remaining three peptides were mutated to corresponding alanines by site directed mutagenesis to generate constructs TprC-M4-S2046,2047,2049A,   TprC-M4-S2059A and TprC-M4-S2094A and their expression in COS-1 cells were confirmed by western blots (Fig 4.3B). TprC-M4-S2046,2047,2049A mutant had the same pattern of tryptic phosphopeptides as TprC-M4, indicating that none of the serine residues in peptide 1 are targets for phosphorylation (Fig. 4.3C). Both, TprC-M4-S2059A and TprC-M4-S2094A displayed altered maps with spot 2 and 3, respectively missing in the peptide maps (Fig 4.3C). These results demonstrate S2059 and S2094 to be the ERK2 independent phosphorylation sites *in vivo*.

4.2.3 Characterization of phospho-specific antibodies of Tpr

In order to understand the functional significance of both ERK2 dependent and independent phosphorylation of Tpr protein, we raised phospho-specific antibodies that can specifically recognize phosphorylations on T2123, one of the major ERK2 target sites or S2059 or S2094, ERK2 independent sites. Prior to utilization of antibodies as
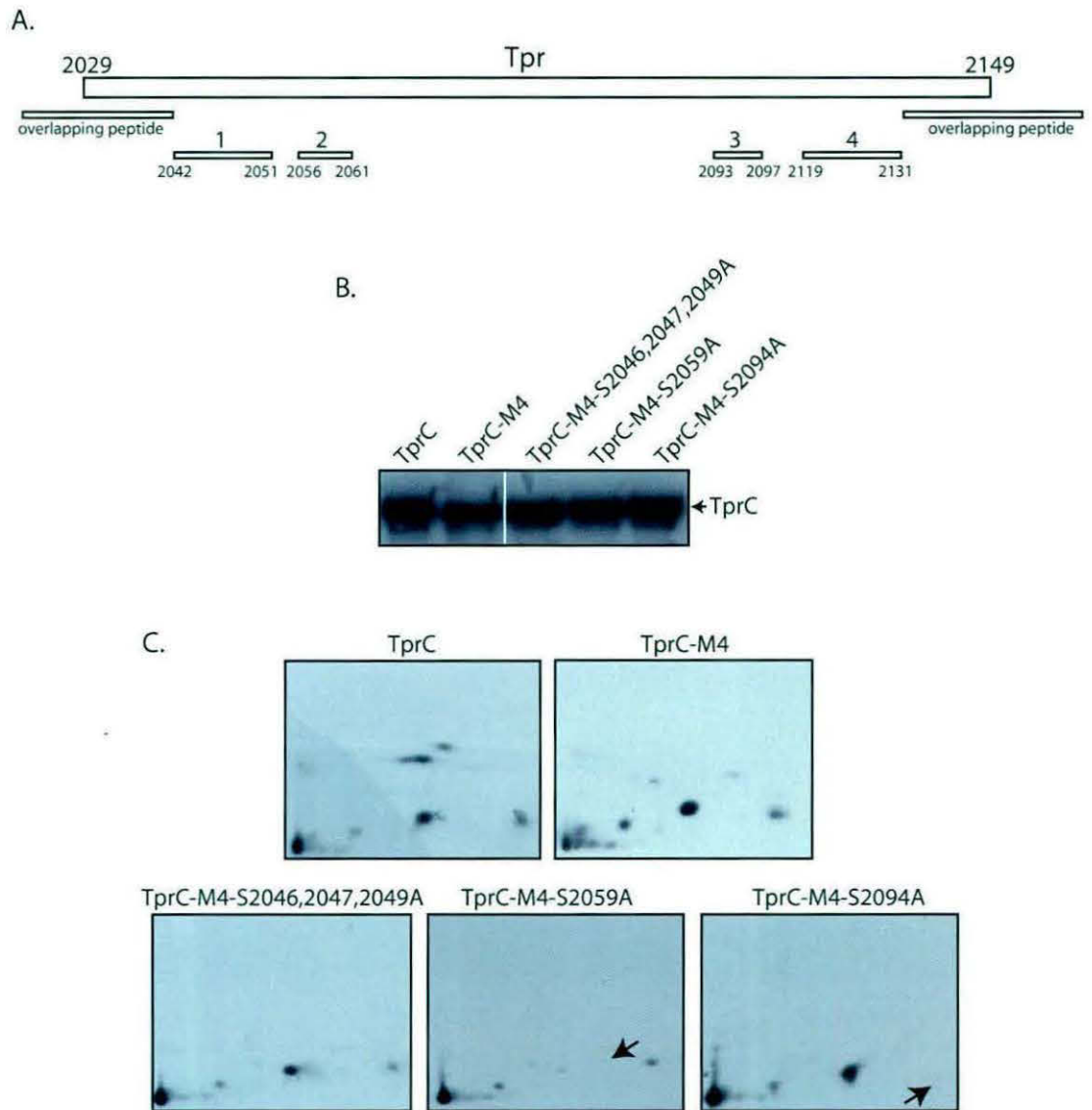
Figure 4.3. Identification of ERK2 independent phosphorylation sites on Tpr – (A) Schematic representation showing the serine containing peptides generated upon digestion from the region 2029-2149 of the Tpr. (B) 100 mm dishes of COS-I cells were individually transfected with 8 µg each of the wild-type TprC or TprC-M4 or TprC-M4-S2046,2047,2049A or TprC-M4-S2059A or TprC-M4-S2094A constructs. The cells were metabolically labelled for 3 hours and stimulated with EGF for 10 min. The FLAG-tagged proteins were immunoprecipitated, resolved, transferred, and autoradiographed. (C) The labeled proteins were digested with trypsin, and the resulting phosphopeptides were mapped by two-dimensional TLC. Arrows indicate the disappearance of labelled phospho-peptide spots in TprC-M4-S2059A and TprC-M4-S2094A.

anti-pTpr antibodies, one has to authenticate their specificity, which requires Tpr protein devoid of any phosphorylations as a negative control. Towards this, the TprC fragment, containing the carboxy terminal 800 aa of Tpr, was cloned into pQEII to generate pQEII-TprC construct, wherein the sequence of TprC was preceded by N-terminal hexa histidine tag. *E. coli* BL21 codon plus cells transformed with pQEII-TprC were induced with IPTG either at 37°C or 18°C to standardize the expression conditions (Fig 4.4A). While the expression could not be detected when the cultures were induced at 18°C, induction of cultures at 37°C clearly resulted in expression of TprC (Fig 4.4A; indicated by an arrow). Clarified *E. coli* lysates were bound to the Ni-NTA-agarose affinity matrix and His-TprC was eluted at different concentrations of imidazole (Fig 4.4B). Though, His-TprC started eluting from the matrix at 20 mM imidazole, it's elution was very efficient at 50 mM imidazole (Fig 4.4B). Peak His-TprC fractions were pooled, dialyzed and resolved on SDS-PAGE along with immunoprecipitated FLAG-TprC. As expected the migration of His-TprC was similar to FLAG-TprC, however, we did observe few additional bands corresponding to degraded His-TprC (Fig 4.4C).

To characterize the Tpr-p2059 antibody, COS-I cells were transfected with pCDNA3-FLAG or FLAG-TprC or FLAG-TprC-S2059A constructs. Lysates from the transfected cells and purified His-TprC were resolved on SDS-PAGE, and probed with anti-Tpr, anti-FLAG, anti-ERK2 and anti-Tpr-pS2059 antibodies. Though both bacterially expressed and immunoprecipitated FLAG-TprC could be efficiently detected with anti-Tpr antibodies, anti-Tpr-pS2059 antibodies could only detect FLAG-TprC (Fig 4.5A). FLAG-TprC-S2059A with serine to alanine mutation in the target site or the unphosphorylated His-TprC could not be detected by the anti-Tpr-p2059 antibody, demonstrating the ability of the antibody to specifically detect Tpr protein phosphorylated on S2059 residue (Fig. 4.5A). Next, we asked if anti-Tpr-pS2059 antibodies are capable of specifically detecting phosphorylation on full length Tpr in the western blot. COS-1 cells transfected with either the vector control or FLAG-Tpr-FL-Si or Tpr-FL-Si-S2059A or S2094A and lysates were probed with FLAG and anti-Tpr-pS2059 antibodies. anti-Tpr-pS2059 antibodies efficiently detected both Tpr and S2094A mutant. As expected, these antibodies failed to detect Tpr in which S2059 residue was mutated. Moreover, we observed that band corresponding to Tpr could be
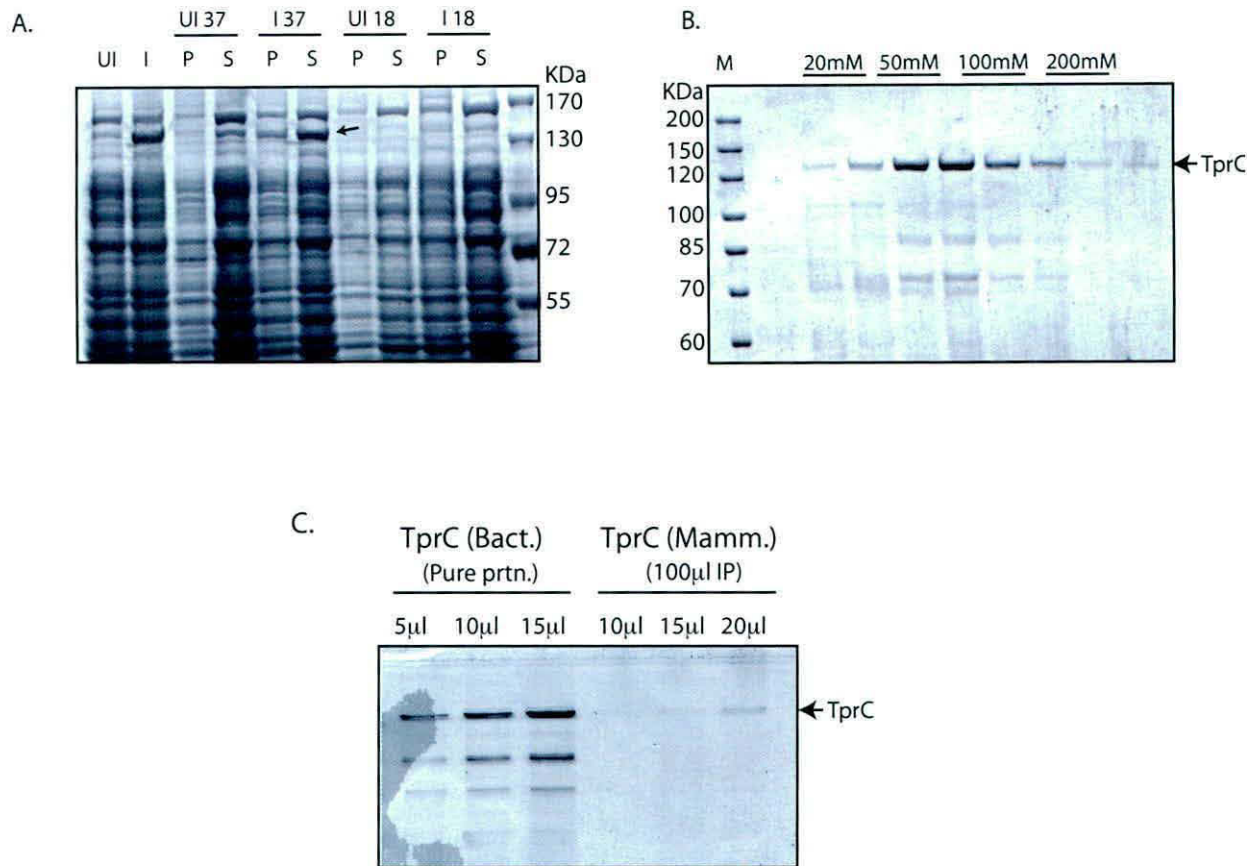
Figure 4.4. Expression and purification of His-tagged TprC protein – (A) E. coli BL-21 cells transformed with pQE-II-TprC construct were induced at 37 degrees Celsius and 18 degrees Celsius with 1 mM IPTG for 3 hours. The cells were lysed by sonication and the pellet and supernatant fractions were resolved by SDS-PAGE. Arrow indicates the expression of TprC protein in the soluble fraction upon the induction at 37 degrees Celsius. (B) Purification of the overexpressed His-TprC from the E.coli BL-21 cells transformed with pQE-II-TprC construct. Concentration of imidazole used for elutions are indicated on the top. (C) COS-I cells were transfected with FLAG-TprC construct and the lysates obtained were immunoprecipitated with α-FLAG antibodies. Different amounts of the immunoprecipitated mammalian TprC protein was loaded along side purified bacterial His-TprC in order to standardize the loading concentrations.
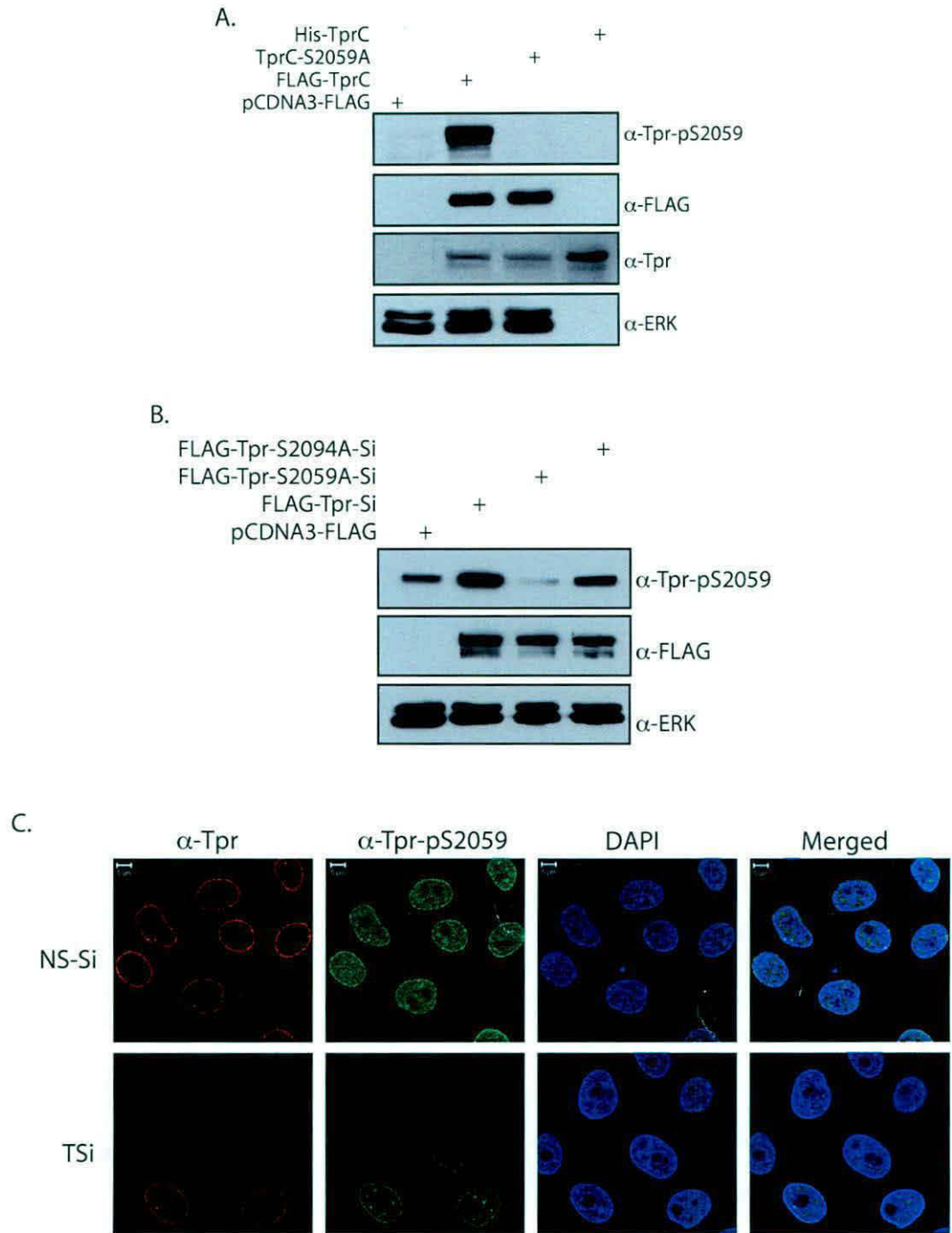
Figure 4.5. Characterization of the phospho-S2059 antibody – (A) COS-I cells in 6-well plates were transfected with 2 µg each of vector or FLAG-TprC or FLAG-TprC-S2059A constructs. Cells were lysed 36 h post transfection and the lysates along with purified His-TprC were resolved on 10% SDS-PAGE, transferred to nitrocellulose membranes and probed with α-FLAG, α-ERK2, α-Tpr (rabit) and α-Tpr-pS2059 antibodies. (B) COS-I cells in 6 well plates were transfected with 2 µg each of vector alone or FLAG-Tpr-Si or Tpr-S2059A-Si or Tpr-S2094A-Si constructs. The lysates were probed with α-FLAG, α-ERK2 and α-Tpr-pS2059 antibodies. (C) HeLa cells in 6 well plates were transfected with Non-specific siRNA (NS-Si) or Tpr-siRNA (TSi). 24 hours post transfection, the cells were trypsinzed and replated on coverslips. 24 hours post replating cells were stained with α-Tpr (red) and α-Tpr-pS2059 (green) antibodies and visualized by confocal microscopy.

detected even in vector transfected lanes, suggesting that these are effective in detecting phosphorylation on endogenous Tpr (Fig. 4.5B). While it is gratifying to know that anti-Tpr-pS2059 antibodies can specifically detect endogenous phosphorylation on Tpr, it is not always necessary that they also work for immunofluorescence. In order to establish the ability of anti-Tpr-pS2059 antibodies to detect phosphorylated Tpr, we performed indirect Immunofluoresence microscopy using the anti-p-S2059 antibodies. Results demonstrated rim staining with the anti-Tpr-pS2059 antibodies, which co-localized with the Tpr staining (Fig. 4.5C). Upon the siRNA treatment, characteristic Tpr rim staining disappeared with both anti-Tpr and anti-Tpr-pS2059 antibodies, establishing the ability of anti-Tpr-pS2059 to detect endogenous Tpr phosphorylated on S2059 (Fig. 4.5C).

To demonstrate the specificity and sensitivity of anti-Tpr-pS2094 antibodies, lysates from COS-1 cells transfected with the vector or pcDNA3-FLAG-TprC or pcDNA3-FLAG-TprC-S2094A were resolved along with His-TprC and probed with anti-Tpr, anti-FLAG, anti-ERK2 and anti-Tpr-pS2094 antibodies. Similar to the results obtained earlier both FLAG tagged as well as His tagged TprC proteins could be detected with anti-Tpr antibodies. While FLAG-TprC could be detected with anti-Tpr-pS2094 antibodies, both FLAG-TprC-S2094A and His-TprC could not be detected signifying the specificity of the antibodies in western blots for Tpr phosphorylated on S2094 residue (Fig. 4.6A). To ascertain the ability of anti-Tpr-pS2094 antibodies in recognizing the full-length Tpr protein, lysates from COS-1 cells transfected with wild type or the mutants of full length Tpr were probed. Analogous to the results obtained with TprC, anti-Tpr-pS2094 antibodies efficiently detected both TprFL and TprFL-S2059A, but not the TprFL-S2094A. Further, we observed that the anti-Tpr-pS2094 antibodies could detect endogenous phosphorylated Tpr (Fig. 4.6B). Indirect immunofluoresence microscopy using the anti-Tpr-pS2094 antibodies demonstrated rim staining, which co-localized with the Tpr staining detected using anti-Tpr antibodies (Fig. 4.6C). When the cells were treated with siRNA against Tpr, it was observed that in the cells where Tpr was knockdown, the pS2094-Tpr staining was also diminished (Fig. 4.6C). Interestingly, only ~ 50- 60% of the cell population showed rim staining with anti-Tpr-pS2094 antibodies, even though Tpr rim staining could be seen in all the cells (Fig.4.6C), suggesting probable modulation of S2094 phosphorylation during the cell

A.

B.

C.
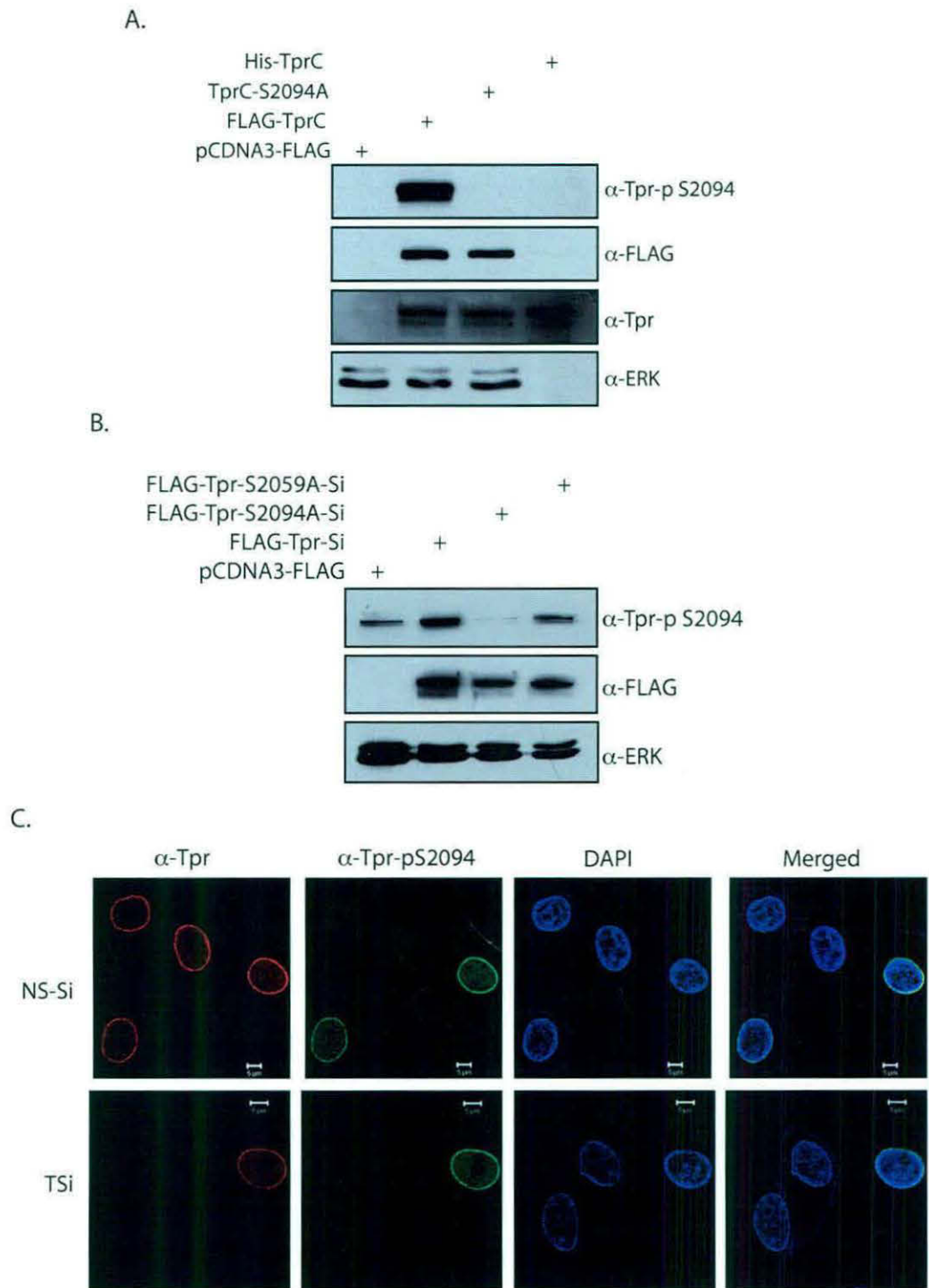
Figure 4.6. Characterization of the phospho-S2094 antibody - (A) COS-I cells in 6-well plates were individually transfected with 2 μg each of pCDNA3-FLAG, FLAG-TprC or FLAG-TprC-S2094A constructs. The lysates obtained 36 hours after transfection were loaded along with the purified bacterial His-TprC protein. Western blot analysis of the samples probed with α-FLAG, α-ERK2, α-Tpr and α-Tpr-pS2094 antibodies. (B) COS-I cells were transfected with 2 μg each of pCDNA3-FLAG, Tpr-Si, Tpr-S2059A-Si and Tpr-S2094A-Si constructs. The lysates were probed with α-FLAG, α-ERK2 and α-Tpr-pS2094 antibodies. (C) Immunoflourescence analysis of HeLa cells transfected with NS-Si or TSi for 48 hours post transfection and stained with α-Tpr (red) and α-Tpr-pS2094 (green) antibodies.

cycle. Taken together, data clearly demonstrate specificity and sensitivity of anti-Tpr-pS2059 and anti-Tpr-pS2094 antibodies to detect endogenous phosphorylation of Tpr on these residues through both western blots and in indirect immunofluorescence.

Previously we showed that ERK2 mediated phosphorylation of Tpr decreases upon serum starvation, and increases significantly upon EGF stimulation. In order to characterize anti-Tpr-pT2123 antibodies, lysates from COS-1 cells transfected with vector or FLAG-TprC or FLAG-TprC-M4 were either serum starved or stimulated post starvation with EGF, were resolved and probed with various antibodies. When the lysates were probed with anti-Tpr-pT2123 antibodies, band corresponding to TprC could only be detected in wild type not in the mutant (Fig 4.7A). Moreover, the levels detected increased significantly upon EGF stimulation, suggesting the specificity of anti-Tpr-pT2123 antibodies (Fig 4.7A; Lanes 3, 4). While the antibodies were specific, their ability to detect phosphorylated Tpr was observed to be poor compared with the anti-Tpr-pS2059 and anti-Tpr-S2094 antibodies. Poor detection of Tpr-T2123 phosphorylation could either be due to the insensitivity of antibody or due to low stoichiometry of T2123 phosphorylation *in vivo*. In order to decipher the reasons for the low levels of detection, COS-1 cells were transfected with pcDNA3 or FLAG-TprC or FLAG-TprC-M4 or HA-ERK2 and FLAG tagged Tpr and HA-tagged ERK2 were immunoprecipitated. Immunoprecipitated FLAG-TprC or TprC-M4 were either mixed with the vector control or HA-ERK2 and *in vitro* kinase reactions were in the presence of 1 mM ATP. Reactions were resolved and probed with either anti-FLAG or anti-Tpr-pT2123 antibodies (Fig 4.7B). It is apparent from the data that, while the antibody could efficiently detect phosphorylation of Tpr on T2123, we could not detect any signal either in the absence of ERK2 or when the reaction were carried out with the TprC-M4 mutant. These results indicate that the weak detection observed is most likely due to low stoichiometry of T2123 phosphorylation *in vivo*. Immunofluoresence microscopy using the anti-p-T2123 antibodies demonstrated a very mild rim staining that co-localized with the staining with Tpr antibodies. In addition to the rim staining, we detected strong intra-nuclear staining, which did not diminish when MAP kinase ERK2 pathway was inhibited by MEK inhibitor CI1040 (data not shown). These results raised concerns regarding the specificity of the antibody to detect endogenous Tpr protein in indirect immunofluorescence experiments.

A.

FLAG-TprCM4					+	+
FLAG-TprC			+	+		
pCDNA3-FLAG	+	+				
EGF		+		+		+

α-Tpr -pT2123
Short exposure

α-FLAG

α-ERK

B.

FLAG-TprCM4			+	+
FLAG-TprC	+	+		
HA-ERK2		+		+

α-Tpr -p2123 (6125)

α-Tpr -p2123 (6126)

α-FLAG

α-HA
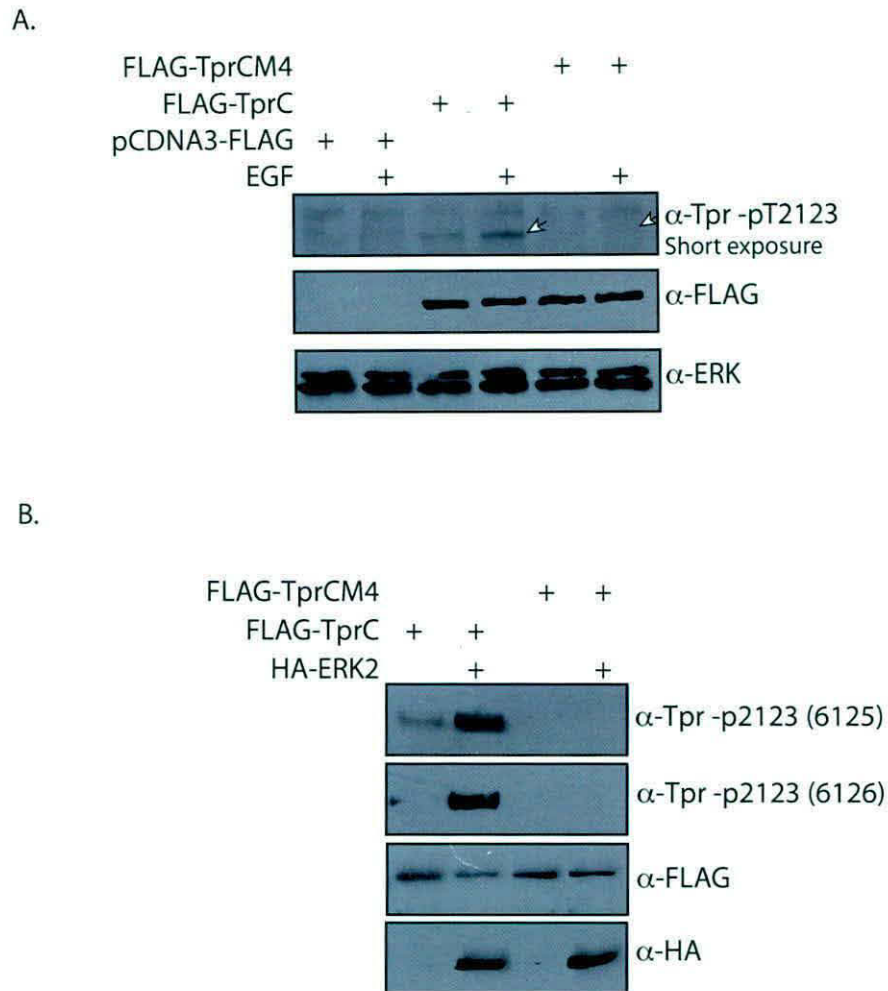
Figure 4.7. Characterization of the phospho-S2123 antibody – (A) COS-I cells in 6 well plates were transfected with 2 µg each of pCDNA3-FLAG or FLAG-TprC or FLAG-TprCM4 constructs. For the EGF-stimulated samples, EGF (20 ng/ml) was added for 10 min after 4 hours of serum starvation. The cell lysates were probed with anti-FLAG, anti-ERK, and anti-Tpr-pT2123antibodies. (B) COS-I cells were individually transfected with HA-ERK2, FLAG-TprC and FLAG-TprCM4 constructs. The HA-ERK2 sample was stimulated with EGF (20 ng/ml) for 10 min after 4 hours of serum starvation. The lysates were immunoprecipitated with anti-FLAG or anti-HA antibodies. The immunoprecipitated vector control or HA-ERK2 sample was mixed either with the immunoprecipitated FLAG-TprC or FLAG-TprCM4 proteins and Kinase reactions were carried out with 1 mM ATP at 30°C for 10 min. The samples were resolved, transferred onto nitrocellulose membrane and the blot was probed with two different bleeds of and anti-Tpr- pT2123antibodies.

4.2.4. Protein Kinase A (PKA) phosphorylates Tpr at the S2094 residue

The primary sequence of the TprC terminal fragment was analyzed with the help of phospho-site prediction software Scan-Site to identify the kinases that may phosphorylate S2059 and S2094 residues on Tpr (Table 4.1). To determine if these predictions are indeed true, we have performed *in vitro* kinase assays by mixing immunoprecipitated kinases with immunoprecipitated TprC or TprC-S2059A or TprC-S2094A proteins. In order to determine if PKA indeed phosphorylates S2094 residue, Cos-I cells were individually transfected with wild-type TprC, TprC-S2059A, TprC-S2094A and the kinases HA-ERK2 and CMV-PKA constructs. In agreement with our previous data, we observed robust phosphorylation of TprC by ERK2 (Fig 4.8A). While PKA strongly phosphorylated both TprC and TprC-S2059A, phosphorylation of TprC-S2094A mutant by PKA was almost negligible indicating the S2094 is indeed an *in vitro* target for PKA (Fig. 4.8.A). The bands corresponding to TprC phosphorylated by ERK2 and PKA were trypsinized and the peptide maps obtained were compared with those obtained for metabolically labelled TprC. As expected all the spots corresponding to ERK2 sites on migrated quite high up in the map (indicated by dotted elipse; Fig 4.8B). Spot corresponding to S2094 (spot 3) was only spot that could be detected upon phosphorylation by PKA, validating the bioinformatic prediction that S2094 residue on Tpr is indeed a target for PKA. Our efforts to identify the kinase for S2059 phosphorylation of Tpr have not been successful. *In vitro* kinase assays carried out with activated p38α and Cdk5 did not given any signal above the background with the C-terminal fragments of Tpr (data not shown).

Site S2094	Protein Kinase A	Sequence IQMTRRQSVGRGLQL	Score 0.3313
Site S2059	p38 MAPK	Sequence QAPRAPQSPRRPPHP	Score 0.2826
Site S2059	Cdk5 Kinase	Sequence QAPRAPQSPRRPPHP	Score 0.3673
Site S2059	Cdc2 Kinase	Sequence QAPRAPQSPRRPPHP	Score 0.3313

Table 4.1: Putative cellular kinases that may phosphorylate S2059 and S2094 residues on Tpr identified by phospho-site prediction *software* Scan-Site.
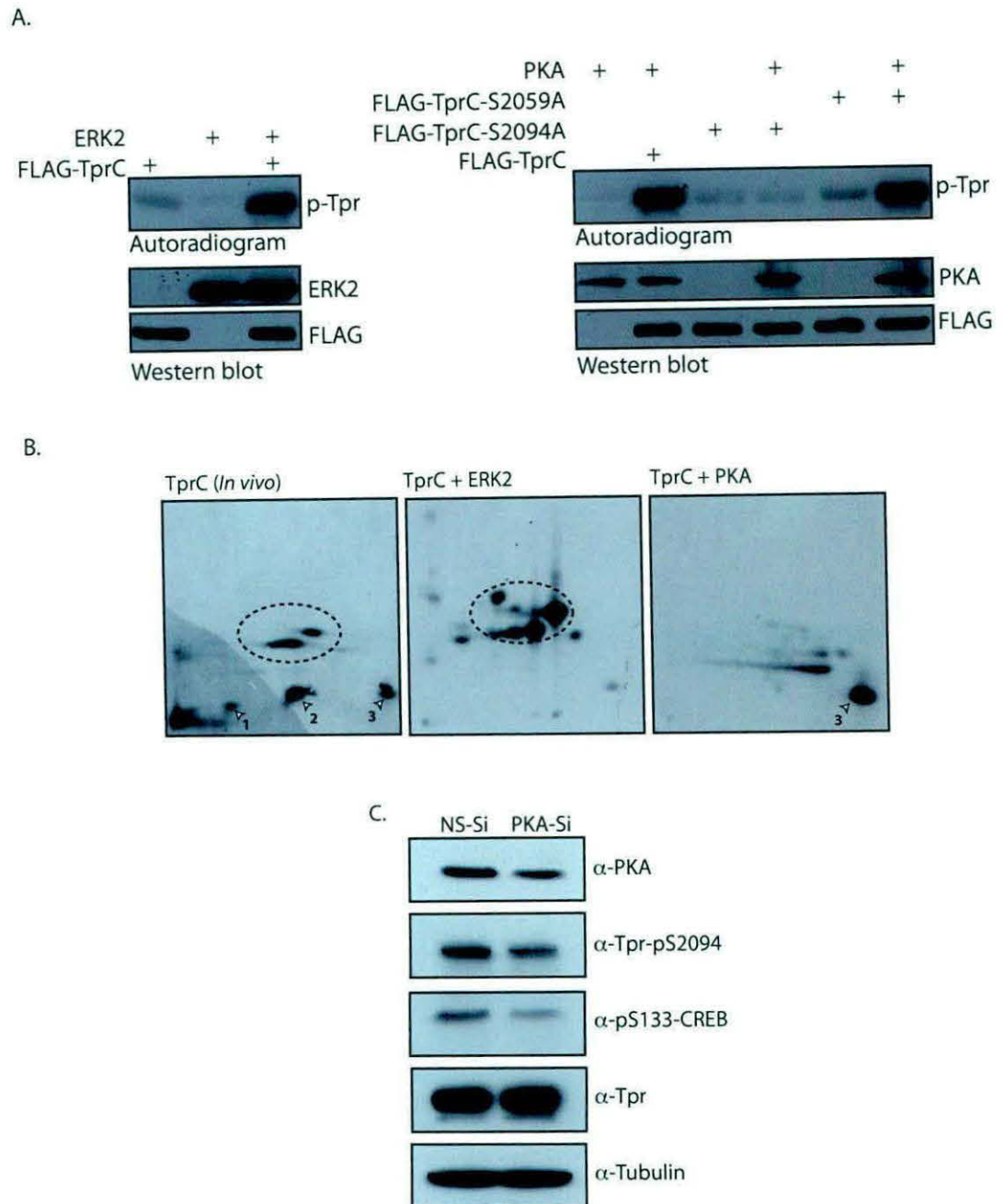
Figure 4.8. PKA phosphorylates Tpr at S2094 residue both in vitro and in vivo – (A) COS-I cells were transfected individually with 8 µg each of wild-type FLAG-TprC, FLAG-TprC-S2059A, FLAG-TprC-S2094A, HA-ERK2, CMV-PKA constructs. The lysates of cell obtained 36 hours post transfection were immunoprecipitated with α-FLAG, α-HA or α-PKA antibodies. The immunoprecipitated FLAG-TprC was mixed with immunoprecipitated HA-ERK2 and Kinase reactions were carried out with [γ-32P]ATP at 30°C for 10 min. The immunoprecipitated CMV-PKA sample was distributed and mixed either with the immunoprecipitated FLAG-TprC, FLAG-TprC-S2059A or FLAG-TprC-S2094A samples. Kinase reactions were carried out with [γ-32P] ATP at 30°C for 10 min. (B) In vitro phosphorylated TprC by either ERK2 or PKA was digested with trypsin, and the resulting phosphopeptides were mapped by two-dimensional TLC. Comparative peptide map of the in vivo labeled TprC protein is also represented. (C) COS-I cells were transfected with siRNA against PKA. 48 hours after the siRNA treatment, the cell lysates were probed with α-PKA, α-Tubulin, α-pS133-CREB, α-Tpr and α-Tpr-pS2094 antibodies.

Next we asked if S2094 of Tpr is a bonafide target for PKA *in vivo*. HeLa cells were transfected either with Non-Specific siRNA (NS-Si) or PKA-siRNA and lysates were probed with various antibodies. PKA is known to be required for phosphorylating CREB on S133. Western blot results showed that partial depletion of PKA resulted in decreased phosphorylation of CREB on S133 (Fig 4.8C). Interestingly, while the Tpr levels were unchanged, phosphorylation of Tpr on S2094 also showed reduction upon PKA depletion (Fig 4.8C). Collectively, data demonstrates that Tpr is a bona fide substrate of PKA both *in vitro* and *in vivo*, and that the PKA phosphorylates Tpr on S2094 residue.

4.2.5 Tpr protein levels and its phosphorylation are regulated during cell cycle

Several studies shed light on the crucial role played by Tpr and its homologs during mitosis [18, 19, 185, 188]. Further, mitotic-specific hyper phosphorylation of nucleoporins has also been demonstrated [31-34, 90-92]. We therefore sought to investigate the phosphorylation status of Tpr during the cell cycle and specifically during mitosis. Towards this, HeLa cells were arrested at pro-metaphase stage by treatment with nocadazole and the arrested cells were released at specific time points to obtain synchronized cell population at different stages of the cell cycle. FACS analysis of the samples stained with Propidium Iodide confirmed the mitotic arrest and the subsequent synchronized release into the G1 and S Phases of cell cycle (Fig. 4.9A). Analysis of Tpr protein levels during different stages of mitosis by immunoblot provided preliminary evidence that Tpr levels are higher during the mitotic stages compared with the interphase (Fig. 4.9B). We plan to determine the levels of Tpr phosphorylation on S2059 and 2094 residues after mitotic arrest and subsequent release.

Immunofluoresence analysis of HeLa cells at different stages of mitosis by phospho-S2059 antibody indicated that Tpr is phosphorylated at S2059 both at interphase and during the mitosis (Fig. 4.10A). Tpr-p2059 co-localized with unphosphorylated Tpr during Interphase and all the way up to anaphase of the mitosis. Interestingly, during the telophase we observed that localization of Tpr-p2059 to be different from the localization of unphosphorylated Tpr. Tpr-p2059 seemed to co-localize with chromatin whereas the unphosphorylated Tpr appeared to localize away

A.

B.

0' 15' 30' 45' 1h 4h 8h 12h

α-Tpr

α–β-Actin
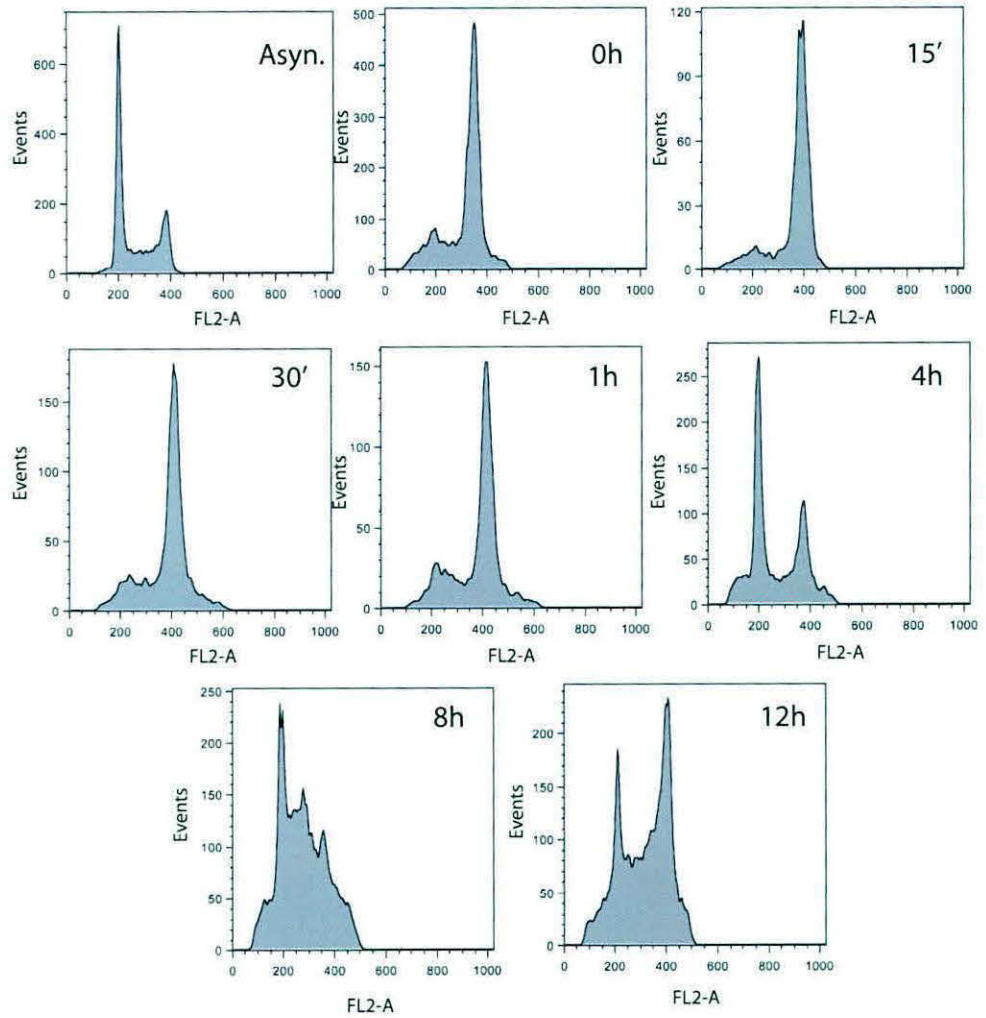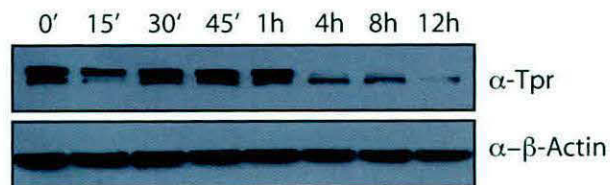
Figure 4.9. Tpr protein levels are regulated during the cell cycle - HeLa cells were arrested at pre-mitotic stage by treatment with 40 ng/ml Nocadazole for 16 hours and were subsequently released at different time points by washing off the drug. (A) FACS analysis of the samples stained with Propidium Iodide to check for the synchronization of cells post release of the Nocodazole block. (B) Western blot analysis of the lysates obtained from cells harvested at different time points after release of Nocadazole block and probed with α-Tpr α-β-Actin antibodies.
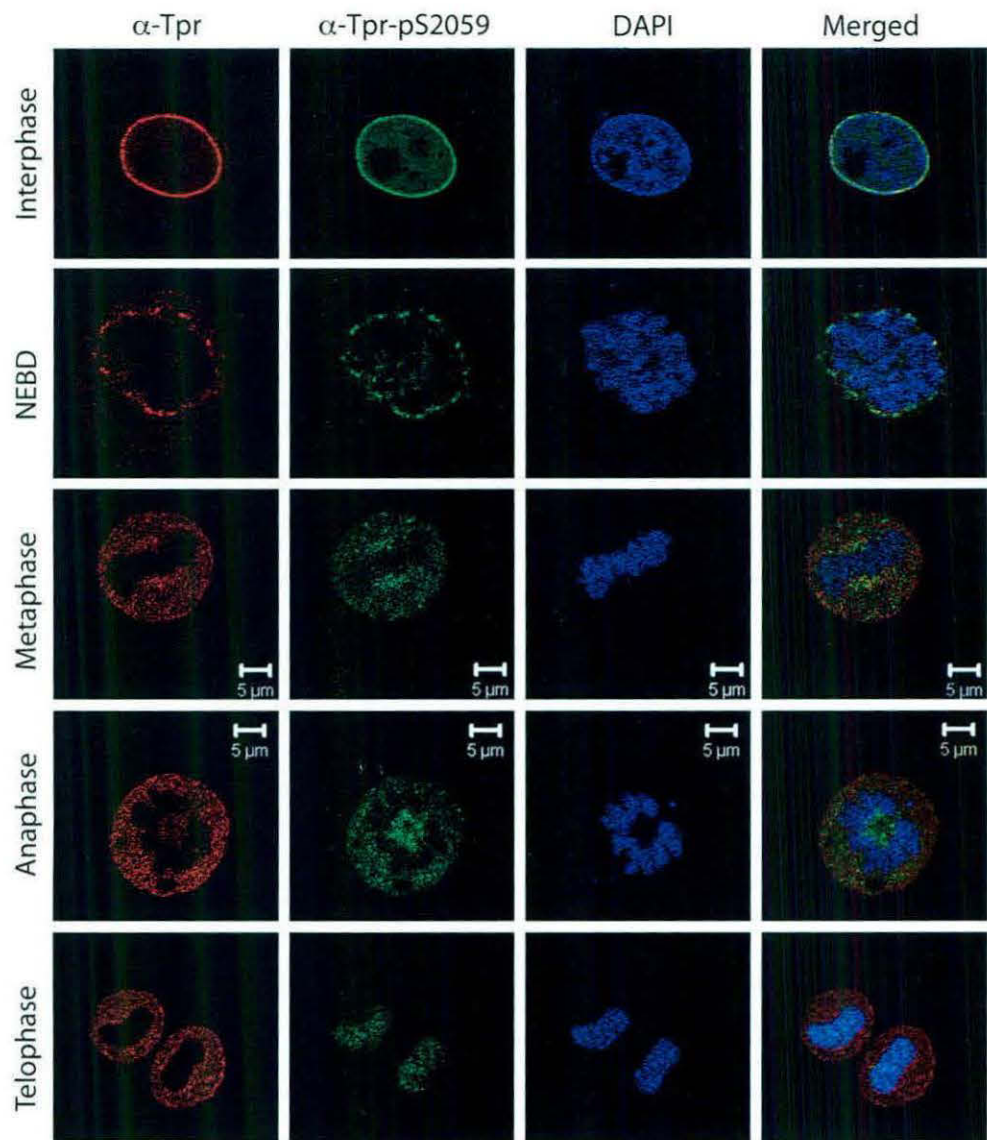
Figure 4.10. Status of S2059 phosphorylation during mitosis- Immunofluorescence analysis of asynchronous HeLa cell population stained with DAPI (blue), α-Tpr (red) and α-Tpr-pS2059 (green) antibodies. Confocal microscopic images of the cells captured at different stages of mitosis are represented (Scale bar, 5 μM).

from the chromatin. Work is underway to decipher the biological significance of Tpr-p2059 localization with the chromatin during the telophase.

When a similar analysis was performed with phospho-S2094 antibody, significant dephosphorylation as reflected by the absence of green fluoresence, was observed during the telophase (Fig. 4.11A). However, it was apparent that all the other mitotic stages had the presence of S2094 phosphorylation (Fig. 4.11A). The localization of Tpr-pS2094 was observed to be the same as unphosphorylated Tpr both during Interphase and the mitosis. We speculate based on the data presented here and in Fig.4.6C, that phosphorylation of Tpr on S2094 is modulated during the cell cycle. We need to validate our hypothesis and determine the precise biological role played by the phosphorylation of Tpr on S2094 residue. Collectively, results provide critical preliminary data that phosphorylation of Tpr may modulate the stability and localization during the mitosis.

4.2.6. Tpr is mislocalized when all the target phosphorylation sites are mutated.

To understand the functional significance of Tpr phosphorylation, we generated siRNA resistant phosphorylation site mutants of Tpr, namely Tpr-Si-S2059A, Tpr-Si-S2094A and Tpr-Si-M6 by site directed mutagenesis. In Tpr-Si-M6 construct, we have mutated both ERK2 target sites and ERK2 independent sites (S2059 and S2094) to corresponding alanine residues. Western blot analysis of the lysates clearly confirmed the expression of the proteins (Fig 4.12A). Interestingly, we observed anomalous migration pattern of the Tpr-Si-M6 mutant in the immunoblot (Fig 4.12A; compare Lanes 2 and 6). In the indirect immunofluoresence microscopy experiments, distinct nuclear rim staining was observed in cells transfected with Tpr-Si, Tpr-Si-M4, Tpr-Si-S2094A constructs (Fig 4.12B). However, the rim localization of Tpr-Si-S2059A mutant was not very apparent (Fig 4.12B). Importantly, the localization of Tpr-Si-M6 mutant was found to be entirely in the cytoplasmic region (Fig 4.12B). Taken together, the expression profile and the cytosolic localization of the Tpr-Si-M6 mutant are suggestive of the fact that the phosphorylation on Tpr protein is critical for maintaining the structural integrity, stability and localization.
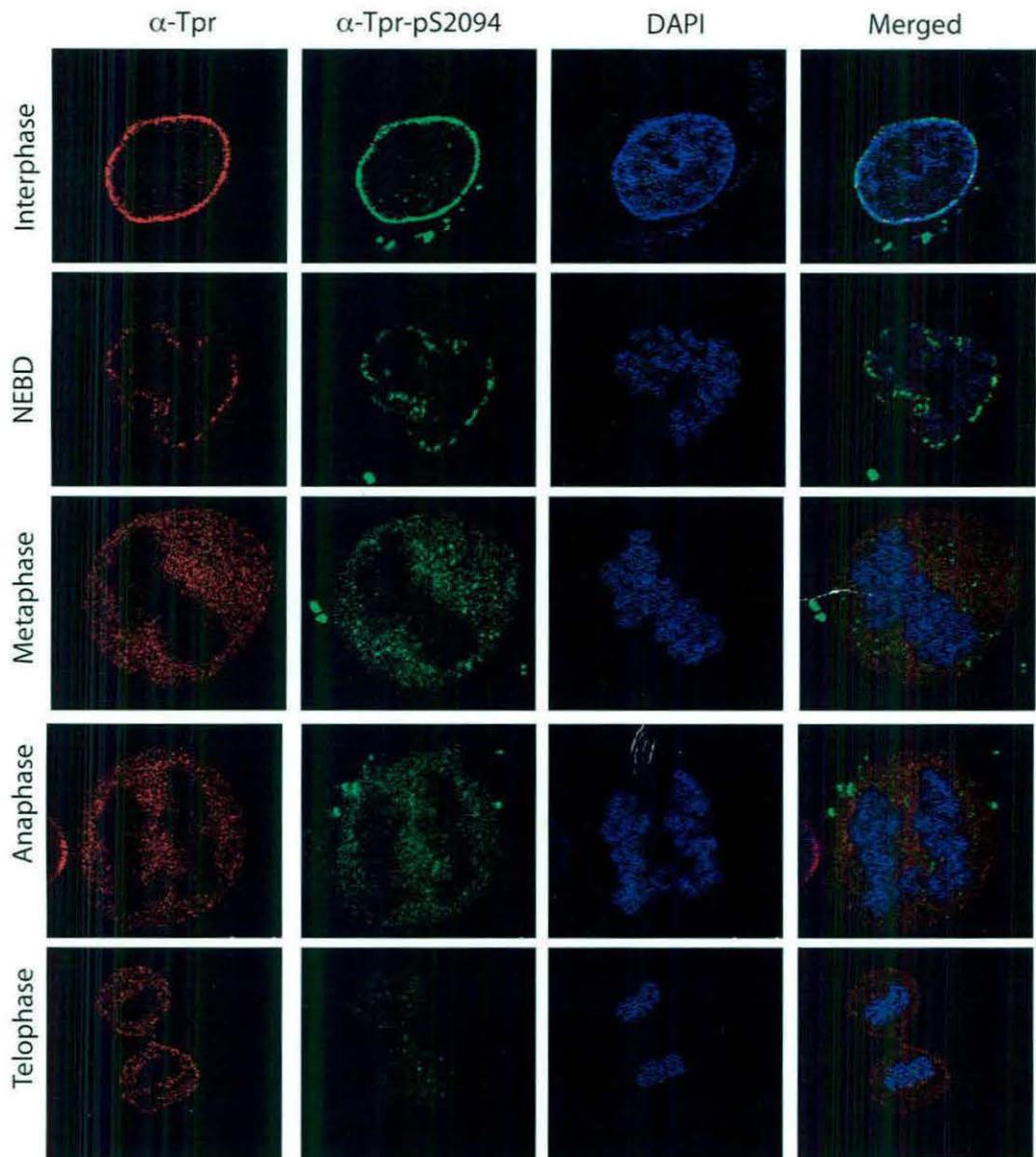
Figure 4.11. Status of S2094 phosphorylation during mitosis - Immunofluoresence analysis of asynchronous HeLa cell population stained with DAPI (blue), α-Tpr (red) and α-Tpr-pS2094 (green) antibodies. Confocal microscopic images of the cells captured at different stages of mitosis are represented (Scale bar, 5 μM).
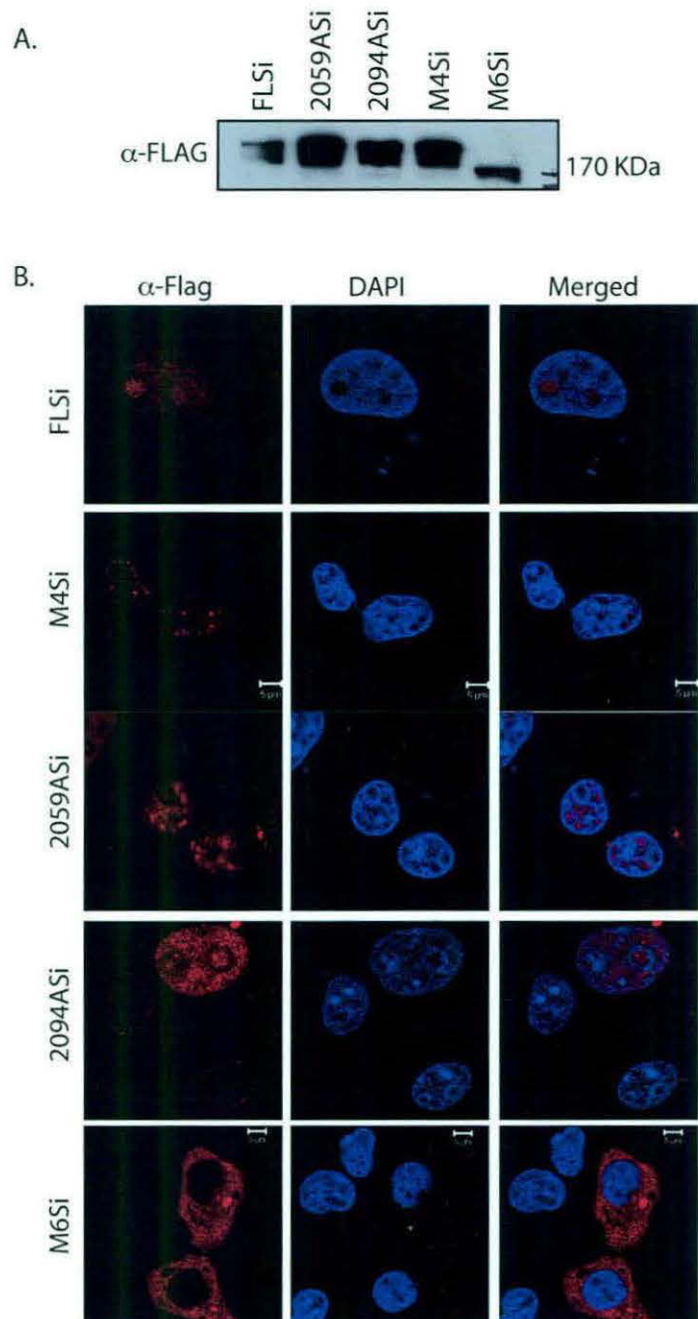
Figure 4.12. Expression and localization of Tpr phospho mutants – (A) COS-I cells were transfected with 2 µg each of FLAG-tagged Tpr-Si, Tpr-M4Si, Tpr-S2059ASi, Tpr-S2094A and Tpr-M6Si constructs. 24 hours post transfection, the lysates were resolved on SDS-PAGE, transferred on to nitrocellulose membrane and probed with α-FLAG antibodies to check for the expression of these constructs. (B) Immunofluoresence analysis of COS-I cells transfected with Tpr-Si and various phospho mutants of Tpr, stained with DAPI (blue) and α-FLAG antibodies (red) (Scale bar, 5 µM).

4.3. Discussion

In the present study, we have identified novel *in vivo* ERK2 independent phosphorylation sites, S2059 and S2094 on the Tpr protein. We demonstrated that one of the residues on Tpr protein is phosphorylated by Protein Kinase A and this phosphorylation may be regulated at different stages of the cell cycle. Phosphospecific antibodies were raised against these residues and they were found to be specific to the phosphorylated form of the protein. Collectively, our data provides evidence that Tpr is phosphorylated by multiple kinases inside the cell and these phosphorylations may play a critical role during mitosis.

Mammalian protein kinase A (PKA), protein kinase C (PKC), the *S. cerevisiae* casein kinase and the *Aspergillus nidulands* Ser/Thr kinase NIMA have also been shown to phosphorylate NPC components [166, 167]. Phosphorylation of structural proteins of the nuclear pore complex appears to be necessary for nuclear import [69, 168], and the kinases responsible for the phosphorylation may be cAMP-dependent protein kinase [169-171], protein kinase C [172], or both[169]. Results showed that Protein Kinase A (PKA) phosphorylates Tpr *in vivo* at S2094 residue. It can be inferred from the results presented in Chapter 3 that Tpr has limited role in the protein transport across the NPC. Moreover, results also suggest that C-terminal region of the Tpr protein may not be involved in regulating the CTE-dependent unspliced RNA export. Hence, we speculate that PKA mediated phosphorylation of S2094 of Tpr may not influence the export of intron containing mRNA. Data presented in Fig 4.6C and 4.11 suggested that phosphorylation of S2094 residue may be modulated during the cell cycle occurs and specifically phosphorylation of S2094 was observed be dephosphorylated during telophase. Previous studies have demonstrated that PKA mediated phosphorylation enhances the protein stability [207-209]. In few instances, it has been shown that increase in the protein stability is due to the inhibition of ubiquitination [207, 210]. Efforts are underway to elucidate the functional significance of stage specific regulation of S2094 phosphorylation and its role, if any, in the stability of Tpr.

Across species, Tpr and its homologs have been shown to be critical for the progression of Mitosis. Yeast homolog, Mlp2 was shown to promote spindle assembly by binding to the yeast spindle body [185]. The recruitment of Mad2 and Mps1 proteins to the unattached kinetochores is promoted by Mtor protein resulting in the progression of

91

spindle checkpoint and thereby resulting in the normal duration of Mitosis [188]. The association of Mad1 and Mad2 proteins with Tpr has been shown to affect mitotic spindle checkpoint signalling [18]. Depletion of Tpr results in a chromosome lagging phenotype and this phenomenon is due to the loss of interaction between Tpr and dynein complex [19]. Cell cycle defects such as multinucleation and presence of micronuclei were reported to occur upon Tpr depletion [18]. Further, nucleoporins were reported to be extensively phosphorylated during the mitosis and this mitotic-specific hyperphosphorylation was demonstrated both *in vitro* and *in vivo* [31-34, 90-92]. Mitotic phosphorylation of FG-Nups was shown to be critical for the organization of spindle microtubules and chromosomes [157-160]. We observed significant phosphorylation of Tpr at both S2059 and S2094 residues during the metaphase and anaphase. Moreover, we observed localization of Tpr phosphorylated on S2059 along with chromatin during the telophase, while the unphosphorylated Tpr was localized around chromatin. These observations are suggestive of the fact that the phosphorylations may be crucial for mediating Tpr's function during mitosis. Further attempts would be directed towards delineating as to whether these phosphorylations play any role in regulating the interaction between Tpr and the Mad proteins or the dynein complex.

Phosphorylation mediated by Ser/Thr kinase Cdk1 was thought to regulate the breakdown of the nuclear envelope and the disassembly of the NPC into different subcomplexes during mitosis [33, 162, 163]. A recent report demonstrated that the phosphorylation of Nup98 by various cellular kinases was necessary for NPC disassembly during mitosis [161]. A study using temperature-sensitive Cdk1 *Drosophila* embryos showed that Cdk1 activity is required for maintaining the NPCs dissociated during mitosis, while the reassembly may be phosphatase- dependent [162]. While we did not see significant changes in the level of Tpr phosphorylated at S2059 residue, the levels of S2094 at telophase were significantly lower. We aim to decipher if dephosphorylation of S2094 residue at the end of the mitosis is a pre-requisite for the post-mitotic reassembly of Tpr at the NPC.

A recent study has shown that nucleoporin Tpr is important for establishing nucleopore associated heterochromatin exclusion zones and thereby mediating the formation of distinct intra-nuclear sub-compartments [190]. Results obtained in this study specifically indicate that Tpr phosphorylated at S2059 residue was found to be

associated with the chromatin at the telophase, just before the NPC reassembly. Future investigations would shed light on whether such chromatin bound phosphorylated form of Tpr is critical in the establishing the perinuclear heterochromatin exclusion zones during the re-formation of nuclear envelope.

Taken together, these results provide evidence that Tpr protein, similar to its other counterpart nucleoporins, also exhibits mitotic-specific hyperphosphorylation. The identification of novel phosphorylation sites on Tpr and the observations presented in this study would open up fresh avenues. A Detailed study of the mechanistic details of Tpr phosphorylation would thereby assist us to delve deeper in to the crucial roles played by Tpr, such as spindle assembly and chromatin organization. These insights obtained by further research may provide a better understanding as to how various cellular processes are regulated at the Nucleopore complex during various stages of the cell cycle.

Appendix – I

List of Abbreviations

NPC	Nucleopore Complex
Nups	Nucleoporins
Tpr	Translocated promoter region
FG repeats	Phenyl alanine-Glycine repeats
NES	Nuclear export signal
NLS	Nuclear localization signal
RNA	Ribonucleic acid
mRNA	Messenger Ribonucleic acid
DNA	Deoxyribonucleic acid
cDNA	Complementary Deoxyribonucleic Acid
mRNPs	messenger ribonucleoproteins
HIV	Human Immunodeficiency virus
RRE	Rev response element
MMPV	Mason-pfizer monkey virus
CTE	Constitutive transport element
ERK	Extracellular signal regulated kinase
Nxf1	Nuclear export factor 1
Sam68	Src associated in mitosis, 68 kDa
Cdk1	Cyclin dependent kinase 1
PKA	Protein Kinase A
GFP	Green Fluorescent Protein
kDa	Kilo Dalton(s)
aa	Amino acids

siRNA	Small interfering ribonucleic acid
ELISA	Enzyme linked immunosorbent assay
PBS	Phosphate buffered saline
PBST	Phosphate buffered saline and 0.05% Tween 20
ATP	Adenosine triphosphate
EDTA	Ethylenediaminetetraacetic acid
EGTA	Ethylene glycol tetraacetic acid
HEPES	N-2-Hydroxyethylpiperazine-N'-2-ethanesulphonic acid
ONPG	o-nitrophenyl-β-D-galactopyranoside
EGF	Epidermal Growth Factor
ml	millilitre
mg	milligram
mM	millimolar
μl	microlitre
μM	micromolar
μg	microgram
ng	nanogram(s)
SDS	Sodium dodecyl sulphate
PAGE	Polyacrylamide gel electrophoresis
qRT-PCR	Quanititative real-time Polymerase chain reaction
DMEM	Dulbecco's modified Eagle's medium
FBS	Fetal bovine serum
NCS	Normal Chicken serum
M	Molar

rpm	Revolutions per minute
h	Hours
min	minutes
PMSF	phenylmethylsulphonyl flouride
IPTG	isopropyl 1-thio-β-D-galactopyranoside

Table A1: List of Plasmid Constructs used in the study

Construct	Description	Source
pcDNA3	**Mammalian expression vector, CMV promoter, T7 promoter for cloning in *E.coli*, Amp^R Neo^R**	**Invitrogen**
Luciferase	Luciferase gene cloned into NotI and XbaI sites	Dr.Sudanshu Vrati
Luc-CTE	Casette containing 3' splice site with part of pol region, 5'Splicesite and CTE from MMPV genome along with the kuciferase gene cloned into NotI and XbaI sites.	This study
pcDNA3-FLAG	**Mammalian expression vector, CMV promoter, T7 promoter for cloning in *E.coli*, Amp^R Neo^R with an N-terminal FLAG tag.**	
FLAG-TprC	C-terminal 800 amino acids of Tpr cloned into NotI and ApaI	Vomastek *et al.*, MCB 2008 [36].
FLAG-TprCM4	C-terminal 800 amino acids of Tpr containing mutations in ERK2 target sites, cloned into NotI and ApaI	Vomastek *et al.*, MCB 2008 [36].
FLAG-Tpr -FL	Tpr cloned into NotI and ApaI	Vomastek *et al.*, MCB 2008 [36].
FLAG-Tpr-FLSi	Tpr containing silent mutations in the siRNA target region, cloned into NotI and ApaI	Vomastek *et al.*, MCB 2008 [36].
FLAG-Tpr-FLM4	Tpr containing mutations in ERK2 target site cloned into NotI and ApaI	Vomastek *et al.*, MCB 2008 [36].
FLAG-TprFLSiM4	Tpr containing silent mutations in the siRNA target region and also has mutated ERK2 target sites cloned into NotI / ApaI	Vomastek *et al.*, MCB 2008 [36].
FLAG-ERK2	ERK2 cloned into NotI / XbaI	Vomastek *et al.*, MCB 2008 [36].
FLAG-TprN	N-terminal 800 aa of Tpr cloned into NotI / ApaI	This study
FLAG-TprM	The region of Tpr between 800aa-1600aa	This study

	cloned into NotI / ApaI	
FLAG-TprNM	N-terminal 1600 aa of Tpr cloned into NotI / ApaI	This study
FLAG-TprMC	The region of Tpr between 1600 aa – 2349 aa cloned into NotI / ApaI	This study
FLAG-Tpr– 1627-2249	The region of Tpr between 1627 aa-2249aa cloned into NotI / ApaI	This study
FLAG-Tpr – 1627-2149	The region of Tpr between 1627aa-2149aa cloned into NotI / ApaI	This study
FLAG-Tpr – 1627-2049	The region of Tpr between 1627aa-2049aa cloned into NotI / ApaI	This study
FLAG-Tpr – 1728-2349	The region of Tpr between 1728 aa-2349aa cloned into NotI / ApaI	This study
FLAG-Tpr – 1826-2349	The region of Tpr between 1826 aa-2349aa cloned into NotI / ApaI	This study
FLAG-Tpr – 1926-2349	The region of Tpr between 1926 aa-2349aa cloned into NotI / ApaI	This study
FLAG-Tpr-Si - L458P/M489P	Tpr containing silent mutations in the siRNA target region and mutated L458P/M489P residues, cloned into NotI and ApaI	This study
FLAG-TprCM4- S349, 355A	C-terminal 800 amino acids of Tpr containing mutations in ERK2 target sites along with mutated serine residues at 349, and 355 positions, cloned into NotI and ApaI	This study
FLAG-TprCM4-S395, 398A	C-terminal 800 amino acids of Tpr containing mutations in ERK2 target sites along with mutated serine residues at 395, and 398 positions, cloned into NotI and ApaI	This study
FLAG-TprCM4- S408, 409A	C-terminal 800 amino acids of Tpr containing mutations in ERK2 target sites along with mutated serine residues at 408, 409, 424 positions, cloned into NotI and ApaI	This study

FLAG-TprCM4- S411A	C-terminal 800 amino acids of Tpr containing mutations in ERK2 target sites along with with mutated S411 residue, cloned into NotI and ApaI	This study
FLAG-TprCM4- S415A	C-terminal 800 amino acids of Tpr containing mutations in ERK2 target sites along with with mutated S415 residue, cloned into NotI and ApaI	This study
FLAG-TprCM4- S434A (S2059A)	C-terminal 800 amino acids of Tpr containing mutations in ERK2 target sites along with with mutated S434 residue, cloned into NotI and ApaI	This study
FLAG-TprCM4- S469A (S2094A)	C-terminal 800 amino acids of Tpr containing mutations in ERK2 target sites along with mutated S469 residue, cloned into NotI and ApaI	This study
FLAG-TprCM4-S421, 422, 424A	C-terminal 800 amino acids of Tpr containing mutations in ERK2 target sites along with mutated serine residues at 421, 422, 424 positions, cloned into NotI and ApaI	This study
FLAG-Tpr-FLSi - S2059A	Tpr containing silent mutations in the siRNA target region and mutated S2059A residue, cloned into NotI and ApaI	This study
FLAG-Tpr – FLSi - S2094A	Tpr containing silent mutations in the siRNA target region and mutated S2094A residue, cloned into NotI and ApaI	This study
FLAG-Tpr - FLSi - S2046, 2047, 2049A	Tpr containing silent mutations in the siRNA target region and mutated S2046, 2047, 2049A residues, cloned into NotI and ApaI	This study
FLAG-Tpr-FLSi-M6	Tpr containing silent mutations in the siRNA target region and also has mutated ERK2 target sites & S2094A, S2059A residues, cloned into NotI / ApaI	This study
FLAG-Tat	Tat cloned into NotI/XbaI	This study
FLAG-Rev	Rev cloned into NotI/XbaI	This study

FLAG-Tap/Nxf1	Tap/Nxf1 cloned into NotI/XbaI	This study
FLAG-Nxt1	Nxt1 cloned into NotI/XbaI	This study
pcDNA3-HA	**Mammalian expression vector, CMV promoter, T7 promoter for cloning in *E.coli*, Amp^R Neo^R with an N-terminal HA tag.**	**Invitrogen**
HA-ERK2	ERK2 cloned into NotI / XbaI	Vomastek *et al.*, MCB 2008 [36].
HA-Sam68	Sam68 cloned into NotI/ApaI	**Addgene**
HA-Tap/Nxf1	Tap/Nxf1 cloned into NotI/XbaI	This study
HA-Nxt1	Nxt1 cloned into NotI/XbaI	This study

Table A2: Sequence of siRNA oligonucleotides used in the study

Name	Sequence
Tpr-siRNA	GCACAACCAGGATAAGGTTA
Tpr-siRNA1	GAAGAAGUGCGUAAGAAUA
Tpr-siRNA2	GGCAUACACUUACUAGAAA
Nup153-siRNA	GAUAGGAGUGGGAUAGAUA
Nup214-siRNA	UCAAAUACCUCUAACCUAU
Nup358-siRNA	GCGAAGUGAUGAUAUGUUU
Nup98-siRNA	GAACAACCAACCUAAGAUU
Nup50-siRNA	CCAAAGUAGUAGUUACCGA
Sam68-siRNA	GCACCCAUAUGGACGUUAU
Tap/Nxf-1-siRNA	GGGAAGUCGUACAGCGAAC
Tap-siRNA-2	GCGCCAUUCGCGAACGAUU
Tap-siRNA-SP	CGAUGAUGAACGCGUUAAU
	AAUUGAAGUCUGAGCGGGA
	GGGAAGUCGUACAGCGAAC
	GCGCCAUUCGCGAACGAUU

Table A3: List of primers used in this study

Number	Primer Description	Primer Sequence
VK135	Nup153 forward NdeI site	CACCCATATGGCCTCGGGAGCCGGAGGAGTC
VK136	Nup153 Reverse NotI site	AAGCGGCCGCTTATTTCCTGCGTCTAACAGCAGTC
VK219	Nup214 Forward (EcoRI & NdeI)	CACCGAATTCAGATCTCATATGGGAGACGAGATGGATGCC
VK220	Nup214 Reverse (HindIII & XbaI)	TCTAGAAAGCTTAGCTTCGCCAGCCACCAAAACC
VK310	pCDNA3 Forward	TAATACGACTCACTATAGGG
VK311	pCDNA3 Reverse	TAGAAGGCACAGTCGAGG
VK315	5'splice site–Forward- Nhe-1	CACCGCTAGAGAGGAGCTCTCTCGACGCAGG
VK316	5'splice site-Reverse- HindIII	TTCAAGCTTACCCATCTCTCTCCTTCTAGC
VK317	Luciferase –Forward – HindIII	CACCAAGCTTGAAGATGCCAAAAACATTAAGAAG
VK318	Luciferase –Reverse - KpnI	TGCGGTACCTTACACGGCGATCTTGCCGCC
VK319	EGFP – Forward - HindIII site	CACCAAGCTTGTGAGCAAGGGCGAGGAGCTG
VK320	EGFP – Reverse - KpnI site	GCAGGTACCTTACTTGTACAGCTCGTCCATGCC
VK321	3'splice site-Forward- KpnI	CACCGGTACCAGCAGAAGTTATTCCAGCAGA
VK322	3'splice site–Reverse-XbaI & EcoRV	ATCTCTAGATATCTCGACACCCAATTCTGAAAATG

VK323	CTE – Forward - EcoRV	CACCGATATCACCTCCCCTGTGAGCTAGACTG
VK325	CTE – Reverse – XbaI and XhoI	TCTAGACTCGAGCGGGATCAACAGTAGGAACCTG
VK330	Rev Forward primer	CACCGCGGCCGCAATGGCAGGAAGAAGCGGAGAC
VK331	Rev Middle forward primer	CAAGCTTCTCTATCAAAGCAACCCACCTCCCAACCCCGAGG
VK333	Rev Reverse primer	AGTCTAGACTATTCTTTAGTTCCTGACTC
VK329	Tat forward primer	CACCGCGGCCGCAATGGAGCCAGTAGATCCTAGAC
VK331	Tat Middle forward primer	CAAGCTTCTCTATCAAAGCAACCCACCTCCCAACCCCGAGG
VK332	Tat reverse primer	CCTCGGGGTTGGGAGGTGGGTTGCTTTGATAGAGAAGCTTG
VK382	Nup98 Forward - NotI and BamHI	CACCGGATCCGCGGCCGCAATGTTTAACAAATCATTTGGA
VK383	Nup98 reverse - EcoRI and XbaI	GTACGAATTCTCTAGATCACATCTCCTTCAAAATAGATTG
VK547	Sam68 Forward EcoRI	CACCGAATTCATGCAGCGCCGGGACGACC
VK385	Sam68 Reverse EcoRI and ApaI	GAGAATTCGGGCCCTTAATAACGTCCATATGGGTGC
VK380	Nxt1 Forward - NdeI and EcoRI	CACCGAATCCCATATGGCATCTGTGGATTTCAAG
VK381	Nxt1 Reverse - XbaI and HindIII	GATCTCTAGAAGCTTAGCTGGCCCAGTCCTGGAAGC
VK386	Nxf1/TAP Forward - BamHI and NdeI	CACCGGATCCCATATGGCTGACGAGGGGAAGTCG
VK387	Nxf1/TAP Reverse - XbaI and EcoRI	GATCTCTAGAATTCTCACTTCATGAATGCCACTTC

VK684	TPR shRNA Oligo – Top Strand	CACCGCACAACAGGATAAGGTTATGCGAACATAACCTTATCCTGTTGTGC
VK685	TPR shRNA Oligo – Bottom Strand	AAAAGCACAACAGGATAAGGTTATGTTCGCATAACCTTATCCTGTTGTGC
VK738	Tpr L458P Forward Primer	TTATCTGTTAAGCCTGAACAAGCTATGAAG
VK739	Tpr L458P Reverse Primer	CTTCATAGCTTGTTCAGGCTTAACAGATAA
VK740	Tpr M489P Forward Primer	AGAGATAATCGAAGACCGGAAATACAAGTA
VK741	Tpr M489P Reverse Primer	TACTTGTATTTCCGGTCTTCGATTATCTCT
VK743	Tpr Forward Primer- NdeI site:	CACCCATATGGCGGCGGTGTTGCAGCAAGT
VK742	Tpr Reverse [~200 bp away from Mutagenesis site M489]	GGTACCTCAAGTGATTTTGGATGAAGTTGT
VK792	TprC 93-724 Forward	CACCGCGGCCGCAATGCCCACTACACAAGTGGAA
VK793	TprC 201-724 Forward	CACCGCGGCCGCATCTTTGCCAAAGCGTACACGT
VK794	TprC 301-724 Forward	CACCGCGGCCGCAGATCAGCAGACGACAACTTCA
VK795	TprC 1-404 Reverse	GACTGGGCCCTTAACCTGTATTTCCTTCACCACT
VK796	TprC 1-522 Reverse	GACTGGGCCCTTAACCAGCAACCTGCGGCGAATG
VK797	TprC 1-624 Reverse	GACTGGGCCCTTATCCATCATCACCTGTTGCTGT
VK905	Tpr S349, 355A Forward	GGTGAAGATGCTAATGAAGGAACTGGTGCTGCCGATGG
VK906	Tpr S349, 355A Reverse	CCATCGGCAGCACCAGTTCCTTCATTAGCATCTTCACC

VK907	Tpr S395, 398A Forward	AGAGCTGCTGATGCTCAAAACGCTGGTGAAGGA
VK908	Tpr S395, 398A Reverse	TCCTTCACCAGCGTTTTGAGCATCAGCAGCTCT
VK909	Tpr S408, 409A Forward	ACAGGTGCTGCAGAAGCTGCTTTTTCTCAGGAGGTT
VK910	Tpr S408, 409A Reverse	AACCTCCTGAGAAAAAGCAGCTTCTGCAGCACCTGT
VK911	Tpr S411A Forward	GCAGAATCTTCTTTTGCTCAGGAGGTTTCTAGA
VK912	Tpr S411A Reverse	TCTAGAAACCTCCTGAGCAAAAGAAGATTCTGC
VK913	Tpr S415A Forward	TTTTCTCAGGAGGTTGCTAGAGAACAACAGCCA
VK914	Tpr S415A Reverse	TGGCTGTTGTTCTCTAGCAACCTCCTGAGAAAA
VK917	Tpr S434A (S2059A) Forward	CCTCGAGCACCTCAGGCACCGAGACGCCCACCA
VK918	Tpr S434A (S2059A) Reverse	TGGTGGGCGTCTCGGTGCCTGAGGTGCTCGAGG
VK919	Tpr S469A (S2094A) Forward	ATGACCCGAAGGCAGGCTGTAGGACGTGGCCTT
VK920	Tpr S469A (S2094A) Reverse	AAGGCCACGTCCTACAGCCTGCCTTCGGGTCAT
VK915	Tpr S421, 422, 424A Forward	GAACAACAGCCAGCAGCAGCAGCTGAAAGACAGGCC
VK916	TprS421, 422, 424A Reverse	GGCCTGTCTTTCAGCTGCTGCTGCTGGCTGTTGTTC
VKN29	TprM Forward - NotI site	CACCGCGGCCGCAGGAATACTGGAGCGATCTGAA
VKN30	TprM Reverse - ApaI	TATGGGCCCTTATTCTTGAGGCTCATCTCTCTG

105

VKN58	Mad1 Forward NotI	CACCGCGGCCGCAATGGAAGACCTGGGGGAAAAC
VKN59	Mad1 reverse ApaI	AGTCGGGCCCCTACGCCACGGTCTGGCGGCT
VKN60	TTK Forward NotI	CACCGCGGCCGCAATGGAATCCGAGGATTTAAGTG
VKN61	TTK reverse ApaI	AGTCGGGCCCTAGGTGGTATCTGACATTACG
VKN62	PKA Forward NotI	CACCGCGGCCGCAATGGGCAACGCCGCCGCCGCC
VKN63	PKA reverse XbaI	AGCTTCTAGACTAAAACTCAGAAAACTCCTTGC
VKN203	Mad2 Forward NotI	CACCGCGGCCGCAATGGACTACAAAGACGATGAC
VKN204	Mad2 Reverse ApaI	AGTCGGGCCCTCAGTCATTGACAGGAATTTT

<table>
<tr><td colspan="3" align="center">Primers for Reverse Transcriptase Reactions</td></tr>
</table>

Number	Primer Description	Primer Sequence
VKN71	ERK2 Forward	TTCCTGACAGAATATGTGGCC
VKN69	ERK2 Reverse reverse	CATGTCGAACTTGAATGGTGC
VKN70	ERK2 Reverse	TAAGTCCAGAGCTTTGGAGTC
VKN74	Gag-Pol Forward	CTTTAAGCAATCCTCAGGAGG
VKN72	Gag-Pol Reverse reverse	GAGCGGACTCATTGTTGCTAT
VKN73	Gag-Pol Reverse	AATTTGTCCACTGATGGGAGG

VKN68	Tpr Forward	TTTACTGAGAGCACCACCTCT
VKN66	Tpr Reverse reverse	CTCACACCTCTCTGTCTGTTA
VKN67	Tpr Reverse	AGTCTTACTCGTCTGAAAGGC

Appendix – II
Publications

PLoS one

Localization of Nucleoporin Tpr to the Nuclear Pore Complex Is Essential for Tpr Mediated Regulation of the Export of Unspliced RNA

Kalpana Rajanala, Vinay Kumar Nandicoori*

National Institute of Immunology, Aruna Asaf Ali Marg, New Delhi, India

Abstract

Nucleoporin Tpr is a component of the nuclear pore complex (NPC) that localizes exclusively to intranuclear filaments. Tpr functions as a scaffolding element in the nuclear phase of the NPC and plays a role in mitotic spindle checkpoint signalling. Export of intron-containing mRNA in Mason Pfizer Monkey Virus is regulated by direct interaction of cellular proteins with the cis-acting Constitutive Transport Element (CTE). In mammalian cells, the transport of Gag/Pol-CTE reporter construct is not very efficient, suggesting a regulatory mechanism to retain this unspliced RNA. Here we report that the knockdown of Tpr in mammalian cells leads to a drastic enhancement in the levels of Gag proteins (p24) in the cytoplasm, which is rescued by siRNA resistant Tpr. Tpr's role in the retention of unspliced RNA is independent of the functions of Sam68 and Tap/Nxf1 proteins, which are reported to promote CTE dependent export. Further, we investigated the possible role for nucleoporins that are known to function in nucleocytoplasmic transport in modulating unspliced RNA export. Results show that depletion of Nup153, a nucleoporin required for NPC anchoring of Tpr, plays a role in regulating the export, while depletion of other FG repeat-containing nucleoporins did not alter the unspliced RNA export. Results suggest that Tpr and Nup153 both regulate the export of unspliced RNA and they are most likely functioning through the same pathway. Importantly, we find that localization of Tpr to the NPC is necessary for Tpr mediated regulation of unspliced RNA export. Collectively, the data indicates that perinuclear localization of Tpr at the nucleopore complex is crucial for regulating intron containing mRNA export by directly or indirectly participating in the processing and degradation of aberrant mRNA transcripts.

Competing Interests: The authors have declared that no competing interests exist.

* E-mail: vinaykn@nii.res.in

Introduction

Nucleoporin Tpr was originally identified as the oncogenic activator of the met, raf, and trk protooncogenes [1,2,3]. Tpr is a large 270 kDa protein with a bipartite structure consisting of a ~1600-residue α-helical coiled-coil N-terminal domain and a highly acidic noncoiled ~800 amino acid carboxy terminus [4]. Cellular transformations and human tumors have been shown to occur due to the fusion of N-terminal residues of Tpr (residues 140–230) with the protein kinase domains of the protooncogenes met, raf, and trk [1,2,3]. Tpr has been shown to be localized exclusively to intranuclear filaments associated with the nucleoplasmic side of the NPC, by directly binding to Nup153 [5,6,7]. Different metazoan species have been shown to contain only one Tpr ortholog, whereas two homologs, Mlp1 and Mlp2, are present in Saccharomyces cerevisiae and Schizosaccharomyces pombe [8,9,10].

The functions of Tpr include roles in intranuclear and nucleocytoplasmic transport and as a scaffolding element in the nuclear phase of the NPC [11,12,13,14]. Tpr has been shown to play a role in nuclear export of proteins containing leucine rich nuclear export signal (NES) and it also aids in the export of proteins with no apparent NES, as in the Huntington protein [12,15]. The association of Mad1 and Mad2 proteins with Tpr has been shown to affect mitotic spindle checkpoint signalling [16].

Depletion of Tpr causes a chromosome lagging phenotype and this phenomenon is due to the loss of interaction between Tpr and dynein complex [17]. The Tpr homolog of Arabidopsis has been implicated in the regulation of mRNA export and SUMO homeostasis, and has been shown to influence various aspects of plant development like flowering time [18,19]. The interaction between transcription factor HSF-1 and Tpr has been shown to facilitate the export of stress induced Hsp-70 mRNA [20]. In a previous study we have identified Tpr as a substrate of MAP kinase ERK2 and identified the ERK2 mediated phosphorylation sites on Tpr [21,22]. Tpr has been demonstrated to act as an ERK2 scaffold in NPC, in turn resulting in phosphorylation of substrates that interact with Tpr.

Conventionally in eukaryotes, unspliced RNA is retained in the nucleus, and only processed mRNA is exported through the NPC. However, retroviruses have developed mechanisms to overcome this regulation, thus enabling unspliced genomic RNA to be exported and finally packaged. These mechanisms can be classified into two types, Rev dependent and Rev independent. The Rev dependent pathway, employed by the Human Immuno deficiency Virus (HIV), utilizes retroviral Rev protein bound to the Rev response element (RRE) [3] present in the unspliced transcripts [23,24]. Once bound to RRE, Rev recruits host cellular factors such as Exportin-1 [25] and Sam68 (Src associated

Histone H4 lysine 14 acetylation in *Leishmania donovani* is mediated by the MYST-family protein HAT4

Devanand Kumar,[1] Kalpana Rajanala,[2] Neha Minocha[1] and Swati Saha[1]

Correspondence
Swati Saha
ss5gp@yahoo.co.in

[1]Department of Microbiology, University of Delhi South Campus, Benito Juarez Road, New Delhi 110021, India

[2]National Institute of Immunology, Aruna Asaf Ali Marg, New Delhi 110067, India

Post-translational modifications (PTMs) of histones regulate almost all facets of DNA metabolism in eukaryotes, such as replication, repair, transcription and chromatin condensation. While histone PTMs have been exhaustively examined in yeast and higher eukaryotes, less is known of their functional consequences in trypanosomatids. Trypanosome histones are highly divergent from those of other eukaryotes, and specific PTMs have been identified in histones of *Trypanosoma* species. The characterization of three MYST-family histone acetyltransferases (HATs) in *Trypanosoma brucei* had earlier identified the HATs responsible for acetylation of two lysine residues, K4 and K10, in the N-terminal tail of histone H4. This report presents the results of what we believe to be the first study of a HAT in a *Leishmania* species. The HAT4 gene of *Leishmania donovani*, the causative pathogen of visceral leishmaniasis, was cloned and expressed in fusion with GFP in *Leishmania* promastigotes. We found that HAT4–GFP behaves differently from typical eukaryotic MYST-family HATs, which are usually constitutively nuclear, in that it is cytosolic throughout the cell cycle, although the protein is also present in the nucleus in post-mitotic cells. Substrate-specificity analyses revealed that LdHAT4 acetylates the N terminus of histone H4, but not those of H2A, H2B or H3. Nor does it acetylate the C terminus of H2A. The primary target of HAT4-mediated acetylation is the K14 residue of H4, although K2 may be a minor site as well. H4K14 acetylation in *Leishmania* may occur either in the cytoplasm prior to histone deposition, or soon after mitosis in the nucleus.

INTRODUCTION

Histones are a part of the nucleosomal structure of eukaryotic chromatin, and they carry a host of various post-translational modifications (PTMs), especially on their tail domains, that act in consortium or sequentially to regulate several activities such as chromatin condensation, transcriptional activation, replication timing, and DNA repair. Over 60 different residues on histones have been detected to have PTMs, and the roles of specific modifications in various biological processes have been determined. While the best-characterized histone modifications are acetylations, methylations and phosphorylations, other modifications such as ubiquitylations and sumoylations of lysine residues have also been reported

(reviewed by Kouzarides, 2007; Bannister & Kouzarides, 2011). These PTMs on specific residues form the histone code, and a multitude of histone-modifying enzymes are responsible for the formation of this code. The histone code hypothesis, first proposed by Strahl and Allis over a decade ago (Strahl & Allis, 2000), postulates that histone PTMs modulate cellular processes through effector proteins that recognize specific histone modifications, via specific domains present in them. The interaction of effector protein with chromatin may lead to one or more useful outcomes, such as the recruitment of essential transcription factors to promoters, or the further modification of other histone residues, which in turn influence downstream processes (Yun *et al.*, 2011). Histone modifications are not uniformly distributed throughout the genome. Microarray analysis in *Saccharomyces cerevisiae* has revealed that histones are hyperacetylated in promoters of genes that are actively expressed (Millar & Grunstein, 2006), and lysine trimethylation is enriched in coding regions of genes. In general, acetylation, methylation, phosphorylation and ubiquitination are implicated in transcriptional activation, while methylation, ubiquitination,

Characterization of *Leishmania donovani* MCM4: Expression Patterns and Interaction with PCNA

Neha Minocha[1], Devanand Kumar[1], Kalpana Rajanala[2], Swati Saha[1]*

1 Department of Microbiology, University of Delhi South Campus, New Delhi, India, 2 National Institute of Immunology, New Delhi, India

Abstract

Events leading to origin firing and fork elongation in eukaryotes involve several proteins which are mostly conserved across the various eukaryotic species. Nuclear DNA replication in trypanosomatids has thus far remained a largely uninvestigated area. While several eukaryotic replication protein orthologs have been annotated, many are missing, suggesting that novel replication mechanisms may apply in this group of organisms. Here, we characterize the expression of *Leishmania donovani* MCM4, and find that while it broadly resembles other eukaryotes, noteworthy differences exist. MCM4 is constitutively nuclear, signifying that, unlike what is seen in *S.cerevisiae*, varying subcellular localization of MCM4 is not a mode of replication regulation in *Leishmania*. Overexpression of MCM4 in *Leishmania* promastigotes causes progress through S phase faster than usual, implicating a role for MCM4 in the modulation of cell cycle progression. We find for the first time in eukaryotes, an interaction between any of the proteins of the MCM2-7 (MCM4) and PCNA. MCM4 colocalizes with PCNA in S phase cells, in keeping with the MCM2-7 complex being involved not only in replication initiation, but fork elongation as well. Analysis of a LdMCM4 mutant indicates that MCM4 interacts with PCNA via the PIP box motif of MCM4 - perhaps as an integral component of the MCM2-7 complex, although we have no direct evidence that MCM4 harboring a PIP box mutation can still functionally associate with the other members of the MCM2-7 complex- and the PIP box motif is important for cell survival and viability. In *Leishmania*, MCM4 may possibly help in recruiting PCNA to chromatin, a role assigned to MCM10 in other eukaryotes.

Introduction

Eukaryotic DNA replication involves the licensing and activation of multiple origins. Origins are licensed by the assembly of pre-replication complexes (pre-RCs) in G1 phase [1–3], a process involving the ordered loading of ORCs 1-6, Cdc6, Cdt1, MCM2-7, and MCM10. At the G1/S transition, Cdc7/Dbf4 and Cdk2/cyclin E kinase activity transform pre-RCs into pre-initiation complexes. GINS, Sld2, Dpb11 and Cdc45 associate with the complexes to trigger origin activation, and with the recruitment of the elongation machinery, DNA synthesis commences [4,5]. While replication has been extensively examined in higher eukaryotes and yeasts, the pre-replication and replication apparatus of protozoans remains largely uninvestigated, with most reports being from studies in *Plasmodium falciparum* [6-9] and *Tetrahymena thermophila* [10-12].

The trypanosomatid *Leishmania* causes the group of diseases collectively called Leishmaniasis. Leishmaniasis occurs in three main forms – cutaneous, subcutaneous and visceral, and different *Leishmania* species cause different forms of the disease. Leishmaniasis is prevalent in 88 countries across the globe, and inflicts mostly people of the economically weaker sections of society. Every year ~1.6 million new cases are reported, of which about 500,000 are cases of visceral leishmaniasis (VL). Around 90% of the cases of VL occur in South Asia and East Africa. VL can be fatal if not treated early and appropriately, and several research groups are engaged in investigating the biology of the causative pathogens of VL, with the aim of developing more effective means of therapeutic intervention. *Leishmania donovani* is one of the causative agents of VL, prevalent in Sudan and the Indian subcontinent.

Leishmania species cycle between two hosts – the insect sandfly, and the mammalian host. In the insect host they exist as flagellate promastigotes. The promastigotes remain attached to the wall of the anterior region of the midgut, as non-infective procyclic forms in the early stages. As the parasites further develop, they detach from the midgut and migrate to the salivary glands. These metacyclic forms are infective. When the insect bites the mammalian host the promastigotes are released into the mammalian host's bloodstream where they are taken up by host macrophages. Within the macrophages they transform into aflagellate amastigotes, and propagate. The amastigotes are transferred to the insect host with a bloodmeal where they transform into promastigotes again. Microarray analysis reveals the absence of stage-specific putative DNA replication proteins in *Leishmania* promastigotes and amastigotes [13], not unexpectedly, as both forms of the parasite reproduce asexually by binary fission. The components of pre-RCs are conserved from yeast to

The distribution pattern of proliferating cell nuclear antigen in the nuclei of *Leishmania donovani*

Devanand Kumar,[1] Neha Minocha,[1] Kalpana Rajanala[2] and Swati Saha[1]

Correspondence
Swati Saha
ss5gp@yahoo.co.in

[1]Department of Microbiology, University of Delhi South Campus, Benito Juarez Road, New Delhi 110021, India

[2]National Institute of Immunology, Aruna Asaf Ali Marg, New Delhi 110067, India

DNA replication in eukaryotes is a highly conserved process marked by the licensing of multiple origins, with pre-replication complex assembly in G1 phase, followed by the onset of replication at these origins in S phase. The two strands replicate by different mechanisms, and DNA synthesis is brought about by the activity of the replicative DNA polymerases Pol δ and Pol ε. Proliferating cell nuclear antigen (PCNA) augments the processivity of these polymerases by serving as a DNA sliding clamp protein. This study reports the cloning of PCNA from the protozoan *Leishmania donovani*, which is the causative agent of the systemic disease visceral leishmaniasis. PCNA was demonstrated to be robustly expressed in actively proliferating *L. donovani* promastigotes. We found that the protein was present primarily in the nucleus throughout the cell cycle, and it was found in both proliferating procyclic and metacyclic promastigotes. However, levels of expression of PCNA varied through cell cycle progression, with maximum expression evident in G1 and S phases. The subnuclear pattern of expression of PCNA differed in different stages of the cell cycle; it formed distinct subnuclear foci in S phase, while it was distributed in a more diffuse pattern in G2/M phase and post-mitotic phase cells. These subnuclear foci are the sites of active DNA replication, suggesting that replication factories exist in *Leishmania*, as they do in higher eukaryotes, thus opening avenues for investigating other *Leishmania* proteins that are involved in DNA replication as part of these replication factories.

DNA replication in eukaryotes is the culmination of events occurring in two distinct stages. In the first stage, origins get licensed to replicate by the establishment of multi-protein complexes called pre-replication complexes (pre-RCs) at origins in G1 phase, and, in the second stage, these licensed origins get activated, and fire in S phase (Bell & Dutta, 2002; Diffley, 2004). DNA synthesis of the two strands occurs by two different mechanisms, wherein one strand is synthesized continuously, and the other is synthesized discontinuously. Several enzymes and protein factors are responsible for these processes, and DNA polymerases δ and ε play a major role in DNA synthesis. The DNA polymerase processivity factor proliferating cell nuclear antigen (PCNA) considerably augments the processivity of these enzymes (Moldovan *et al.*, 2007; Bravo *et al.*, 1987; Prelich *et al.*, 1987). Replication proteins and their auxiliary factors are organized in complexes

called replisomes. Several replicons and their replisomes are ordered into clusters called replication factories or foci. Replication foci can be indirectly or directly labelled by short pulses with fluorescently labelled nucleotides, and they are visible by fluorescence microscopy (Lengronne *et al.*, 2001; Pasero *et al.*, 1997; Gilbert, 2001; Kitamura *et al.*, 2006). Each replication focus is believed to harbour several replication forks (Berezney *et al.*, 2000; Cook, 2001).

Replication foci are rich in the enzymes and accessory proteins that are involved in DNA replication. These enzymes and proteins include DNA polymerases, PCNA, replication factor C, replication protein A and DNA ligases, and cell cycle regulators such as cyclin A (Leonhardt *et al.*, 2000; Cardoso *et al.*, 1993). PCNA was the first protein to be identified at these replication foci, and it has been widely used as a marker for these foci in higher eukaryotes, as it is conserved, and is absolutely essential for DNA replication. Though first identified as the DNA polymerase δ processivity factor, PCNA forms a trimeric ring around DNA, anchoring not only DNA polymerases, but also interacting with other replication-associated factors, such as Cdt1 and MCM10 (Das-Bradoo *et al.*, 2006; Arias & Walter, 2006).

Bibliography

BIBLIOGRAPHY

1. Greco A, Pierotti MA, Bongarzone I, Pagliardini S, Lanzi C, Della Porta G. TRK-T1 is a novel oncogene formed by the fusion of TPR and TRK genes in human papillary thyroid carcinomas. Oncogene 1992; 7:237-42.

2. Park M, Dean M, Cooper CS, Schmidt M, O'Brien SJ, Blair DG, et al. Mechanism of met oncogene activation. Cell 1986; 45:895-904.

3. Soman NR, Correa P, Ruiz BA, Wogan GN. The TPR-MET oncogenic rearrangement is present and expressed in human gastric carcinoma and precursor lesions. Proc Natl Acad Sci U S A 1991; 88:4892-6.

4. Mitchell PJ, Cooper CS. The human tpr gene encodes a protein of 2094 amino acids that has extensive coiled-coil regions and an acidic C-terminal domain. Oncogene 1992; 7:2329-33.

5. Cordes VC, Reidenbach S, Rackwitz HR, Franke WW. Identification of protein p270/Tpr as a constitutive component of the nuclear pore complex-attached intranuclear filaments. J Cell Biol 1997; 136:515-29.

6. Shah S, Tugendreich S, Forbes D. Major binding sites for the nuclear import receptor are the internal nucleoporin Nup153 and the adjacent nuclear filament protein Tpr. J Cell Biol 1998; 141:31-49.

7. Hase ME, Cordes VC. Direct interaction with nup153 mediates binding of Tpr to the periphery of the nuclear pore complex. Mol Biol Cell 2003; 14:1923-40.

8. Kuznetsov NV, Sandblad L, Hase ME, Hunziker A, Hergt M, Cordes VC. The evolutionarily conserved single-copy gene for murine Tpr encodes one prevalent isoform in somatic cells and lacks paralogs in higher eukaryotes. Chromosoma 2002; 111:236-55.

9. Kosova B, Pante N, Rollenhagen C, Podtelejnikov A, Mann M, Aebi U, et al. Mlp2p, a component of nuclear pore attached intranuclear filaments, associates with nic96p. J Biol Chem 2000; 275:343-50.

10. Strambio-de-Castillia C, Blobel G, Rout MP. Proteins connecting the nuclear pore complex with the nuclear interior. J Cell Biol 1999; 144:839-55.

11. Fontoura BM, Dales S, Blobel G, Zhong H. The nucleoporin Nup98 associates with the intranuclear filamentous protein network of TPR. Proc Natl Acad Sci U S A 2001; 98:3208-13.

12. Frosst P, Guan T, Subauste C, Hahn K, Gerace L. Tpr is localized within the nuclear basket of the pore complex and has a role in nuclear protein export. J Cell Biol 2002; 156:617-30.

13. Shibata S, Matsuoka Y, Yoneda Y. Nucleocytoplasmic transport of proteins and poly(A)+ RNA in reconstituted Tpr-less nuclei in living mammalian cells. Genes Cells 2002; 7:421-34.

14. Zimowska G, Paddy MR. Structures and dynamics of Drosophila Tpr inconsistent with a static, filamentous structure. Exp Cell Res 2002; 276:223-32.

15. Cornett J, Cao F, Wang CE, Ross CA, Bates GP, Li SH, et al. Polyglutamine expansion of huntingtin impairs its nuclear export. Nat Genet 2005; 37:198-204.

16. Bangs P, Burke B, Powers C, Craig R, Purohit A, Doxsey S. Functional analysis of Tpr: identification of nuclear pore complex association and nuclear localization domains and a role in mRNA export. J Cell Biol 1998; 143:1801-12.

17. Galy V, Gadal O, Fromont-Racine M, Romano A, Jacquier A, Nehrbass U. Nuclear retention of unspliced mRNAs in yeast is mediated by perinuclear Mlp1. Cell 2004; 116:63-73.

18. Lee SH, Sterling H, Burlingame A, McCormick F. Tpr directly binds to Mad1 and Mad2 and is important for the Mad1-Mad2-mediated mitotic spindle checkpoint. Genes Dev 2008; 22:2926-31.

19. Nakano H, Funasaka T, Hashizume C, Wong RW. Nucleoporin translocated promoter region (Tpr) associates with dynein complex, preventing chromosome lagging formation during mitosis. J Biol Chem 2010; 285:10841-9.

20. Xu XM, Rose A, Muthuswamy S, Jeong SY, Venkatakrishnan S, Zhao Q, et al. NUCLEAR PORE ANCHOR, the Arabidopsis homolog of Tpr/Mlp1/Mlp2/megator, is involved in mRNA export and SUMO homeostasis and affects diverse aspects of plant development. Plant Cell 2007; 19:1537-48.

21. Jacob Y, Mongkolsiriwatana C, Veley KM, Kim SY, Michaels SD. The nuclear pore protein AtTPR is required for RNA homeostasis, flowering time, and auxin signaling. Plant Physiol 2007; 144:1383-90.

22. Skaggs HS, Xing H, Wilkerson DC, Murphy LA, Hong Y, Mayhew CN, et al. HSF1-TPR interaction facilitates export of stress-induced HSP70 mRNA. J Biol Chem 2007; 282:33902-7.

23. Love DC, Sweitzer TD, Hanover JA. Reconstitution of HIV-1 rev nuclear export: independent requirements for nuclear import and export. Proc Natl Acad Sci U S A 1998; 95:10608-13.

24. Smith AJ, Cho MI, Hammarskjold ML, Rekosh D. Human immunodeficiency virus type 1 Pr55gag and Pr160gag-pol expressed from a simian virus 40 late replacement vector are efficiently processed and assembled into viruslike particles. J Virol 1990; 64:2743-50.

25. Srinivasakumar N, Hammarskjold ML, Rekosh D. Characterization of deletion mutations in the capsid region of human immunodeficiency virus type 1 that affect particle formation and Gag-Pol precursor incorporation. J Virol 1995; 69:6106-14.

26. Wodrich H, Schambach A, Krausslich HG. Multiple copies of the Mason-Pfizer monkey virus constitutive RNA transport element lead to enhanced HIV-1 Gag expression in a context-dependent manner. Nucleic Acids Res 2000; 28:901-10.

27. Jin L, Guzik BW, Bor YC, Rekosh D, Hammarskjold ML. Tap and NXT promote translation of unspliced mRNA. Genes Dev 2003; 17:3075-86.

28. Coyle JH, Guzik BW, Bor YC, Jin L, Eisner-Smerage L, Taylor SJ, et al. Sam68 enhances the cytoplasmic utilization of intron-containing RNA and is functionally regulated by the nuclear kinase Sik/BRK. Mol Cell Biol 2003; 23:92-103.

29. Kang Y, Bogerd HP, Cullen BR. Analysis of cellular factors that mediate nuclear export of RNAs bearing the Mason-Pfizer monkey virus constitutive transport element. J Virol 2000; 74:5863-71.

30. Reddy TR, Tang H, Xu W, Wong-Staal F. Sam68, RNA helicase A and Tap cooperate in the post-transcriptional regulation of human immunodeficiency virus and type D retroviral mRNA. Oncogene 2000; 19:3570-5.

31. Blethrow JD, Glavy JS, Morgan DO, Shokat KM. Covalent capture of kinase-specific phosphopeptides reveals Cdk1-cyclin B substrates. Proc Natl Acad Sci U S A 2008; 105:1442-7.

32. Glavy JS, Krutchinsky AN, Cristea IM, Berke IC, Boehmer T, Blobel G, et al. Cell-cycle-dependent phosphorylation of the nuclear pore Nup107-160 subcomplex. Proc Natl Acad Sci U S A 2007; 104:3811-6.

33. Macaulay C, Meier E, Forbes DJ. Differential mitotic phosphorylation of proteins of the nuclear pore complex. J Biol Chem 1995; 270:254-62.

34. Mansfeld J, Guttinger S, Hawryluk-Gara LA, Pante N, Mall M, Galy V, et al. The conserved transmembrane nucleoporin NDC1 is required for nuclear pore complex assembly in vertebrate cells. Mol Cell 2006; 22:93-103.

35. Eblen ST, Kumar NV, Shah K, Henderson MJ, Watts CK, Shokat KM, et al. Identification of novel ERK2 substrates through use of an engineered kinase and ATP analogs. J Biol Chem 2003; 278:14926-35.

36. Vomastek T, Iwanicki MP, Burack WR, Tiwari D, Kumar D, Parsons JT, et al. Extracellular signal-regulated kinase 2 (ERK2) phosphorylation sites and docking domain on the nuclear pore complex protein Tpr cooperatively regulate ERK2-Tpr interaction. Mol Cell Biol 2008; 28:6954-66.

37. Ulbert S, Antonin W, Platani M, Mattaj IW. The inner nuclear membrane protein Lem2 is critical for normal nuclear envelope morphology. FEBS Lett 2006; 580:6435-41.

38. D'Angelo MA, Hetzer MW. The role of the nuclear envelope in cellular organization. Cell Mol Life Sci 2006; 63:316-32.

39. Cronshaw JM, Krutchinsky AN, Zhang W, Chait BT, Matunis MJ. Proteomic analysis of the mammalian nuclear pore complex. J Cell Biol 2002; 158:915-27.

40. Rout MP, Aitchison JD, Suprapto A, Hjertaas K, Zhao Y, Chait BT. The yeast nuclear pore complex: composition, architecture, and transport mechanism. J Cell Biol 2000; 148:635-51.

41. Watson ML. Further observations on the nuclear envelope of the animal cell. J Biophys Biochem Cytol 1959; 6:147-56.

42. Jarnik M, Aebi U. Toward a more complete 3-D structure of the nuclear pore complex. J Struct Biol 1991; 107:291-308.

43. Beck M, Forster F, Ecke M, Plitzko JM, Melchior F, Gerisch G, et al. Nuclear pore complex structure and dynamics revealed by cryoelectron tomography. Science 2004; 306:1387-90.

44. Stoffler D, Feja B, Fahrenkrog B, Walz J, Typke D, Aebi U. Cryo-electron tomography provides novel insights into nuclear pore architecture: implications for nucleocytoplasmic transport. J Mol Biol 2003; 328:119-30.

45. Kiseleva E, Allen TD, Rutherford S, Bucci M, Wente SR, Goldberg MW. Yeast nuclear pore complexes have a cytoplasmic ring and internal filaments. J Struct Biol 2004; 145:272-88.

46. Goldberg MW, Allen TD. The nuclear pore complex: three-dimensional surface structure revealed by field emission, in-lens scanning electron microscopy, with underlying structure uncovered by proteolysis. J Cell Sci 1993; 106 (Pt 1):261-74.

47. Franke WW. On the universality of nuclear pore complex structure. Z Zellforsch Mikrosk Anat 1970; 105:405-29.

48. Aitchison JD, Blobel G, Rout MP. Nup120p: a yeast nucleoporin required for NPC distribution and mRNA transport. J Cell Biol 1995; 131:1659-75.

49. Miller BR, Powers M, Park M, Fischer W, Forbes DJ. Identification of a new vertebrate nucleoporin, Nup188, with the use of a novel organelle trap assay. Mol Biol Cell 2000; 11:3381-96.

50. Grandi P, Dang T, Pane N, Shevchenko A, Mann M, Forbes D, et al. Nup93, a vertebrate homologue of yeast Nic96p, forms a complex with a novel 205-kDa protein and is required for correct nuclear pore assembly. Mol Biol Cell 1997; 8:2017-38.

51. Siniossoglou S, Wimmer C, Rieger M, Doye V, Tekotte H, Weise C, et al. A novel complex of nucleoporins, which includes Sec13p and a Sec13p homolog, is essential for normal nuclear pores. Cell 1996; 84:265-75.

52. Fontoura BM, Blobel G, Matunis MJ. A conserved biogenesis pathway for nucleoporins: proteolytic processing of a 186-kilodalton precursor generates Nup98 and the novel nucleoporin, Nup96. J Cell Biol 1999; 144:1097-112.

53. Belgareh N, Rabut G, Bai SW, van Overbeek M, Beaudouin J, Daigle N, et al. An evolutionarily conserved NPC subcomplex, which redistributes in part to kinetochores in mammalian cells. J Cell Biol 2001; 154:1147-60.

54. Vasu SK, Forbes DJ. Nuclear pores and nuclear assembly. Curr Opin Cell Biol 2001; 13:363-75.

55. Siniossoglou S, Lutzmann M, Santos-Rosa H, Leonard K, Mueller S, Aebi U, et al. Structure and assembly of the Nup84p complex. J Cell Biol 2000; 149:41-54.

56. Alber F, Dokudovskaya S, Veenhoff LM, Zhang W, Kipper J, Devos D, et al. Determining the architectures of macromolecular assemblies. Nature 2007; 450:683-94.

57. Alber F, Dokudovskaya S, Veenhoff LM, Zhang W, Kipper J, Devos D, et al. The molecular architecture of the nuclear pore complex. Nature 2007; 450:695-701.

58. Devos D, Dokudovskaya S, Alber F, Williams R, Chait BT, Sali A, et al. Components of coated vesicles and nuclear pore complexes share a common molecular architecture. PLoS Biol 2004; 2:e380.

59. Devos D, Dokudovskaya S, Williams R, Alber F, Eswar N, Chait BT, et al. Simple fold composition and modular architecture of the nuclear pore complex. Proc Natl Acad Sci U S A 2006; 103:2172-7.

60. DeGrasse JA, DuBois KN, Devos D, Siegel TN, Sali A, Field MC, et al. Evidence for a shared nuclear pore complex architecture that is conserved from the last common eukaryotic ancestor. Mol Cell Proteomics 2009; 8:2119-30.

61. Radu A, Moore MS, Blobel G. The peptide repeat domain of nucleoporin Nup98 functions as a docking site in transport across the nuclear pore complex. Cell 1995; 81:215-22.

62. Liu SM, Stewart M. Structural basis for the high-affinity binding of nucleoporin Nup1p to the Saccharomyces cerevisiae importin-beta homologue, Kap95p. J Mol Biol 2005; 349:515-25.

63. Strawn LA, Shen T, Shulga N, Goldfarb DS, Wente SR. Minimal nuclear pore complexes define FG repeat domains essential for transport. Nat Cell Biol 2004; 6:197-206.

64. Nehrbass U, Rout MP, Maguire S, Blobel G, Wozniak RW. The yeast nucleoporin Nup188p interacts genetically and physically with the core structures of the nuclear pore complex. J Cell Biol 1996; 133:1153-62.

65. Wente SR, Rout MP. The nuclear pore complex and nuclear transport. Cold Spring Harb Perspect Biol 2010; 2:a000562.

66. Davis LI, Blobel G. Identification and characterization of a nuclear pore complex protein. Cell 1986; 45:699-709.

67. Besirli CG, Wagner EF, Johnson EM, Jr. The limited role of NH2-terminal c-Jun phosphorylation in neuronal apoptosis: identification of the nuclear pore complex as a potential target of the JNK pathway. J Cell Biol 2005; 170:401-11.

68. Hsia KC, Stavropoulos P, Blobel G, Hoelz A. Architecture of a coat for the nuclear pore membrane. Cell 2007; 131:1313-26.

69. Pemberton LF, Paschal BM. Mechanisms of receptor-mediated nuclear import and nuclear export. Traffic 2005; 6:187-98.

70. Terry LJ, Wente SR. Nuclear mRNA export requires specific FG nucleoporins for translocation through the nuclear pore complex. J Cell Biol 2007; 178:1121-32.

71. Lei EP, Silver PA. Protein and RNA export from the nucleus. Dev Cell 2002; 2:261-72.

72. Weis K. Regulating access to the genome: nucleocytoplasmic transport throughout the cell cycle. Cell 2003; 112:441-51.

73. Hoelz A, Debler EW, Blobel G. The structure of the nuclear pore complex. Annu Rev Biochem 2011; 80:613-43.

74. Rabut G, Doye V, Ellenberg J. Mapping the dynamic organization of the nuclear pore complex inside single living cells. Nat Cell Biol 2004; 6:1114-21.

75. Tran EJ, Wente SR. Dynamic nuclear pore complexes: life on the edge. Cell 2006; 125:1041-53.

76. Maul GG, Price JW, Lieberman MW. Formation and distribution of nuclear pore complexes in interphase. J Cell Biol 1971; 51:405-18.

77. Doucet CM, Hetzer MW. Nuclear pore biogenesis into an intact nuclear envelope. Chromosoma 2010; 119:469-77.

78. Dultz E, Zanin E, Wurzenberger C, Braun M, Rabut G, Sironi L, et al. Systematic kinetic analysis of mitotic dis- and reassembly of the nuclear pore in living cells. J Cell Biol 2008; 180:857-65.

79. Burke B, Stewart CL. Life at the edge: the nuclear envelope and human disease. Nat Rev Mol Cell Biol 2002; 3:575-85.

80. Walther TC, Alves A, Pickersgill H, Loiodice I, Hetzer M, Galy V, et al. The conserved Nup107-160 complex is critical for nuclear pore complex assembly. Cell 2003; 113:195-206.

81. Kimura N, Takizawa M, Okita K, Natori O, Igarashi K, Ueno M, et al. Identification of a novel transcription factor, ELYS, expressed predominantly in mouse foetal haematopoietic tissues. Genes Cells 2002; 7:435-46.

82. Rasala BA, Orjalo AV, Shen Z, Briggs S, Forbes DJ. ELYS is a dual nucleoporin/kinetochore protein required for nuclear pore assembly and proper cell division. Proc Natl Acad Sci U S A 2006; 103:17801-6.

83. Franz C, Walczak R, Yavuz S, Santarella R, Gentzel M, Askjaer P, et al. MEL-28/ELYS is required for the recruitment of nucleoporins to chromatin and postmitotic nuclear pore complex assembly. EMBO Rep 2007; 8:165-72.

84. Gillespie PJ, Khoudoli GA, Stewart G, Swedlow JR, Blow JJ. ELYS/MEL-28 chromatin association coordinates nuclear pore complex assembly and replication licensing. Curr Biol 2007; 17:1657-62.

85. Harel A, Chan RC, Lachish-Zalait A, Zimmerman E, Elbaum M, Forbes DJ. Importin beta negatively regulates nuclear membrane fusion and nuclear pore complex assembly. Mol Biol Cell 2003; 14:4387-96.

86. Dawson TR, Lazarus MD, Hetzer MW, Wente SR. ER membrane-bending proteins are necessary for de novo nuclear pore formation. J Cell Biol 2009; 184:659-75.

87. Talamas JA, Hetzer MW. POM121 and Sun1 play a role in early steps of interphase NPC assembly. J Cell Biol 2011; 194:27-37.

88. Drin G, Casella JF, Gautier R, Boehmer T, Schwartz TU, Antonny B. A general amphipathic alpha-helical motif for sensing membrane curvature. Nat Struct Mol Biol 2007; 14:138-46.

89. Dultz E, Ellenberg J. Live imaging of single nuclear pores reveals unique assembly kinetics and mechanism in interphase. J Cell Biol 2010; 191:15-22.

90. Favreau C, Worman HJ, Wozniak RW, Frappier T, Courvalin JC. Cell cycle-dependent phosphorylation of nucleoporins and nuclear pore membrane protein Gp210. Biochemistry 1996; 35:8035-44.

91. Bodoor K, Shaikh S, Salina D, Raharjo WH, Bastos R, Lohka M, et al. Sequential recruitment of NPC proteins to the nuclear periphery at the end of mitosis. J Cell Sci 1999; 112 (Pt 13):2253-64.

92. Nousiainen M, Sillje HH, Sauer G, Nigg EA, Korner R. Phosphoproteome analysis of the human mitotic spindle. Proc Natl Acad Sci U S A 2006; 103:5391-6.

93. Muhlhausser P, Kutay U. An in vitro nuclear disassembly system reveals a role for the RanGTPase system and microtubule-dependent steps in nuclear envelope breakdown. J Cell Biol 2007; 178:595-610.

94. Kiseleva E, Rutherford S, Cotter LM, Allen TD, Goldberg MW. Steps of nuclear pore complex disassembly and reassembly during mitosis in early Drosophila embryos. J Cell Sci 2001; 114:3607-18.

95. Cotter L, Allen TD, Kiseleva E, Goldberg MW. Nuclear membrane disassembly and rupture. J Mol Biol 2007; 369:683-95.

96. Feldherr CM. The nuclear annuli as pathways for nucleocytoplasmic exchanges. J Cell Biol 1962; 14:65-72.

97. Paine PL, Moore LC, Horowitz SB. Nuclear envelope permeability. Nature 1975; 254:109-14.

98. Pante N, Kann M. Nuclear pore complex is able to transport macromolecules with diameters of about 39 nm. Mol Biol Cell 2002; 13:425-34.

99. Shulga N, Goldfarb DS. Binding dynamics of structural nucleoporins govern nuclear pore complex permeability and may mediate channel gating. Mol Cell Biol 2003; 23:534-42.

100. Rout MP, Aitchison JD, Magnasco MO, Chait BT. Virtual gating and nuclear transport: the hole picture. Trends Cell Biol 2003; 13:622-8.

101. Ribbeck K, Gorlich D. Kinetic analysis of translocation through nuclear pore complexes. EMBO J 2001; 20:1320-30.

102. Peters R. Translocation through the nuclear pore complex: selectivity and speed by reduction-of-dimensionality. Traffic 2005; 6:421-7.

103. Lusk CP, Blobel G, King MC. Highway to the inner nuclear membrane: rules for the road. Nat Rev Mol Cell Biol 2007; 8:414-20.

104.Matsubayashi Y, Fukuda M, Nishida E. Evidence for existence of a nuclear pore complex-mediated, cytosol-independent pathway of nuclear translocation of ERK MAP kinase in permeabilized cells. J Biol Chem 2001; 276:41755-60.

105.Suntharalingam M, Wente SR. Peering through the pore: nuclear pore complex structure, assembly, and function. Dev Cell 2003; 4:775-89.

106.Whitehurst AW, Wilsbacher JL, You Y, Luby-Phelps K, Moore MS, Cobb MH. ERK2 enters the nucleus by a carrier-independent mechanism. Proc Natl Acad Sci U S A 2002; 99:7496-501.

107.Rout MP, Aitchison JD. Pore relations: nuclear pore complexes and nucleocytoplasmic exchange. Essays Biochem 2000; 36:75-88.

108.Rodriguez MS, Dargemont C, Stutz F. Nuclear export of RNA. Biol Cell 2004; 96:639-55.

109.Cole CN, Scarcelli JJ. Unravelling mRNA export. Nat Cell Biol 2006; 8:645-7.

110.Lund MK, Guthrie C. The DEAD-box protein Dbp5p is required to dissociate Mex67p from exported mRNPs at the nuclear rim. Mol Cell 2005; 20:645-51.

111.Alcazar-Roman AR, Tran EJ, Guo S, Wente SR. Inositol hexakisphosphate and Gle1 activate the DEAD-box protein Dbp5 for nuclear mRNA export. Nat Cell Biol 2006; 8:711-6.

112.Weirich CS, Erzberger JP, Flick JS, Berger JM, Thorner J, Weis K. Activation of the DExD/H-box protein Dbp5 by the nuclear-pore protein Gle1 and its coactivator InsP6 is required for mRNA export. Nat Cell Biol 2006; 8:668-76.

113.Cochrane AW, Chen CH, Rosen CA. Specific interaction of the human immunodeficiency virus Rev protein with a structured region in the env mRNA. Proc Natl Acad Sci U S A 1990; 87:1198-202.

114.Malim MH, Hauber J, Fenrick R, Cullen BR. Immunodeficiency virus rev trans-activator modulates the expression of the viral regulatory genes. Nature 1988; 335:181-3.

115.Askjaer P, Jensen TH, Nilsson J, Englmeier L, Kjems J. The specificity of the CRM1-Rev nuclear export signal interaction is mediated by RanGTP. J Biol Chem 1998; 273:33414-22.

116.Coyle JH, Bor YC, Rekosh D, Hammarskjold ML. The Tpr protein regulates export of mRNAs with retained introns that traffic through the Nxf1 pathway. RNA 2011.

117.Reddy TR, Xu WD, Wong-Staal F. General effect of Sam68 on Rev/Rex regulated expression of complex retroviruses. Oncogene 2000; 19:4071-4.

118.Modem S, Badri KR, Holland TC, Reddy TR. Sam68 is absolutely required for Rev function and HIV-1 production. Nucleic Acids Res 2005; 33:873-9.

119.Pasquinelli AE, Ernst RK, Lund E, Grimm C, Zapp ML, Rekosh D, et al. The constitutive transport element (CTE) of Mason-Pfizer monkey virus (MPMV) accesses a cellular mRNA export pathway. EMBO J 1997; 16:7500-10.

120.Wiegand HL, Coburn GA, Zeng Y, Kang Y, Bogerd HP, Cullen BR. Formation of Tap/NXT1 heterodimers activates Tap-dependent nuclear mRNA export by enhancing recruitment to nuclear pore complexes. Mol Cell Biol 2002; 22:245-56.

121.Levesque L, Guzik B, Guan T, Coyle J, Black BE, Rekosh D, et al. RNA export mediated by tap involves NXT1-dependent interactions with the nuclear pore complex. J Biol Chem 2001; 276:44953-62.

122.Reddy TR. A single point mutation in the nuclear localization domain of Sam68 blocks the Rev/RRE-mediated transactivation. Oncogene 2000; 19:3110-4.

123.Galy V, Olivo-Marin JC, Scherthan H, Doye V, Rascalou N, Nehrbass U. Nuclear pore complexes in the organization of silent telomeric chromatin. Nature 2000; 403:108-12.

124.Feuerbach F, Galy V, Trelles-Sticken E, Fromont-Racine M, Jacquier A, Gilson E, et al. Nuclear architecture and spatial positioning help establish transcriptional states of telomeres in yeast. Nat Cell Biol 2002; 4:214-21.

125.Fahrenkrog B, Koser J, Aebi U. The nuclear pore complex: a jack of all trades? Trends Biochem Sci 2004; 29:175-82.

126.Akhtar A, Gasser SM. The nuclear envelope and transcriptional control. Nat Rev Genet 2007; 8:507-17.

127.Capelson M, Doucet C, Hetzer MW. Nuclear pore complexes: guardians of the nuclear genome. Cold Spring Harb Symp Quant Biol 2010; 75:585-97.

128. Khadaroo B, Teixeira MT, Luciano P, Eckert-Boulet N, Germann SM, Simon MN, et al. The DNA damage response at eroded telomeres and tethering to the nuclear pore complex. Nat Cell Biol 2009; 11:980-7.

129. Nagai S, Dubrana K, Tsai-Pflugfelder M, Davidson MB, Roberts TM, Brown GW, et al. Functional targeting of DNA damage to a nuclear pore-associated SUMO-dependent ubiquitin ligase. Science 2008; 322:597-602.

130. Strambio-De-Castillia C, Niepel M, Rout MP. The nuclear pore complex: bridging nuclear transport and gene regulation. Nat Rev Mol Cell Biol 2010; 11:490-501.

131. Towbin BD, Meister P, Gasser SM. The nuclear envelope--a scaffold for silencing? Curr Opin Genet Dev 2009; 19:180-6.

132. Palancade B, Liu X, Garcia-Rubio M, Aguilera A, Zhao X, Doye V. Nucleoporins prevent DNA damage accumulation by modulating Ulp1-dependent sumoylation processes. Mol Biol Cell 2007; 18:2912-23.

133. Pichler A, Gast A, Seeler JS, Dejean A, Melchior F. The nucleoporin RanBP2 has SUMO1 E3 ligase activity. Cell 2002; 108:109-20.

134. Pichler A, Knipscheer P, Saitoh H, Sixma TK, Melchior F. The RanBP2 SUMO E3 ligase is neither HECT- nor RING-type. Nat Struct Mol Biol 2004; 11:984-91.

135. Joseph J, Dasso M. The nucleoporin Nup358 associates with and regulates interphase microtubules. FEBS Lett 2008; 582:190-6.

136. D'Angelo MA, Anderson DJ, Richard E, Hetzer MW. Nuclear pores form de novo from both sides of the nuclear envelope. Science 2006; 312:440-3.

137. Galy V, Antonin W, Jaedicke A, Sachse M, Santarella R, Haselmann U, et al. A role for gp210 in mitotic nuclear-envelope breakdown. J Cell Sci 2008; 121:317-28.

138. Salina D, Enarson P, Rattner JB, Burke B. Nup358 integrates nuclear envelope breakdown with kinetochore assembly. J Cell Biol 2003; 162:991-1001.

139. Antonin W, Franz C, Haselmann U, Antony C, Mattaj IW. The integral membrane nucleoporin pom121 functionally links nuclear pore complex assembly and nuclear envelope formation. Mol Cell 2005; 17:83-92.

140.Franz C, Askjaer P, Antonin W, Iglesias CL, Haselmann U, Schelder M, et al. Nup155 regulates nuclear envelope and nuclear pore complex formation in nematodes and vertebrates. EMBO J 2005; 24:3519-31.

141.Hawryluk-Gara LA, Platani M, Santarella R, Wozniak RW, Mattaj IW. Nup53 is required for nuclear envelope and nuclear pore complex assembly. Mol Biol Cell 2008; 19:1753-62.

142.Capelson M, Hetzer MW. The role of nuclear pores in gene regulation, development and disease. EMBO Rep 2009; 10:697-705.

143.Kohler A, Hurt E. Gene regulation by nucleoporins and links to cancer. Mol Cell 2010; 38:6-15.

144.Zhang X, Chen S, Yoo S, Chakrabarti S, Zhang T, Ke T, et al. Mutation in nuclear pore component NUP155 leads to atrial fibrillation and early sudden cardiac death. Cell 2008; 135:1017-27.

145.Kerscher O, Hieter P, Winey M, Basrai MA. Novel role for a Saccharomyces cerevisiae nucleoporin, Nup170p, in chromosome segregation. Genetics 2001; 157:1543-53.

146.Joseph J, Liu ST, Jablonski SA, Yen TJ, Dasso M. The RanGAP1-RanBP2 complex is essential for microtubule-kinetochore interactions in vivo. Curr Biol 2004; 14:611-7.

147.Arnaoutov A, Azuma Y, Ribbeck K, Joseph J, Boyarchuk Y, Karpova T, et al. Crm1 is a mitotic effector of Ran-GTP in somatic cells. Nat Cell Biol 2005; 7:626-32.

148.Knauer SK, Bier C, Habtemichael N, Stauber RH. The Survivin-Crm1 interaction is essential for chromosomal passenger complex localization and function. EMBO Rep 2006; 7:1259-65.

149.Mishra RK, Chakraborty P, Arnaoutov A, Fontoura BM, Dasso M. The Nup107-160 complex and gamma-TuRC regulate microtubule polymerization at kinetochores. Nat Cell Biol 2010; 12:164-9.

150.Mackay DR, Elgort SW, Ullman KS. The nucleoporin Nup153 has separable roles in both early mitotic progression and the resolution of mitosis. Mol Biol Cell 2009; 20:1652-60.

151.Whalen WA, Bharathi A, Danielewicz D, Dhar R. Advancement through mitosis requires rae1 gene function in fission yeast. Yeast 1997; 13:1167-79.

152.Blower MD, Nachury M, Heald R, Weis K. A Rae1-containing ribonucleoprotein complex is required for mitotic spindle assembly. Cell 2005; 121:223-34.

153.Jeganathan KB, Malureanu L, van Deursen JM. The Rae1-Nup98 complex prevents aneuploidy by inhibiting securin degradation. Nature 2005; 438:1036-9.

154.Wong RW, Blobel G, Coutavas E. Rae1 interaction with NuMA is required for bipolar spindle formation. Proc Natl Acad Sci U S A 2006; 103:19783-7.

155.Lussi YC, Shumaker DK, Shimi T, Fahrenkrog B. The nucleoporin Nup153 affects spindle checkpoint activity due to an association with Mad1. Nucleus 2010; 1:71-84.

156.Cross MK, Powers MA. Nup98 regulates bipolar spindle assembly through association with microtubules and opposition of MCAK. Mol Biol Cell 2011; 22:661-72.

157.Hetzer M, Gruss OJ, Mattaj IW. The Ran GTPase as a marker of chromosome position in spindle formation and nuclear envelope assembly. Nat Cell Biol 2002; 4:E177-84.

158.Harel A, Forbes DJ. Importin beta: conducting a much larger cellular symphony. Mol Cell 2004; 16:319-30.

159.Clarke DJ, Bachant J. Kinetochore structure and spindle assembly checkpoint signaling in the budding yeast, Saccharomyces cerevisiae. Front Biosci 2008; 13:6787-819.

160.Tahara K, Takagi M, Ohsugi M, Sone T, Nishiumi F, Maeshima K, et al. Importin-beta and the small guanosine triphosphatase Ran mediate chromosome loading of the human chromokinesin Kid. J Cell Biol 2008; 180:493-506.

161.Laurell E, Beck K, Krupina K, Theerthagiri G, Bodenmiller B, Horvath P, et al. Phosphorylation of Nup98 by multiple kinases is crucial for NPC disassembly during mitotic entry. Cell 2011; 144:539-50.

162.Onischenko EA, Gubanova NV, Kiseleva EV, Hallberg E. Cdk1 and okadaic acid-sensitive phosphatases control assembly of nuclear pore complexes in Drosophila embryos. Mol Biol Cell 2005; 16:5152-62.

163. Lusk CP, Waller DD, Makhnevych T, Dienemann A, Whiteway M, Thomas DY, et al. Nup53p is a target of two mitotic kinases, Cdk1p and Hrr25p. Traffic 2007; 8:647-60.

164. Swaminathan S, Kiendl F, Korner R, Lupetti R, Hengst L, Melchior F. RanGAP1*SUMO1 is phosphorylated at the onset of mitosis and remains associated with RanBP2 upon NPC disassembly. J Cell Biol 2004; 164:965-71.

165. Kosako H, Yamaguchi N, Aranami C, Ushiyama M, Kose S, Imamoto N, et al. Phosphoproteomics reveals new ERK MAP kinase targets and links ERK to nucleoporin-mediated nuclear transport. Nat Struct Mol Biol 2009; 16:1026-35.

166. De Souza CP, Osmani AH, Hashmi SB, Osmani SA. Partial nuclear pore complex disassembly during closed mitosis in Aspergillus nidulans. Curr Biol 2004; 14:1973-84.

167. Miller MW, Caracciolo MR, Berlin WK, Hanover JA. Phosphorylation and glycosylation of nucleoporins. Arch Biochem Biophys 1999; 367:51-60.

168. Terry LJ, Shows EB, Wente SR. Crossing the nuclear envelope: hierarchical regulation of nucleocytoplasmic transport. Science 2007; 318:1412-6.

169. Nigg EA. Mechanisms of signal transduction to the cell nucleus. Adv Cancer Res 1990; 55:271-310.

170. Wen W, Meinkoth JL, Tsien RY, Taylor SS. Identification of a signal for rapid export of proteins from the nucleus. Cell 1995; 82:463-73.

171. Karin M, Hunter T. Transcriptional control by protein phosphorylation: signal transmission from the cell surface to the nucleus. Curr Biol 1995; 5:747-57.

172. Nigg EA. Nucleocytoplasmic transport: signals, mechanisms and regulation. Nature 1997; 386:779-87.

173. Azuma Y, Takio K, Tabb MM, Vu L, Nomura M. Phosphorylation of Srp1p, the yeast nuclear localization signal receptor, in vitro and in vivo. Biochimie 1997; 79:247-59.

174. Yoon SO, Shin S, Liu Y, Ballif BA, Woo MS, Gygi SP, et al. Ran-binding protein 3 phosphorylation links the Ras and PI3-kinase pathways to nucleocytoplasmic transport. Mol Cell 2008; 29:362-75.

175.Makhnevych T, Lusk CP, Anderson AM, Aitchison JD, Wozniak RW. Cell cycle regulated transport controlled by alterations in the nuclear pore complex. Cell 2003; 115:813-23.

176.Schneider R, Grosschedl R. Dynamics and interplay of nuclear architecture, genome organization, and gene expression. Genes Dev 2007; 21:3027-43.

177.Kosako H, Imamoto N. Phosphorylation of nucleoporins: signal transduction-mediated regulation of their interaction with nuclear transport receptors. Nucleus 2010; 1:309-13.

178.Ben-Efraim I, Frosst PD, Gerace L. Karyopherin binding interactions and nuclear import mechanism of nuclear pore complex protein Tpr. BMC Cell Biol 2009; 10:74.

179.Zimowska G, Aris JP, Paddy MR. A Drosophila Tpr protein homolog is localized both in the extrachromosomal channel network and to nuclear pore complexes. J Cell Sci 1997; 110 (Pt 8):927-44.

180.Byrd DA, Sweet DJ, Pante N, Konstantinov KN, Guan T, Saphire AC, et al. Tpr, a large coiled coil protein whose amino terminus is involved in activation of oncogenic kinases, is localized to the cytoplasmic surface of the nuclear pore complex. J Cell Biol 1994; 127:1515-26.

181.Mendjan S, Taipale M, Kind J, Holz H, Gebhardt P, Schelder M, et al. Nuclear pore components are involved in the transcriptional regulation of dosage compensation in Drosophila. Mol Cell 2006; 21:811-23.

182.Walther TC, Fornerod M, Pickersgill H, Goldberg M, Allen TD, Mattaj IW. The nucleoporin Nup153 is required for nuclear pore basket formation, nuclear pore complex anchoring and import of a subset of nuclear proteins. EMBO J 2001; 20:5703-14.

183.Cordes VC, Hase ME, Muller L. Molecular segments of protein Tpr that confer nuclear targeting and association with the nuclear pore complex. Exp Cell Res 1998; 245:43-56.

184.Vinciguerra P, Iglesias N, Camblong J, Zenklusen D, Stutz F. Perinuclear Mlp proteins downregulate gene expression in response to a defect in mRNA export. EMBO J 2005; 24:813-23.

185.Niepel M, Strambio-de-Castillia C, Fasolo J, Chait BT, Rout MP. The nuclear pore complex-associated protein, Mlp2p, binds to the yeast spindle pole body and promotes its efficient assembly. J Cell Biol 2005; 170:225-35.

186.Zhao Y, Kwon SW, Anselmo A, Kaur K, White MA. Broad spectrum identification of cellular small ubiquitin-related modifier (SUMO) substrate proteins. J Biol Chem 2004; 279:20999-1002.

187.Qi H, Rath U, Wang D, Xu YZ, Ding Y, Zhang W, et al. Megator, an essential coiled-coil protein that localizes to the putative spindle matrix during mitosis in Drosophila. Mol Biol Cell 2004; 15:4854-65.

188.Lince-Faria M, Maffini S, Orr B, Ding Y, Claudia F, Sunkel CE, et al. Spatiotemporal control of mitosis by the conserved spindle matrix protein Megator. J Cell Biol 2009; 184:647-57.

189.Vaquerizas JM, Suyama R, Kind J, Miura K, Luscombe NM, Akhtar A. Nuclear pore proteins nup153 and megator define transcriptionally active regions in the Drosophila genome. PLoS Genet 2010; 6:e1000846.

190.Krull S, Dorries J, Boysen B, Reidenbach S, Magnius L, Norder H, et al. Protein Tpr is required for establishing nuclear pore-associated zones of heterochromatin exclusion. EMBO J 2010; 29:1659-73.

191.David-Watine B. Silencing nuclear pore protein Tpr elicits a senescent-like phenotype in cancer cells. PLoS One 2011; 6:e22423.

192.Livak KJ, Schmittgen TD. Analysis of relative gene expression data using real-time quantitative PCR and the 2(-Delta Delta C(T)) Method. Methods 2001; 25:402-8.

193.Herold A, Klymenko T, Izaurralde E. NXF1/p15 heterodimers are essential for mRNA nuclear export in Drosophila. RNA 2001; 7:1768-80.

194.Herold A, Suyama M, Rodrigues JP, Braun IC, Kutay U, Carmo-Fonseca M, et al. TAP (NXF1) belongs to a multigene family of putative RNA export factors with a conserved modular architecture. Mol Cell Biol 2000; 20:8996-9008.

195.Levesque L, Bor YC, Matzat LH, Jin L, Berberoglu S, Rekosh D, et al. Mutations in tap uncouple RNA export activity from translocation through the nuclear pore complex. Mol Biol Cell 2006; 17:931-43.

196.Katahira J, Inoue H, Hurt E, Yoneda Y. Adaptor Aly and co-adaptor Thoc5 function in the Tap-p15-mediated nuclear export of HSP70 mRNA. EMBO J 2009; 28:556-67.

197.Cochrane AW, Perkins A, Rosen CA. Identification of sequences important in the nucleolar localization of human immunodeficiency virus Rev: relevance of nucleolar localization to function. J Virol 1990; 64:881-5.

198.Ernst RK, Bray M, Rekosh D, Hammarskjold ML. A structured retroviral RNA element that mediates nucleocytoplasmic export of intron-containing RNA. Mol Cell Biol 1997; 17:135-44.

199.Skruzny M, Schneider C, Racz A, Weng J, Tollervey D, Hurt E. An endoribonuclease functionally linked to perinuclear mRNP quality control associates with the nuclear pore complexes. PLoS Biol 2009; 7:e8.

200.Ohnishi T, Yamashita A, Kashima I, Schell T, Anders KR, Grimson A, et al. Phosphorylation of hUPF1 induces formation of mRNA surveillance complexes containing hSMG-5 and hSMG-7. Mol Cell 2003; 12:1187-200.

201.Unterholzner L, Izaurralde E. SMG7 acts as a molecular link between mRNA surveillance and mRNA decay. Mol Cell 2004; 16:587-96.

202.Glavan F, Behm-Ansmant I, Izaurralde E, Conti E. Structures of the PIN domains of SMG6 and SMG5 reveal a nuclease within the mRNA surveillance complex. EMBO J 2006; 25:5117-25.

203.Powers MA, Forbes DJ, Dahlberg JE, Lund E. The vertebrate GLFG nucleoporin, Nup98, is an essential component of multiple RNA export pathways. J Cell Biol 1997; 136:241-50.

204.Ren Y, Seo HS, Blobel G, Hoelz A. Structural and functional analysis of the interaction between the nucleoporin Nup98 and the mRNA export factor Rae1. Proc Natl Acad Sci U S A 2010; 107:10406-11.

205.Bastos R, Lin A, Enarson M, Burke B. Targeting and function in mRNA export of nuclear pore complex protein Nup153. J Cell Biol 1996; 134:1141-56.

206.Ullman KS, Shah S, Powers MA, Forbes DJ. The nucleoporin nup153 plays a critical role in multiple types of nuclear export. Mol Biol Cell 1999; 10:649-64.

207.Meyer RD, Srinivasan S, Singh AJ, Mahoney JE, Gharahassanlou KR, Rahimi N. PEST motif serine and tyrosine phosphorylation controls vascular endothelial

growth factor receptor 2 stability and downregulation. Mol Cell Biol 2011; 31:2010-25.

208.Taurin S, Sandbo N, Qin Y, Browning D, Dulin NO. Phosphorylation of beta-catenin by cyclic AMP-dependent protein kinase. J Biol Chem 2006; 281:9971-6.

209.Moujalled D, Weston R, Anderton H, Ninnis R, Goel P, Coley A, et al. Cyclic-AMP-dependent protein kinase A regulates apoptosis by stabilizing the BH3-only protein Bim. EMBO Rep 2011; 12:77-83.

210.Hino S, Tanji C, Nakayama KI, Kikuchi A. Phosphorylation of beta-catenin by cyclic AMP-dependent protein kinase stabilizes beta-catenin through inhibition of its ubiquitination. Mol Cell Biol 2005; 25:9063-72.